Republic of Iraq
Ministry of Higher Education
and Scientific Research
University of Babylon
College of Engineering

Design and Simulation of Hybrid Single-Carrier Frequency-Division Multiple Access and Direct Sequence Code-Division Multiple Access

A Thesis
Submitted to the Department of Electrical Engineering / College of Engineering / University of Babylon in Partial Fulfillment
of the Requirements for the Degree of Master in Engineering/ Electrical Engineering/ Communications.

By

Mohammed Hamzah Owaid Abd

Supervised by

Prof. Dr. Samir Jasim Mohammed AL-Muraab

2022 A.D. 1444 A.H.

بِسْمِ اللَّـهِ الرَّحْمَـٰنِ الرَّحِيمِ

﴿يَرْفَعِ اللَّهُ الَّذِينَ آمَنـــــوُا مِنكُمْ
وَالَّذِينَ أُوتُـــــوا الْعِلْمَ دَرَجَاتٍ﴾

صدق الله العظيم

سورة المجادلة : 11

Supervisors Certification

I certify that this thesis titled **"Design and Implementation of Single-Carrier Direct Sequence Frequency-Division Multiple Access Communication System Code Division Multiple Access "** was prepared by **Mohammed Hamzah Owaid** under my supervision at the Electrical Engineering Department, College of Engineering at University of Babylon, in a partial fulfillment of the requirements for the degree of Master of Science in Electrical Engineering/Communications.

Supervisors

Signature:

Name*:* ***Prof. Dr. Samir Jasim Mohammed AL-Muraab***

Date: / / 2022

In view of the available recommendation, we forward this thesis for debate by the examining committee.

Head of the Electrical Engineering Department

Signature:

Name:

Date: / / 2022

Acknowledgements

Thanks be to God for the insight that inspired me, and praise be to Him for the blessings He has bestowed upon me, and to Him is the credit for achieving what I aspire to in this research. Praise be to God, who by His praise opens every book and by His remembrance every speech is issued, and by His praise the people of blessings enjoy the abode of reward.

It gives me great pleasure to extend my thanks and gratitude to ***(Prof. Dr. Samir Jasim Mohammed AL-Muraab)****, who provided me with the information I needed in my research*

And for the great efforts he made for me since he proposed the subject of the research and his continuous supervision, and for his advice that helped me a lot in overcoming the difficulties I faced, calling from God success and brilliance in the scientific career.

I would like to extend my thanks and gratitude to the Deanship of the College of Engineering and the Presidency of the Electrical Engineering Department for the facilities and administrative procedures they provided me, which effectively contributed to the completion of the requirements of this research.

.

Researcher

Dedication

To the fruit of the Ibrahemic Imamate and the Muhammadian tree, to the person who will fill the earth with value and equity after it was fill up with Injustice and tyranny.

To my kind father.... who taught me how to stand firmly above the earth, my role model, and my ideal in life; He is the one who taught me how to live with dignity and honor.

To my tender mother... the source of love, altruism and generosity, I cannot find words that can give her her due, for she is the epic of love and the joy of a lifetime, and an example of dedication and giving.

To my brothers... Those who support me and share my sorrows before my joys.

To my beloved wife... Who supports me and strengthens me when I am weak, my love and my queen.

To all my friends and to all those from whom I received advice and support;

I dedicate to you the summary of my scientific effort.

Abstract

Orthogonal Frequency Division Multiple Access (OFDMA) is a new version of Orthogonal Frequency Division Multiplexing (OFDM) that allows multi-user access based on orthogonal frequency division by allocating time-frequency sub-channels to distinct users, making it possible for multiple users to send data simultaneously. Despite the many advantages, which have led to the deployment of OFDMA technology in many applications, OFDMA has a high Peak to Avarage Power Ratio (PAPR) problem.

Single Carrier-Frequency Division Multiple Access (SC-FDMA) is one of the approaches proposed by The 3rd Generation Partnership Project (3GPP) to reduce the OFDMA PAPR and is now used in 4G uplink. The Single Carrier-Frequency Division Multiple Access Direct Sequence-Code Division Multiple Access (SC-FDMA DS-CDMA) technology is proposed in this thesis to lower the PAPR of SC-FDMA.

In this thesis the simulation scenarios started by simulate the OFDMA system to know its performance in terms of PAPR and BER and then simulate the SC-FDMA system and comparing it with the OFDMA system. When the Complementary Cumulative Distribution Function (CCDF) of PAPR is 10^{-3} with localized subcarrier mapping and QPSK modulation, the PAPR of SC-FDMA is 7 dB, while the PAPR of OFDMA is 9.8 dB. SC-FDMA has a BER of 6.2×10^{-4} at SNR of 17.5 dB, while OFDMA requires SNR of 26.8 dB to achieve the same BER.

The rest of the simulation scenarios implemented the SC-FDMA-DS-CDMA approach and compared its performance with the traditional SC-FDMA method. The proposed system was implemented using two modulation schemes (QPSK and 16PSK) with two kinds of sub-carrier mapping (localized and interleaved). Also, two models of the communication channel have been implemented (AWGN, Rayleigh), with multiple types of code sequences

(Walsh-Hadamard sequences, OVSF codes, Maximum-length sequences “m-sequences”, and Gold codes). The proposed system simulation was carried out on multiple users, starting with 8 and up to 128 users and using the MATLAB program.

When the CCDF of PAPR is 10^{-2} under localized subcarrier mapping, QPSK modulation, and Walsh codes, the SC-FDMA-DSCDMA PAPR with 8 users is 7.85 dB, while the SC-FDMA PAPR is 8.9 dB. The suggested SC-FDMA-DSCDMA system's PAPR with 32 users is 10 dB, compared to the SC-FDMA system's PAPR of 10.4 dB. The suggested SC-FDMA-DSCDMA system has a PAPR of 11.26 dB with 128 users, compared to 11.47 dB for SC-FDMA. SC-FDMA-DSCDMA BER is the same as SC-FDMA BER when comparing BER performance.

List of Contents

List of Tables

List of Figures

List of Figures

List of Figures

List of Figures

List of Figures

List of Figures

List of Abbreviations

Abbreviation	Definition
3GPP	third Generation Partnership Project.
4G	Fourth Generation.
ADSL	Asymmetric Digital Subscriber Line
AJ	Anti-Jamming
ASK	Amplitude Shift Keying
AWGN	Additive White Gaussian Noise.
AWGN	Additive White Gaussian Noise
BER	Bit Error Rate.
BPSK	Binary Shift Keying
CCDF	Complementary Commutative Distribution Function
CDMA	Code Division Multiple Access
CP	Cyclic Prefix
DAB	Digital Audio Broadcast
DFDMA	Distributed Frequency Division Multiple Access
DFT	Discrete Fourier Transform.
DFT	Discrete Fourier Transform
DS	Direct Sequencing
DS-CDMA	Direct Sequence-Code Division Multiplexing Access**.**
DSSS	Direct Sequence Spread Spectrum
DVB	Digital Video Broadcasting
FDMA	Frequency Division Multiple Access
FFT	Fast Fourier Transform
FH	Frequency Hopping
FPGA	Field Programmable Gate Array
FSK	Frequency Shift Keying
GSM	Global System for Mobile

List of Abbreviations

Abbreviation	Definition
HPA	High Power Amplifier.
IDFT	Inverse Discrete Fourier Transform
IEEE	Institute of Electrical and Electronics Engineers
IFDMA	Interleaved Frequency Division Multiple Access
IFFT	Inverse Fast Fourier Transform
ISI	Inter Symbol Interference.
LFDMA	Localized Frequency Division Multiple Access
LFSR	Linear Feedback Shift Register
LOS	Line Of Sight
LTE	Long Term Evaluation.
MC-CDMA	Multi Carrier- Code Division Multiple Access**.**
MC-DS-CDMA	MultiCarrier Direct Sequence Code Division Multiple Access.
MCM	Multi Carrier Modulation**.**
NTC	Nonlinear Companding Transform.
OFDM	Orthogonal Frequency Division Multiplexing**.**
OFDMA	Orthogonal Frequency Division Multiple Access**.**
OVSF	Orthogonal Variable Spreading Factor.
PAPR	Peak Average Power Ratio.
PNLCP	Proposed New Linear Combination Pulse.
PRK	Phase Reversal Keying
PSD	Power Spectral Density
PSK	Phase Shift Keying
QPSK	Quadrature Phase Shift Keying.
RF	Radio Frequency
SC-FDMA	Single Carrier- Frequency Division Multiple Access**.**

List of Abbreviations

Abbreviation	Definition
SC-FDMA-DSCDMA	Single Carrier- Frequency Division Multiple Access- Direct Sequence-Code Division Multiple Access**.**
SNR	Signal to Noise Ratio
TDMA	Time Division Multiple Access
TH	Time Hopping

List of Symbols

Symbol	Definition
r(t)	Received signal
s(t)	Transmitted signal
w(t)	White noise
μ	Mean power of noise
$f_x(x)$	Power density function of Gaussian distribution
Σ	Noise power
b_s	Bandwidth of the transmitted signal
b_c	Coherence bandwidth
f_d	Doppler frequency
f_c	Carrier frequency
V	Source velocity
C	Velocity of light
T_s	Sample delay
y(n)	Multipath output
a_n	Attenuation factor
z(n)	Gaussain noise
x(m)	Modulated complex data symbols
X(k)	Disecret Fourior transform output samples
N	Total numbers of subcarriers
M	Input block size
Q	Bandwidth spreading factor
x(n)	Inverse disecrete fourier transform output samples
x(l)	Samples after the subcarrier mapping
R	Received signal after removing the cyclic prefix
N	AWGN noise
u^{th}	Number of users

List of Symbols

Symbol	Definition
x^u	User samples
H_c^u	Circulant channel matrix
R_d	Received block
A_c^u	Diagonal matrix
x^u	User's symbols
H	Channel impulse response
G_p	Processing gain
R_c	Chip rate
R_b	Bit rate
g(x)	Generator polynomial
x^m	Generator polynomial coefficient
H	Efficiency
η_{max}	Maximum efficiency
Q(x)	Complementary error function
E_b	Energy bit
N_o	Single sided noise power spectral density

Publication

- M. H. Owaid and S. J. Mohammed, "PAPR Performance Comparison Among Single Carrier Spread Spectrum Techniques for 5G Robust Communication Systems," *5th International Conference on Engineering Technology and its Applications (IICETA)*, 2022, pp. 91–96.

- M. H. Owaid and S. J. Mohammed, "Performance Analysis of SC-FDMA and SC-FDMA-DSCDMA," *8th International Conference on Contemporary Information Technology and Mathematics (ICCITM)*, 2022.

Chapter One Introduction

CHAPTER ONE

INTRODUCTION

1.1 Background

The major challenge faced by every digital communication system is starting to find out how to boost the data throughput while simultaneously lowering the error rate. Therefore, to meet this challenge's requirements, the method of Multi-Access Modulation known as Multi-Carrier Modulation (MCM) is utilized. MCM relies on partitioning the transmitted data stream into a symbol stream, with a much lower symbol rate modulated on the multiple Sub-Carrier. The most popular technology of the MCM system is Orthogonal Frequency Division Multiplexing (OFDM)[1]. OFDM employs several carriers, each transmitting data at a low bit rate. Thus, it effectively utilizes the spectrum and is resistant to multipath effects, interference, and selective fading. Multi-Carrier modulation systems are getting more attention due to their ability to combat multipath channel fading. Despite the many advantages provided by the OFDMA system, which made it used in many essential systems, it suffers from the problem of high Peak to Average Ratio (PAPR)[2].

A high PAPR affects the entire system's performance and the complexity and cost of implementing the transmitter. The nature of transmission in the uplink is by sending the signal from all the devices within the geographical area to the base station. That requires an access technique that ensures that the transmitting power of the device is sufficient to send a signal to the base station. Therefore, if the value of PAPR is high, the device needs a large power amplifier with a large linear area to ensure that the signal reaches the base station without distortion[3]. It has been found that if PAPR is lower, power efficiency is higher, increasing battery usage for a long time. One of the essential solutions to get rid of the problem of PAPR is presented by 3rd Generation Partnership Project (3GPP).

This solution suggests applying the Discrete Fourier Transform (DFT) to spread the baseband signal prior to apply the OFDMA modulator, resulting in a reduction in the envelope fluctuation compared to OFDMA. The method provided by 3GPP is named Single Carrier-Frequency Division Multiple Access (SC-FDMA). SC-FDMA transmissions have a lower PAPR than the typical OFDMA, which is a significant advantage, because of this, SC-FDMA is used for 4G uplink transmission[4].

In wireless communication, the DS-CDMA is widely utilized. It provides many benefits, including high-level security because its signal is like noise shape, a good technique for multiple access, reduction of the effects of multipath fading, and resistance to narrowband jamming. Thus, further research into new methods to lower the PAPR value while ensuring the data errors rate doesn't go up is still required. For SC-FDMA, this thesis used a hybrid approach to lower PAPR. The proposed technology combines Single Carrier-FDMA and Direct Sequences-CDMA and is named SC-FDMA-DSCDMA. Used many simulated scenarios to compare how the suggested system behaves to SC-FDMA [5].

1.2 Literature Survey

This section will review and highlight a few research studies that have focused on reducing the PAPR value.

J. Gazda et al, 2010, This work compared the performance of the SC-FDMA system and the OFDMA system in the nonlinear AWGN environment. Simulated with only one user to eliminate multipath distortion and leave only the distortion from nonlinear AWGN. Many different numbers have been used for the Input Back Off (IBO). The simulation results show that an SC-FDMA system works better than an OFDMA system when the value of IBO is low, which means that the nonlinear distortion is high. But if the nonlinear distortion

is reduced by increasing the value of IBO or using one of the PAPR reduction techniques and the terminal is close to the base station, and a high data rate is needed, it is better to use OFDMA. In the end, both systems have advantages that depend on how they are used. Thus SC-FDMA is not always better than OFDMA[6].

Z. Luo et al, 2011, This work presented a comparison between MC-CDMA and SC-FDMA-CDMA. The work discussed the theoretical part of the two systems and the implementation of the two systems using Matlab simulation. Different subcarrier assignments are used, such as the localized and the interleaved subcarrier mapping as well as the AWGN channel and QPSK modulation are used in the simulation. Then the hybrid subcarrier is used that combines the localized and the interleaved subcarrier mapping. One type of orthogonal spreading code is used which is the Walsh Code and the simulation is carried out on 16 users. The simulation results proved that the SC-FDMA-CDMA system showed better performance of PAPR than MC-CDMA. As for the performance of BER, the two systems have almost the same performance. The use of hybrid subcarrier mapping gives a good performance but spoils the orthogonality between the subcarriers. It needs other techniques to be used better, such as adaptive modulation[7].

C. A. Azurdia-Meza et al, 2012, Proposed a new group of Nyquist pulses was generated by linearly merging two free ISI parametric pulses. The generated pulses are employed in the pulse shaping filter to diminish the SC-FDMA PAPR value. The simulation of the SC-FDMA system was done using the MATLAB program, where 16QAM was used in the simulation as a modulation method, interleaved subcarrier mapping, the number of subcarriers is 64, uniform random data is 10^6, and the roll of factor is 0.35. Simulations indicate that the SC-FDMA system's interleaved subcarrier method has a lower PAPR than alternative current filters[8].

S. Shukla et al, 2013, In this work, the Nonlinear Transformation Technology (NTC) is a new scheme that has been added to the SC-FDMA system. This work aims mainly to reduce the PAPR of the SC-FDMA system. It converts the SC-FDMA signal by carefully selecting the transform parameters to achieve a fair tradeoff between PAPR reduction and bit error rate (BER) performances. The employment of two forms of carrier mapping allows the system designer additional freedom to adapt to various radio situations. The simulation of the SC-FDMA system was done using the MATLAB program, where QPSK and 16QAM are used in the simulation as modulation methods, and interleaved and localized subcarriers are used as mapping forms. The simulation results proved that the proposed system performed well as it significantly reduced PAPR compared with the traditional SC-FDMA system[9].

D. Kedia, A. Modi, 2014, This study compares the SC-FDMA-CDMA system to SC-FDMA, OFDMA, and MC-DS-CDMA with 8 and 16 users in terms of PAPR and BER. AWGN, Rayleigh, and Rician channels are used as channel models, and localized subcarrier mapping and QPSK are used as mapping forms, also the convolution with rate 1/2 is used as the channel coding technique. Pseudo Noise (PN) is used as spreading sequences with a maximum length is 16 which is equal to the maximum number of users. Simulations demonstrate that the SC-FDMA-CDMA system outperforms others techniques [10].

F. S. Al-Kamal et al, 2015, In this research, the discrete cosine transform (DCT) is utilized for SC-FDMA transmission. Firstly, an improved DCTbased SC-FDMA (DCT SC-FDMA) system is introduced. Then, the paper presents a new transceiver architecture design for the uplink SC-FDMA system that implements a cosine basis function or a complex exponential Fourier basis function. The proposed architecture uses the discrete wavelet transform and a

hybrid companding and clipping method for peak-to-average power ratio (PAPR) reduction. The modulation type used in the simulation is QPSK, the transmitted block size is 512, the input block size is 128 symbols, the channel coding is convolution code with a rate is 1/2, the subcarrier mapping is localized, the channel model is AWGN channel with MMSE estimator. From the simulation results, it is shown that the DCT SC-FDMA system achieves a superior bit error rate(BER) performance than that of the discrete Fourier transform-based SC-FDMA (DFT SC-FDMA) system[11].

R. Chisab et al, 2016, This work provided an excellent investigation of the performance of the SC-FDMA system from several viewpoints. The simulation provided by MATLAB was used to implement the system. PAPR and BER were used to evaluate the system's performance. This study uses different modulation forms, including QPSK, 16QAM, and 64QAM. Localized, distributed, and interleaved subcarrier mapping are examples of different forms of subcarrier mapping. The tests were also carried out using a multi-path channel, specifically two paths with various delay and gain levels assigned to them and the Doppler effect.Compared to 16QAM and 64QAM, the simulation results showed that QPSK produces the best results. The performance is better when the Doppler shift value is low. A lower PAPR is obtained by using a higher roll-of-factor value. Finally, interleaved subcarrier mapping outperforms the other modes[12].

S. Singh et al, 2017, In this research work, the PAPR reduction employing transmit Nyquist pulses in SC-FDMA has been taken into consideration and examined . By taking into account the linear combination of three Nyquist pulses, a new pulse has been presented. Evaluation and comparison of the PAPR performance of the suggested Nyquist pulse in the SC-FDMA system with other Nyquist pulses. Additionally assessed is the impact of the roll-off factor on the pulse-shaped SC-FDMA systems' PAPR performance. The

simulation of the SC-FDMA system was done using the MATLAB program, where 16QAM was used in the simulation as a modulation method, interleaved subcarrier mapping, the number of subcarriers is 256, uniform random data is 10^4. The simulation results proved that the performance of the SC-FDMA system is much better when using Proposed New Linear Combination Pulse (PNLCP) in pulse shaping compared to different types[13].

K. Shri Ramtej, S. Anuradha, 2018, This research proposes a companding transform based on a special airy function to limit PAPR without increasing the average signal power. The proposed method maintains the BER performance of the SC-FDMA system without introducing out-of-band radiation, unlike μ law companding. the proposed SC-FDMA is simulated using the Matlab software. The modulation type used in the simulation is QPSK and 16QAM, the input block size is 128 symbol, the channel coding is convolution code with a rate is 1/2, the subcarrier mapping is localized, and the channel model is AWGN channel with MMSE estimator. The results demonstrate that the proposed airy companding technique offers a PAPR reduction of about 1.87 dB when $\alpha = 2$ without increasing average signal power. PAPR reduction is less when compared to other techniques, but it does not degrade the BER performance and introduces minimum out-of-band distortion. The proposed method is simple and does not require bandwidth expansion. So airy companding technique can be used practically to reduce PAPR in LTE uplink communications[14].

G. Naidu and V. Malleswara, 2019, A nonlinear companding function (NCF) based on the Exponential function is proposed in this research to reduce the PAPR and also BER of SC-FDMA. the proposed SC-FDMA is simulated using the Matlab software. The modulation type used in the simulation is QPSK and 16QAM, the input block size is 128 symbol, the subcarrier mapping is localized, and the channel model is AWGN channel with ZF and MMSE estimator. Computer simulations give that the expected method decides

better than the other functions like μ -law companding function in term of BER and PAPR performance[15].

K. Shri Ramtej and S. Anuradha, 2020, This paper discusses error function, exponential, rooting, and logarithmic companding techniques that can be utilized to mitigate PAPR in SC-FDMA systems. the proposed SC-FDMA is simulated using the Matlab software. The modulation type used in the simulation is QPSK and 16QAM, the input block size is 128 symbol, the channel coding is convolution code with a rate is 1/2, the subcarrier mapping is localized, and the channel model is AWGN channel with MMSE estimator. Simulation results show that the exponential companding technique provides better PAPR and Bit Error Rate (BER) performances at the cost of higher side lobes, and error function companding transform provides good PAPR and Power Spectral Density (PSD) performances at the cost of higher BER without increasing average signal power[16].

K. Vaigandla et al, 2021, focuses on the performance evaluation of SC-FDMA and OFDMA models using the AWGN channel. Localized, distributed, and interleaved subcarriers are all utilized. Compared to localized data, the results showed that the interleaved and distributed data has a low error rate. Regarding PAPR and BER, the SC-FDMA system performs better than the OFDMA system[17].

In this research, The behaviour of the SC-FDMA-DSCDMA system is analyzed and compared with the SC-FDMA in terms of the error rate and PAPR using 8,16,32,64, and 128 users using four types of code sequences, which are Walsh-Hadamard sequences, OVSF codes, Maximum-length sequences (m-sequences), and Gold codes. Also, localized and interleaved are used as subcarrier mapping, and AWGN and Rayleigh are used as channel models.

1.3 Problem Statement

1. High PAPR is the most problem in the multi-carriers transmission.
2. OFDMA envelope is not fixed therefore when many subcarriers are added in the same phase duo to the linear combination of the IDFT process results in a high PAPR value.
3. High distortion is happened when transmitted over nonlinear component like High Power Amplifier (HPA)
4. Uplink transmission is based on sending signals from devices to the base station so when the PAPR is high therefore the devices need batteries with long life.

1.4 Aims of the Study

1. single carrier transmission is used to overcome the high PAPR problem stated in the first point of the previous section.
2. The DFT process is applied before the OFDMA modulator (IDFT) to spread the baseband modulator symbols to overcome the second point stated in the previous section.
3. The spread spectrum technology is suggested to spread the baseband modulator symbols before applying the SC-FDMA DFT to improve its performance in terms of PAPR to overcome the third point stated in the previous section.
4. A hybrid system combining the single carrier and spread spectrum technique is proposed to decrease the PAPR value to come to a suitable system for uplink transmission therefore the suggested system overcomes the fourth point in the previous section.

1.5 Thesis Outline

The following chapters comprise the rest of the thesis.

- **Chapter Two** " Theoretical Concepts" discusses the essential concepts that have been used in implementing the proposed work.
- **Chapter Three** " SC-FDMA-DSCDMA proposed system " It covers the key components of the OFDMA system and describes how to simulate each one. Next, it simulates the SC-FDMA system by applying the DFT before the OFDMA modulator. Finally, it incorporates the spreading approach into the SC-FDMA system to simulate the proposed system.
- **Chapter Four** "Results and Discussion" discusses the implemented systems' simulation results and comparisons between them from many aspects.
- **Chapter Five** "Conclusions and Future works" introduces the conclusions and the recommendations for future works to design an advanced PAPR reduction system.

Chapter Two

Theoretical Concepts

Chapter Two

Theoretical Concepts

2.1 Introduction

Many modulation kinds are available in communications in order to ensure data transmission. OFDMA is applied for such reasons in various communication schemes such as Digital Audio Broadcast (DAB), Asymmetric Digital Subscriber Line (ADSL), cellular wide wave connection strategies, and Digital Video Broadcasting (DVB), as well as the modern wireless model generation in LTE, has a downlink transmitter. Another relevant modulation model is SC-FDMA adopted in LTE to the uplink path. SC-FDMA transmissions have a lower PAPR than the typical OFDMA, which is an important advantage. Because of this, SC-FDMA is used for 4G uplink transmission, while OFDMA is used for downlink transmission[18].

The theoretical bases necessary to develop the SC-FDMA model will be presented in this chapter, including The Basic Components Of the Communication System, Communication Types, Multipath Propagation, Multipath Effects, Multiple Access Techniques, OFDMA, SC-FDMA, Spread-Spectrum Technology, PAPR, PSK, and Channel Models.

2.2 The Basic Components of the Communication System

Each communication system comprises three essential parts: the transmitter, which readies the signal to be sent, and the channel is the medium through which the signal passes, arriving at the third and last part, which is the receiver that recovers the signal, as displayed in Figure (2.1)[2].

2.2.1 Transmitter

The information signal is converted into an electrical signal in the transmission part. For example, the microphone converts the audio signal into an electrical signal. Thus, all physical properties, such as heat, pressure, and

light, are converted into an electrical signal through the transducer, which is the first part of the transmitter. The signal to be sent has weak characteristics, so the modulation process needs to strengthen and ensure that the signal reaches the receiving destination.[19].

Figure (2.1): basic components of the communication system.

It can add some blocks to the communications system, such as source coding and channel coding, to be a robust system and have good specifications, as well as reduce the effects of noise that is added when the signal passes through the medium, as shown in Figure (2.2).

• **Source coding** is a procedure used in the transmission section to encrypt data and removed redundant (duplicate) data so that the signal is represented by the fewest number of bits possible, allowing the signal's bandwidth to be adjusted to the channel capacity for efficient transmission[20].

• **Channel coding** is located in the transmitter part, which adds several bits to the data in a certain way. With the help of this addition, errors are detected and corrected in the receiving party by channel decoding[21].

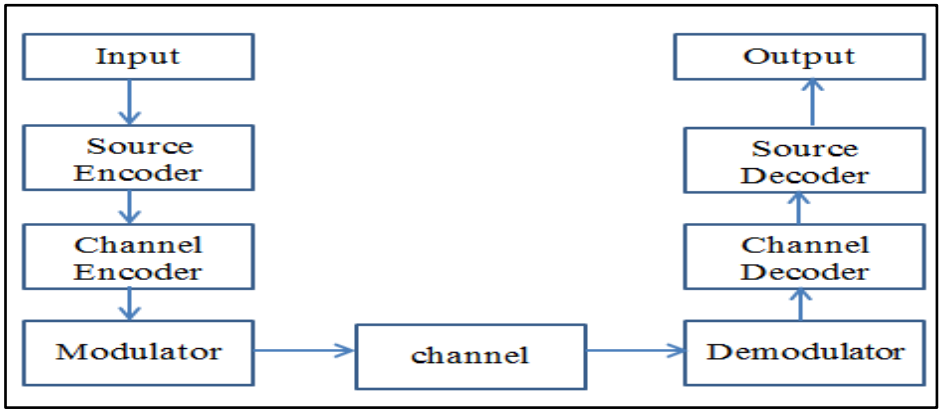

Figure (2.2): communication system block diagram

2.2.2 Channel

It is the intermediate part that connects the sending part and the receiving part, and it may be a wire or wireless. Each channel adds noise to the signal differently, weakening the signal strength as the distance increases. There are many techniques to reduce the impact of the channel on the signal.[19].

2.2.3 Receiver

This part of the communication system works to receive the signal from the channel and also reduces the effects on the signal due to its passage through the medium. In addition, it includes the inverse of the processes that occurred in the transmission part, and thus the original signal is obtained[19].

2.3 Channel Models

The channel is the medium through which the transmitted signal travels before being received by the receiver section. In most circumstances, the signal propagates in wireless environments where reflection, scattering, and attenuation occur. The receiver could be moving, which would cause fading and Doppler frequency shifts. Several channel types, such as additive white Gaussian noise (AWGN), multipath Rician fading channel, multipath Rayleigh fading channel, mobile channel, and 0db echo channel, are used to simulate or develop the performance of the communication system. This thesis considers the AWGN and Rayleigh channels for improving the SC-FDMA system.

2.3.1 Additive White Gaussian Noise Channel

In the presence of thermal noise, the performance of a digital communication system is quantified by the probability of bit detection errors. The primary cause of thermal noise in wireless communications is the addition of random signals resulting from the vibration of atoms in the receiver electronics[22]. The term Additive White Gaussian Noise (AWGN) originates for the following reasons:

❖ **Additive** The noise is additive, meaning that the received signal equals the transmitted signal plus the noise.

$$r(r) = s(t) + w(t) \quad \ldots(2.1)$$

Where $r(r)$ represents the received signal, $s(t)$ Represents the transmitted signal, and $w(t)$ denotes the additive noise. This noise is statistically independent of the signal.

❖ **White** Similar to the white colour, which is comprised of all frequencies in the visual spectrum, white noise refers to the concept that its intensity is uniform over the whole frequency band. As a result, white noise's Power Spectral Density (PSD) is constant for all frequencies ranging from $-\infty$ to $+\infty$.

❖ **Gaussian** The probability distribution of the noise samples is Gaussian with a zero mean, i.e., in the time domain, the samples can acquire both positive and negative values, and values close to zero have a greater chance of occurrence than values far from zero. The PDF of a Gaussian distribution is

$$f_X(x) = \frac{e^{-(x-\mu)^2/2\sigma^2}}{\sqrt{2\pi\sigma^2}} \quad \ldots(2.2)$$

Formally, let X be the random variable of interest, and suppose x can take on any value in the range $(-\infty,\infty)$. The PDF of the random variable is denoted $f_X(x)$. Where $f_X(x)$ means is that the probability that the random variable X takes on a value between x and x + dx, where dx is a vanishingly small increment about x, is given by the product $f_X(x)dx$. the PDF must satisfy a normalization condition because the area under $f_X(x)$ for x $\in$ $(-\infty,\infty)$ is the probability of all possible outcomes and must be exactly one. That is

$$\int_{-\infty}^{+\infty} f_X(x)dx=1 \quad (2.3)$$

Now it can be compute the mean (μX) and variance ($\sigma^2 X$) of the random variable (noise) from its PDF as follows:

$$\mu X = \int_{-\infty}^{+\infty} x f_X(x) dx \quad \ldots (2.4)$$

where μX is the average (mean) of the random variable (noise).

$$\sigma^2 X = \int_{-\infty}^{+\infty} (x - f_X)^2 (x) dx \quad \ldots (2.5)$$

where the standard deviation, (σx), is the square root of the variance[21].

2.4 Multipath Propagation

Multipath propagation is an inherent feature of the wireless communication channel. The transmitter antenna propagates the electromagnetic waveform to the wireless medium in different directions. Many signals are received from the wireless channel, a direct signal known as the Line-Of-Sight signal, which is considered essential, and an indirect set of signals considered delayed copies of the original signal, as shown in Figure (2.3). The delay value is associated with the path taken by the signal. The LOS signal has the least amount of delay. The indirect signals, which are multipath signals, arrive at different delays related to the path taken by the signal. Each path has a delay amount that differs depending on the path length. Among the phenomena that cause multipath propagation are scattering, diffraction and reflection. As a result, the channel effects on a signal, such as attenuation, delay spread, and the Doppler effect, will appear [23].

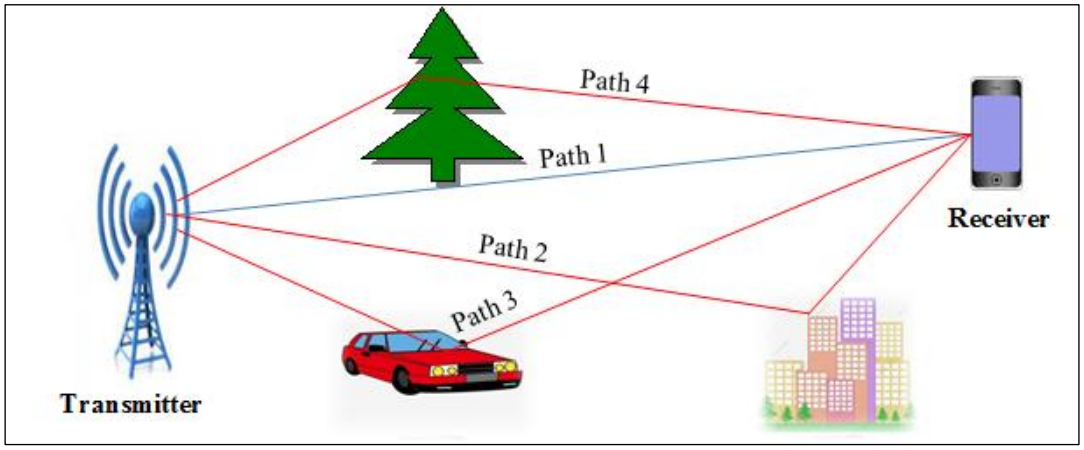

Figure (2.3): Multipath propagation, Path 1 represents LOS and the other represent indirect signals.

2.4.1 Reflection

Reflection occurs when the transmitted signal collides with smooth objects that have a wavelength greater than the transmitted signal wavelength, such as buildings, walls, and concrete, as shown in Figure (2.4). When the signals are received, the phase of the reflected signals might generate either beneficial or harmful interference. When the reflected signals' phases deviate from the sent signal's phase, a phenomenon known as destructive interference may occur, resulting in data corruption[23].

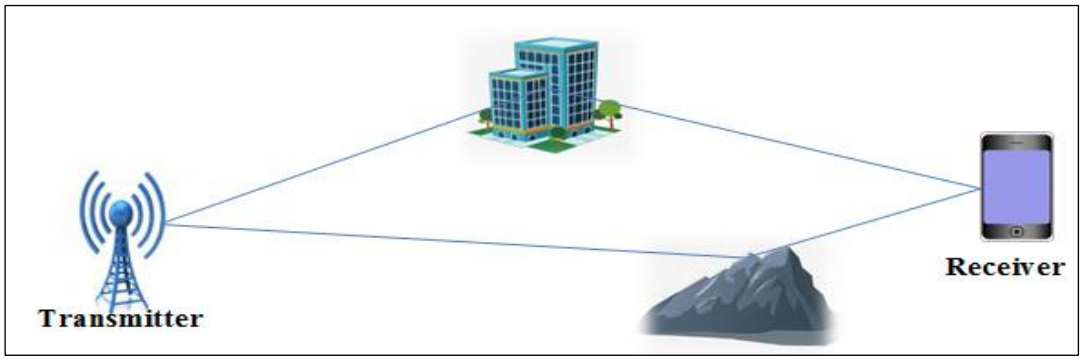

Figure (2.4): Reflection of the transmitted signal

2.4.2 Diffraction

The diffraction phenomenon occurs when the transmitted signal collides with an object with sharp edges, which leads to bending the transmitted signal around this edge. The sharp edges act like a new antenna that transmits the signal around the object, as shown in Figure (2.5).

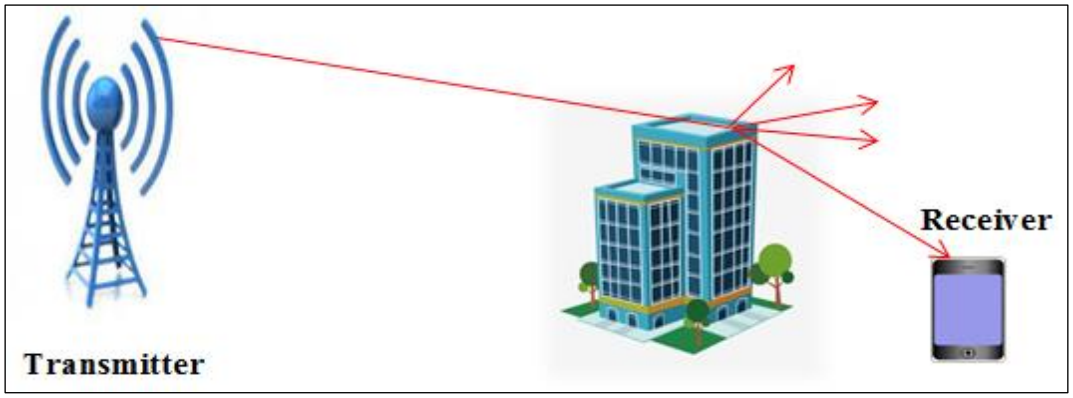

Figure (2.5): Diffraction of the transmitted signal**.**

2.4.3 Scattering

The phenomenon of scattering occurs when the transmitted signal collides with an object with uneven or rough surfaces with a wavelength equal to or greater than the wavelength of the transmitted signal, such as plant leaves, a glass surface with multiple faces, and tiny raindrops. Therefore, The signal will spread in different directions, as shown in Figure (2.6). If the object wavelength is the same as the transmitted signal wavelength, the scattering is called Mie scattering. The scattering is called metric scattering if the wavelength is greater than the transmitted signal wavelength [23].

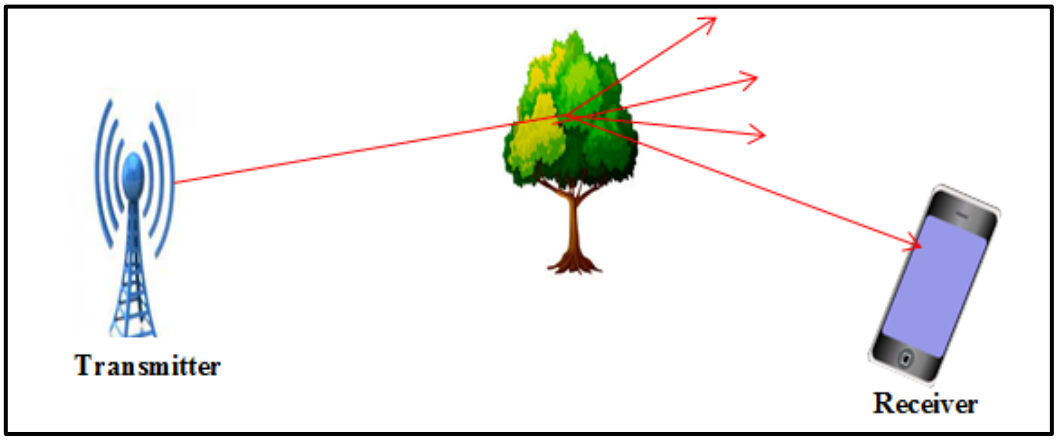

Figure (2.6): Scattering of the transmitted signal.

2.4.4 Attenuation

Signal attenuation, also known as the energy loss due to the effects of the medium over which the signal is transmitted, It is the reduction in the signal's strength as it travels from the transmitter to the receiver. All objects that obstruct the signal when it passes through the medium cause attenuation to the signal. The transmitter is constructed as high as feasible to avoid obstructions in the signal route and lessen this attenuation. The waveform should be robust and abundant to ensure that the detector might reconstruct it. If the attenuation value is large, the detector's ability for reconstruction will decrease, and the signal will be lost[24].

2.4.5 Delay Spread

The delay spread is the relative difference between the time of the first and the last signal received for the same transmitted signal. The delay spread depends on the paths of the reflected signals, which occur because of the obstacles facing the signal. These obstacles are buildings, trees, or other objects, which cannot eliminate, so the delay spread is dealt with statistically. When the delay spread exceeds the symbol time interval, it means that the multipath component of the symbol arrived at a time later than the symbol time, resulting in Inter Symbol Interference (ISI) and the transmission channel being referred to as frequency selective fading. When the delay spread is less than the symbol time interval, in that case, it means that the multipath component of the symbol arrived at a time less than the symbol time, in that case, there is no ISI, and the transmission channel is referred to as frequency nonselective fading or flat fading channel[25].

Another essential metric in the wireless channel is coherence bandwidth, which describes the transmission channel in the frequency domain. The convolution process between the transmitted signal and the channel response produces the received signal in the time domain. The received signal is obtained in the frequency domain by multiplying the transmitted signal by the channel response. Thus, the multiplication in the frequency domain is equivalent to a time-domain convolution. The coherence bandwidth b_c is the frequency of the channel response, and when it is greater than the frequency of the transmitted signal b_s, the received signal is not distorted, and the channel is referred to as a flat fading channel. When the transmitted signal frequency b_s exceeds the coherence bandwidth b_c, distortion occurs in the received signal, and the channel is referred to as a frequency selective fading channel[26].

Coherence bandwidth is the reciprocal of the delay spread, and transmitted bandwidth is the reciprocal of the symbol time. In the case of $b_s < b_c$, that means

the symbol time is greater than the delay spread, and there is no Inter Symbol Interference (ISI), and when $b_s > b_c$, that means the symbol time is less than the delay spread, and this lead to Inter Symbol Interference. Thus the flat fading channel in the frequency domain meets the case in which there is no interference in the time domain[27].

2.4.6 Doppler Effect

The frequency of the received signal differs from that of the transmitted signal when the transmitter, the receiver, or both are moving toward or away from one another. When the transmitter, receiver, or both are getting close to one another, the frequency of the detected signal will be larger than that of the transmitted wave. The frequency of the detected signal will be lower than the frequency of the broadcast signal when the transmitter, the detector, or both move apart. The relative movement between the transmitting and receiving stations causes a frequency difference between the transmitted and received signals, which is called the Doppler effect. Since the doppler effect directly alters a signal's frequency, reducing this impact is crucial for mobile wireless communications. It's important to note that the Doppler effect mostly depends on how fast the sending and receiving stations move to one another[7]. The Doppler effect causes a change in frequency that can be expressed as follows:

$$f_d = f_c \times \frac{v}{c} \quad \ldots(2.6)$$

Where f_c is the carrier frequency, v is the velocity of the source, and c is the velocity of light.

2.4.7 Multipath Rayleigh Fading Channel Model

The Rayleigh fading channel is a statistical channel model that predicts the propagation conditions encountered by wireless signals during transmission. The model assumes that every signal flowing through this channel is subject to an unexpected change in magnitude based on the Rayleigh distribution. The

Rayleigh fading channel is an accurate radio signal model in densely populated locations. This channel is at its strongest when there is no direct line of sight between the transmitter and the receiver and when there are numerous barriers in their path. The barriers scatter the radio waves until they reach the receiver[22].

In the present work, the wireless channel is assumed to be the Rayleigh fading channel as this channel model is simple and very common. The multi-path power profile is assumed to be exponential decaying.

In Figure (2.7), the maximum channel delay spread lasts u samples, the coefficients of a_0, a_1, …. a_u are the attenuations of the different paths. These coefficients are Rayleigh distributed random variables. The delay T_s denotes the unit sample delay. The output of the multi-path channel can be expressed as follows:

$$y(n) = \sum_{i=0}^{u} a_i x(n - T_s) \quad \ldots(2.7)$$

Taking the AWGN noise $z(n)$ into account

$$y(n) = \sum_{i=0}^{u} a_i x(n - T_s) + z(n) \quad \ldots(2.8)$$

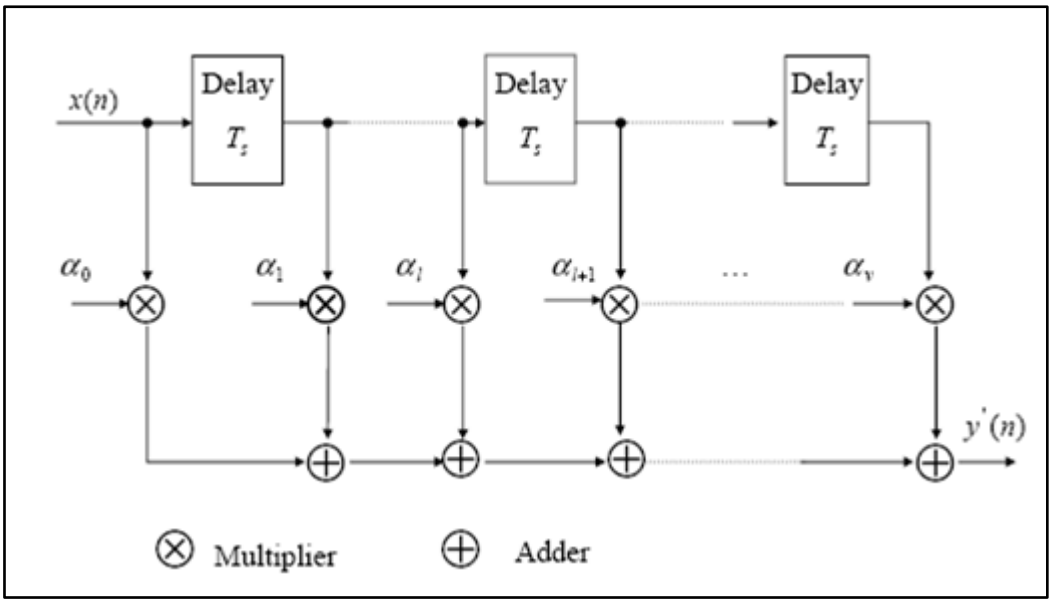

Figure (2.7): A multi-path fading channel model[28].

There are various discrete multi-path channel models for indoor and outdoor cellular systems with different cell sizes have been specified. These channel models define the statistics of the discrete propagation paths. Examples for such models are COST207, COST231, COST273, CODIT, JTC, UMTS/UTRA, and HIPERLAN/2[28].

Table (2.1) lists the corresponding path delay, and power profile for COST207 model as a selected example for the above mentioned models. Hilly terrain causes the longest echoes. The COST207 channel models are based on the channel measurements with bandwidth of 8-10 MHz in the 900MHZ band used for 2G systems such as GSM[28].

Table (2.1) Settings for the COST207 channel models

Path #	Rural area (RA)		Typical urban (TU)		Bad urban (BU)		Hilly terrain (HT)	
	delay	power	delay	power	delay	power	delay	power
	in μsec	in dB	in μsec	in dB	in μsec	in dB	in μsec	in dB
1	0	0	0.2	-3	0	-2.5	0	0
2	0.1	-4	0.5	0	0.3	0	0.1	-1.5
3	0.2	-8	0.5	-2	1.0	-3	0.3	-4.5
4	0.3	-12	1.6	-6	1.6	-5	0.5	-7.5
5	0.4	-16	2.3	-8	5.0	-2	15.0	-8.0
6	0.5	-20	5.0	-10	6.6	-4	17.2	-17.7

2.5 Multiple Access Techniques

Multiple access is an essential scheme for wireless communication that enables several users to transmit signals simultaneously without interfering with one another's transmissions. Several distinct varieties of multiple access techniques will exist like TDMA, FDMA, and CDMA[29].

2.5.1 Time Division Multiple Access (TDMA)

Time Division Multiple Access (TDMA) is a digital modulation technology used in digital cellular telephone and mobile radio transmission. TDMA is one of the two methods for dividing the limited spectrum available on a Radio Frequency (RF) cellular channel[11].TDMA divides the available channel into distinct time slots, allowing several users to share the same frequency based on the time, as shown in Figure (2.8.a).

2.5.2 Frequency Division Multiple Access (FDMA)

FDMA divides the transmission channel into several sub-channels. Sub-channels are allocated to users so that each user gets a sub-channel for transmission and reception, as shown in Figure (2.8.b). FDMA is used in the Global System for Mobile Communications (GSM). FDMA technology is inefficient because when the user is inactive, the user-specific sub-channel cannot use, and therefore the efficiency of the frequency spectrum is reduced[30].

2.5.3 Code Division Multiple Access (CDMA)

In the CDMA technique, users simultaneously transmit data using spread spectrum methods so that the entire bandwidth is used. CDMA is a method through which clients share time and frequency allocations and is channelized by codes that are uniquely issued to them, as shown in Figure (2.8.c). At the receiver, the correlator uses the same code that is used on the transmitter side to separate the user' data [23].

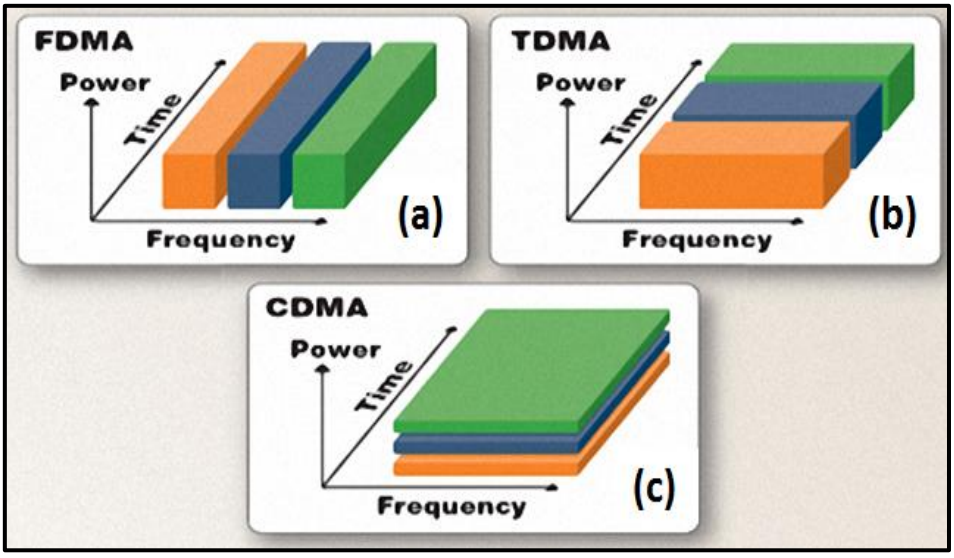

Figure (2.8): Multiple Access Techniques, (a) FDMA, (b) TDMA, and (c) CDMA.

2.6 Orthogonal Frequency Division Multiple Access (OFDMA)

OFDM (Orthogonal Frequency Division Multiplexing) system divides the initial bandwidth into many subcarriers. Every one of these subcarriers can be separately modulated. OFDM systems generally provide hundreds of subcarriers separated by content spacing. Due to the transmission of many subcarriers in parallel in OFDM, every subcarrier can transmit with a lower symbol rate. That improves the robustness of the technology in mobile propagation circumstances[31].

Producing an OFDM signal begins by blocking the symbols that must be transmitted after they have been modulated. They serve as input blocks for an inverse fast Fourier transform. This procedure generates the OFDM symbols that will be transmitted. When the IFFT is utilized, symbols are converted from the frequency domain to the time domain. However, a cyclic prefix is included in the OFDM signals before transmission to avoid inter-symbol interference. The receiving side of the OFDM system should contain an FFT operation to transform the symbol back to the frequency domain[17].

The major difference between an OFDM and an OFDMA (Orthogonal Frequency Division Multiple Access) systems is that in the OFDM, users are distributed only by time. In contrast, in the OFDMA, users are allocated by both time and frequency, as shown in Figure (2.9)[31].

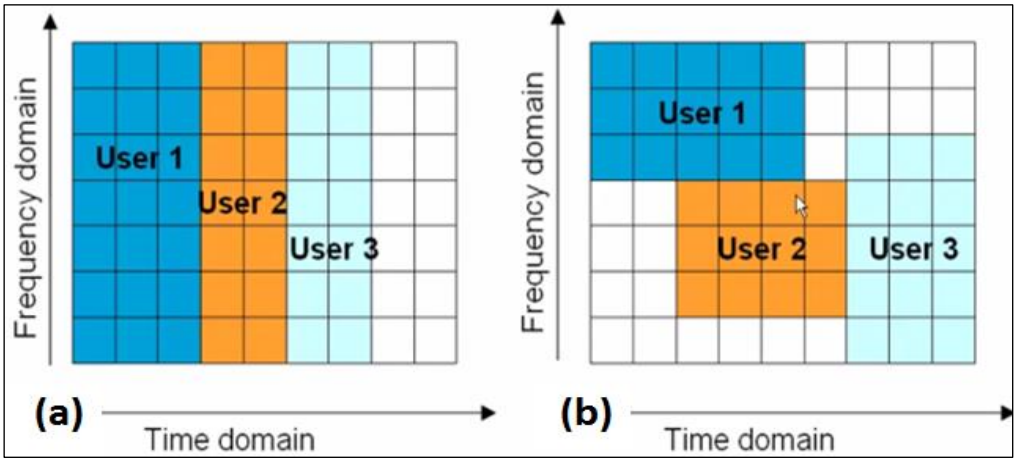

Figure (2.9): allocating resources to users, (a) OFDM, (b) OFDMA

- **Benefits**

The following are some benefits of the OFDMA technique[15]:

- ❖ The ability to overlap transmissions allows for more efficient use of the spectrum.
- ❖ OFDMA is more resistant to frequency selective fading due to the fact that it divides the channel into narrowband flat fading sub-channels.
- ❖ Utilizes a cyclic prefix, which results in the elimination of ISI.
- ❖ Channel equalization is performed, which involves less complexity which is in the frequency domain.
- ❖ OFDMA achieves a high level of computing efficiency by employing FFT algorithms to implement the modulation and demodulation processes.

- **Drawbacks**

The following are some drawbacks of the OFDMA technique[32]:

- ❖ As a result of the fact that the OFDMA technique has a high peak-to-average power ratio, there is a requirement for a high-powered signal amplifier; therefore, it is not employed in 4G uplink transmission.
- ❖ Because the DFT leaks, the OFDMA strategy is more sensitive to carrier frequency offset and drift than single carrier systems.
- ❖ The many paths that the OFDMA spectrum goes over require guard bands to eliminate timing offsets that could cause interference (ISI). Using a cyclic prefix made the spectrum less efficient.

2.7 Single-Carrier Frequency Division Multiple Access (SC-FDMA)

Many base stations offer wireless communication services in a specific geographic region in cellular systems. Uplink and downlink transmission are two types of communication that take place between the base station and users. In downlink transmission, a base station broadcasts signals simultaneously to numerous clients' devices in its service region. As a result, the base station must have a very high transmission power capacity to support this functionality. Concerning uplink transmission, the user can access all available transmission energy for sending data to the base station[13].

Two essential requirements must be satisfied in the uplink for the transmission to succeed. The first of these is the utilization of high-efficiency multiple access technologies. That is connected to the fact that the transmission in the uplink is a transmission from various devices to the base station. Secondly, the signal transmitted by users has a few peak values since the devices' transmission power capacity is limited[32].

One of the primary technologies used in the uplink is OFDMA, a novel variation of OFDM that enables numerous users to share communication resources. OFDMA technology is presently used in both IEEE 802.11 and IEEE

802.16 because of its many benefits, including high spectrum efficiency and fast data transmission with a low data error rate. In any case, because OFDMA employs a multi-carrier transmission method for transmission, this technology suffers from a higher PAPR problem[33].

The Third Generation Partnership Project (3GPP) consortium proposed a potential approach to overcome the OFDMA PAPR problem. This approach depends on spreading the modulated signal in the baseband before applying OFDMA using Discrete Fourier Transform (DFT), which results in lesser envelope fluctuation than OFDMA fluctuation. The 3GPP proposed technique is called Single-Carrier Frequency Division Multiple Access (SC-FDMA)[14].

2.7.1 SC-FDMA Structure

The SC-FDMA schematic diagram is depicted in Figure (2.10). Assuming there is a single basestation and U uplink user. Based on the modulation schemes, the encoded data is converted to a multi-level sequence of complex symbols at the transmitter side. The modulated complex symbols are then arranged into M-symbol blocks, and the DFT is applied to each block [34]. It is possible to give the following representation of the signal after DFT:

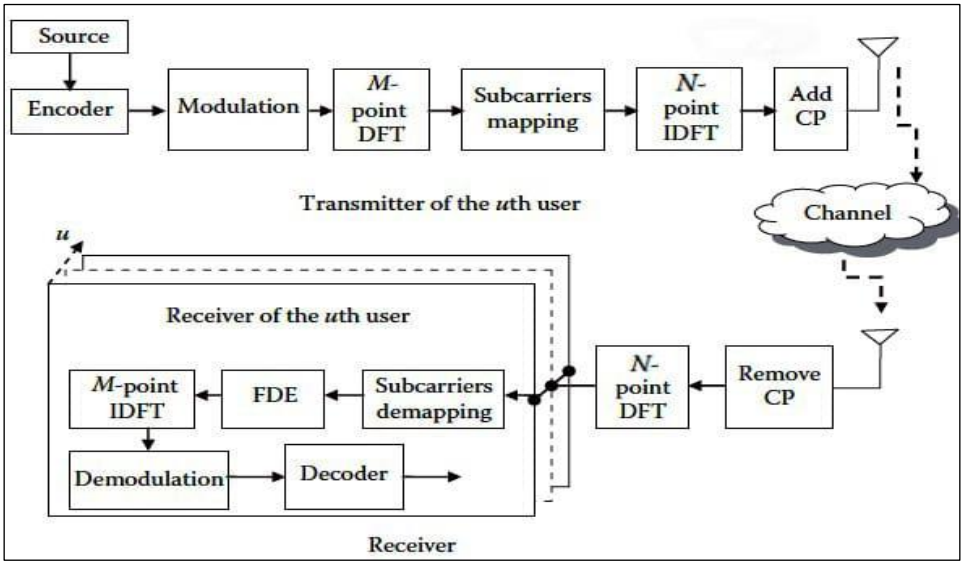

Figure (2.10): SC-FDMA system construction [34].

$$X(k) = \sum_{m=0}^{M-1} x(m) e^{-\frac{j2\pi mk}{M}} \quad \dots (2.9)$$

Where:

M represents the size of the input block

$\{x(m) : m=0,1,2,\dots, M-1\}$ represents the modulated complex data symbols

The time-domain complex symbols are generated after mapping the DFT output to N (N>M) perpendicular subcarriers and using an N-IDFT [34].

The maximum number of users that can be transmitted simultaneously can be represented as follows:

$$Q = \frac{N}{M} \quad \dots (2.10)$$

Where:

Q : represents the maximum number of users that the system can support.

M: represents the input block size and the number of subcarriers allocated for each user.

N: represents the total subcarrier in addition to the size of IDFT

Note that other users may use (N - M) subcarriers. Therefore, multiple access is achieved; sometimes, the remaining subcarriers are zero padding.

The resulting signal after the IDFT can express as follow:

$$\bar{x}(n) = \frac{1}{N} \sum_{l=0}^{N-1} x(l) e^{\frac{j2\pi nl}{N}} \quad \dots (2.11)$$

Where:

x(l): Indicates samples in the spectral domain that resulted after mapping the subcarriers.

$\bar{x}(n)$ Represents the IDFTs' output samples.

Another process is performed before the signal is sent over the wireless channel, which is the addition of the cyclic prefix. The cyclic prefix copies a portion of the block's end and pastes it at the beginning of the block to give guard time for each block and prevent block interference due to the multi-path

effect[4]. Next, the cyclic prefix is eliminated from the received data and converted into the spectrum range using N-DFT. The subcarriers de-mapping and FDE operations are then carried out. Next, M-IDFT is used to transform the equalized signal into a time range, where demodulation and decoding may take place[31].

The signal obtained after CP removal looks like this:

$$r = \sum_{u=1}^{U} H_c^u \bar{x}^u + n \quad \ldots (2.12)$$

Where:

$\bar{x}^u$ is an $N \times 1$ vector representing the block of symbols transmitted by the *u*th user.

n is the $N \times 1$ vector of additive white Gaussian noise (AWGN) with zero mean and variance σ_n^2.

H_c^u is an $N \times N$ circulant channel matrix.

circulant channel matrix is given as follows:

$$\boldsymbol{H_c^u} = \begin{bmatrix} \boldsymbol{h^u}_{[0]} & \mathbf{0} & \cdot & & \mathbf{0} & \boldsymbol{h^u}_{[L-1]} & \cdot & \boldsymbol{h^u}_{[1]} \\ \cdot & \boldsymbol{h^u}_{[0]} & \cdot & & \cdot & \cdot & \cdot & \boldsymbol{h^u}_{[L-1]} \\ \cdot & \cdot & \cdot & & \cdot & \cdot & \cdot & \cdot \\ \boldsymbol{h^u}_{[L-1]} & \cdot & \cdot & & \cdot & \cdot & \cdot & \cdot \\ \mathbf{0} & \cdot & \cdot & & \cdot & \cdot & \cdot & \cdot \\ \cdot & \cdot & \cdot & & \cdot & \cdot & \cdot & \cdot \\ \mathbf{0} & \cdot & \mathbf{0} & & \boldsymbol{h^u}_{[L-1]} & \cdot & \cdot & \boldsymbol{h^u}_{[0]} \end{bmatrix} \quad \ldots (2.13)$$

The circulant matrix H_c^u might be diagonalized efficiently via the DFT (F) and the IDFT ($\bar{F}$). It might be represented as below:

$$H_c^u = \bar{F}\ \Lambda^u\ F \quad \ldots(2.14)$$

Such that Λ^u is an $N \times N$ diagonal matrix including the DFT of the circulant sequence of H_c^u . the DFT(F) is the Frequency domain of H_c^u, and IDFT ($\bar{F}$) is the time domain of H_c^u.

Since there is no interference between users, the $M \times 1$ received block for the *u*th user in the frequency domain is given by:

$$R_d = \Lambda_d^u F_N^{-1} X^u + N \quad \ldots(2.15)$$

Where:

Λ_d^u is the M × M diagonal matrix containing the channel frequency response associated with the *N* subcarriers allocated to the *u*th user.

X^u is the M × 1 vector containing the data symbols of the *u*th user**.**

F_N^{-1} is the M × M DFT matrix.

N is the M × 1 frequency-domain noise vector**.**

2.7.2 SC-FDMA Benefits

The following is a list of benefits that the SC-FDMA system offers:

- SC-FDMA can provide multiple access to share the communication resources without interfering by assigning specific subcarriers to each user [34].
- If the cyclic prefix length exceeds the channel's response, the SC-FDMA system ensures orthogonality between clients via a multipath medium[35].
- Compared to the OFDMA structure, the PAPR for the SC-FDMA model is significantly lower [5].
- SC-FDMA can use the simple equalizer in the frequency domain [34].
- The SC-FDMA model is less susceptible to frequency nulls[29].

2.7.3 SC-FDMA Drawbacks

The following are some drawbacks of the SC-FDMA technique[34]**:**

- SC-FDMA is more sophisticated than the OFDMA system. It needs an extra DFT procedure with a variable size depending on the assigned subcarriers' number on the transmitter end. On the receiving end, an extra IDFT process is required.

- At the linear receiver, noise is amplified. After the IDFT block and equalization, the noise component of the fading subcarriers is spread out over the entire bandwidth and enhanced.
- The SC-FDMA technique is susceptible to carriers' frequency offsets.

2.7.4 Sub-Carrier Mapping Approaches

Localized and distributed mapping are two approaches to map sub-carriers across users. The first method is typically named the localized Frequency Division Multiple Access (LFDMA) scheme, whereas the second is known as a Distributed Frequency Division Multiple Access (DFDMA) transmission scheme. In the LFDMA mapping method, modulation symbols are assigned to M consecutive subcarriers. In the DFDMA, the symbols are equally spaced across the entire channel bandwidth. The DFDMA system is more resistant to frequency-selective fading since the information symbol is spread across the whole signal spectrum. It can therefore attain greater frequency diversity. In the LFDMA approach and across a frequency selective medium, multi-user and frequency selective variety may be obtained if each node has subcarriers with desirable transmission qualities[36].

Interleaved FDMA (IFDMA) refers to the distributed FDMA method with equal distance between occupied subcarriers over the whole band. IFDMA offers low PAPR at the expense of higher susceptibility to phase noise and carrier frequency offset. The LFDMA method is more resistant to Multiple Access Interference (MAI) than the IFDMA system but contains a larger PAPR. The IDFT allocates zero amplitude to the (N-M) left empty subcarriers or assigned to another user[37].

The SC-FDMA system has three distinct subcarrier mapping modes as depicted in Figure (2.11). The size of the input block is M=4 which means four complex symbols in each block, the total orthogonal subcarrier is N=12, and the

bandwidth spreading factor Q=N/M=3. With Q=3, the system supports three users to transmit simultaneously. In the LFDMA method, the four frequency domain complex symbols load to the subcarriers 0,1,2 and 3: $Y_0 = X_0$, $Y_1 = X_1$, $Y_2 = X_2$, $Y_3 = X_3$, and $Y_i = 0$ for $i \neq 0,1,2,3$. In the DFDMA type, the complex symbols are separated by equal spaces overall subcarriers $Y_0 = X_0$, $Y_2 = X_1$, $Y_4 = X_2$, $Y_6 = X_3$, the rest of the subcarriers are zeros and in interleaved mode $Y_0 = X_0$, $Y_3 = X_1$, $Y_6 = X_2$, $Y_9 = X_3$.

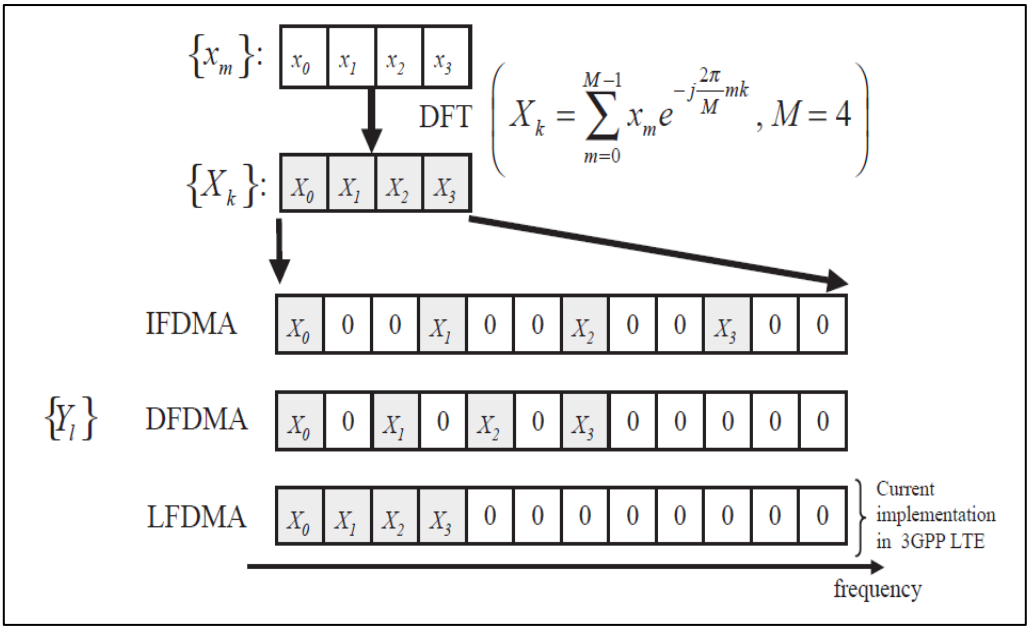

Figure (2.11): Various Subcarrier Mapping modes for M=4, N=12, Q=3[4].

For two users with *M*=4, *N*=12, and *Q*=3, the subcarrier mapping methods are shown in Figure (2.12). In the localized type: the first four subcarriers are allocated to the first user, the second four subcarriers are assigned to the second user, and so on; if there are other users since there are only two users, so the rest of the subcarriers are zeros. As for the distributed type, subcarriers are allocated to users alternately. In this illustrative example, the first subcarrier is assigned to the first user, the second is assigned to the second user, and so on. As for the interleaved mode, each user gets on its subcarriers after Q.

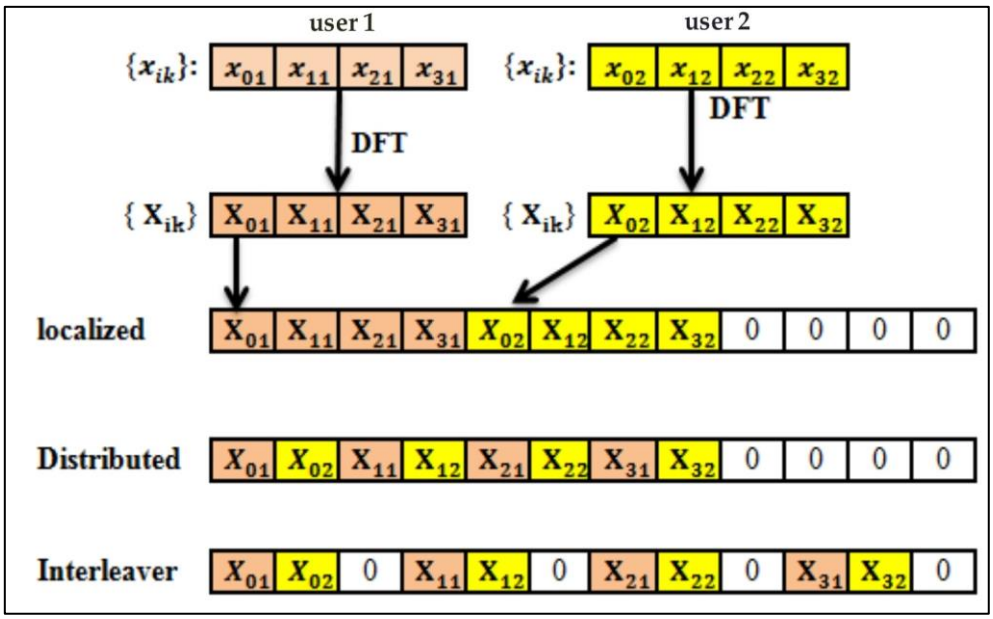

Figure (2.12): An illustrate case of various subcarrier mapping models for two user, $M = 4$, $Q = 3$, and $N = 12$.

2.7.5 Frequency Domain Equalization (FDE)

An equalizer compensates for linear distortion introduced by the multipath propagation channel. For broadband channels, conventional time domain equalizers are impractical because of the very long channel impulse response in the time domain. Frequency domain equalization (FDE) is more practical for such channels.

Channel equalization is essentially an inverse filtering of the linear distortion introduced to the channel by the multipath propagation. From a linear time invariant system perspective, linear filtering is a convolution operation in the time domain and a point-wise multiplication operation in the frequency domain. The Fourier transform, converts the time domain signal to a frequency domain signal, which can be equalized by dividing it point-by-point by an estimate of the channel frequency response. Figure (2.13) shows the basic operation of time domain equalization (convolution) and frequency domain equalization (point-wise multiplication).

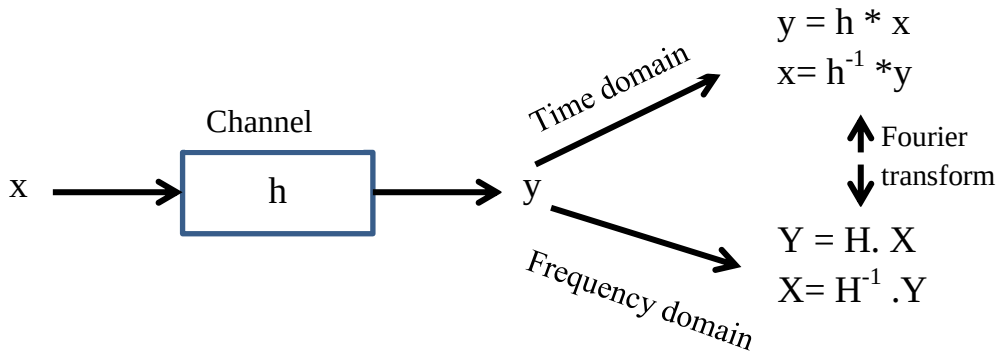

Figure (2.13): Basic idea behind FDE [4]**.**

Using DFT, frequency domain equalization can be easily implemented using modern digital signal processors (DSP). Because the DFT size does not grow linearly with the length of the channel response, the complexity of FDE is much lower than that of the equivalent time domain equalizer for broadband channels.

Single carrier modulation with frequency domain equalization (SC/FDE) is a practical technique for mitigating the effects of frequency-selective fading. It delivers performance similar to OFDM with essentially the same overall complexity, even for a long channel impulse response[4].

2.8 Spread-Spectrum Technology

Primarily developed spread-spectrum technology for military and navigation purposes due to its unique characteristics that enable secure communication in hazardous environments[1]. Spread spectrum signals have Low Probability of Intercept (LPI) qualities, which means they have a low probability of being intercepted by an adversary's communication devices. That is because spread spectrum signals have a low power spectral density, even lower than the background noise level. Spread-spectrum signals provide effective Anti-Jamming (AJ) qualities, which enable them to defend against unwanted interference that reduces the effectiveness of the CDMA system[38].

In modern times, spread-spectrum technology offers practical multiple access for several users who share a single communication channel without needing extra synchronization processes[38].

CDMA is most likely the multiple access mechanism available by spread-spectrum technology. Spread-spectrum communication is based on the principle of spreading a fixed information bandwidth, denoted by B_i, across a somewhat larger transmission bandwidth, denoted by B_t [39].

Direct Sequencing (DS), Frequency Hopping (FH), and Time Hopping (TH) are the three fundamental spread-spectrum techniques. Additionally, several hybrid techniques employ various combinations of these fundamental techniques[40].

2.8.1 Direct Sequence Spread Spectrum (DSSS)

The direct sequence spread spectrum technique is today's most common spread spectrum technique because it is simple and easy to implement. The spreading feature of the DS-SS is achieved by modulating a lower bandwidth data signal with a wide bandwidth spreading signal. DSSS is a method of transmission that, throughout the bandwidth of the transmission, appears in a manner that is close to white noise. The main idea of DSSS is multiplying the signal data with the spreading signal or what is known as a chip sequence, and the signal produced by the multiplication process has a higher bandwidth than the data signal[41]. The chip time interval in the spreading sequence has much lower than the bit time in the data signal. The ratio of the spreading rate R_c to the data rate R_b is known as the processing gain G_p and is given as[18]:

$$G_p = \frac{R_c}{R_b} \tag{2.16}$$

Where:

R_b = data rate.

R_c = spreading rate or chip rate.

The processing gain is an essential factor in spread spectrum technology because it determines the degree of interference r*-ejection. The higher processing gain leads to a decrease in interference. DSSS is a property of Dividing the channel based on the code (CDMA). The transmitter and receiver must use the same spreading code for data transmission. To show how the DSSS mechanism works, Figure (2.14) shows a simple example of sending and receiving data based on the principles of DSSS technology.

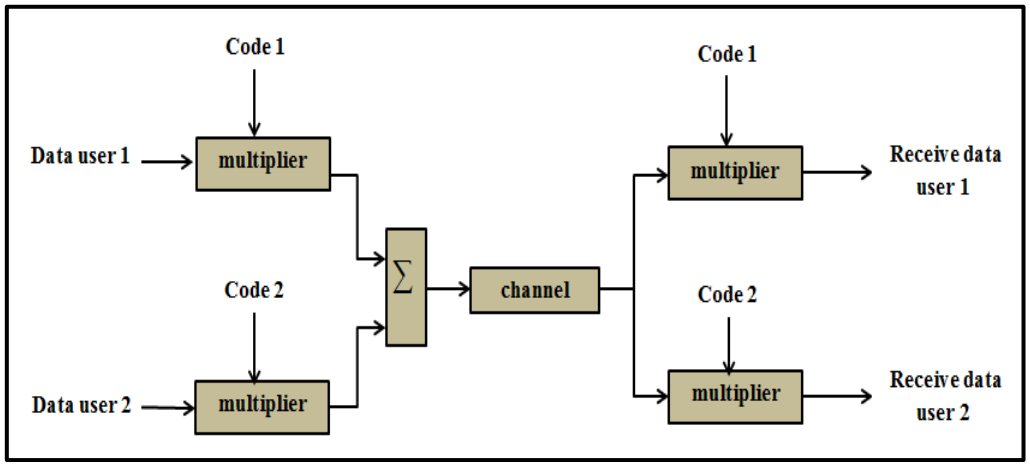

Figure (2.14): DSSS Transceiver

In the detailed example shown in Figure (2.14), two users want to send through one channel. Let's say the first user wants to send (-11) and the second (11). The spreading code assigned to the first user is (1 1 1-1 1 -1 -1 -1), which is code1and the spreading code assigned to the second user is (1 -1 1 1 1 -1 1 1), which is code2.

Firstly, the users' data are multiplied by the code assigned to each user on the transmitter side. Since the spreading code length assigned to each user is 8 bits, each bit of the user's data will be spread to 8 bits. After the users' data is spread, it is combined and transmitted through the channel. After receiving the data from the channel, it is multiplied by the same code assigned to each user to obtain the data of each user, as shown in Table (2.2).

2.8.2 Code sequences

The utilization of code sequences is crucial to any spread spectrum approach. In DSSS, a narrowband signal representing input data is multiplied with a code sequence at a significantly larger bit rate, resulting in a wideband signal[42]. The most commonly used code sequences are Maximum-length (m-sequences), Gold codes, Kasami sequences, Walsh-Hadamard sequences, and Orthogonal variable spreading factor (OVSF).

These codes are used in the spread spectrum to defend against jamming, and interference, protect signals from eavesdropping and allow several users to share the same resource. Application attributes strongly influence the design and selection of a code sequence[43].

Table (2.2): DSSS technique illustration

Data User 1	-1								1							
Code1	1	1	1	-1	1	-1	-1	-1	1	1	1	-1	1	-1	-1	-1
Spreading User1	-1	-1	-1	1	-1	1	1	1	1	1	1	-1	1	-1	-1	-1
Data User2	1								1							
Code2	1	-1	1	1	1	-1	1	1	1	-1	1	1	1	-1	1	1
Spreading User2	1	-1	1	1	1	-1	1	1	1	-1	1	1	1	-1	1	1
Transmitted Data	0	-2	0	2	0	0	2	2	2	0	2	0	2	-2	0	0
Channel	Ideal															
Received Data	0	-2	0	2	0	0	2	2	2	0	2	0	2	-2	0	0
Despreading User1	0	-2	0	-2	0	0	-2	-2	2	0	2	0	2	2	0	0
Data User 1	-8/8=-1								8/8=1							
Despreading User2	0	2	0	2	0	0	2	2	2	0	2	0	2	2	0	0
Data User2	8/8=1								8/8=1							

2.8.2.1 m-sequences

A binary sequence called an m-sequence might be created using an Linear Feedback Shift Register (LFSR) and an initial value. Its autocorrelation characteristics are similar to white noise. Correctly connecting the feedback points allows the LFSR's m registers to create sequences up to 2^m-1. The LFSR

generates a sequence where the number of ones is one bit larger than the number of zeros[25].

The LFSR construction is described by generating polynomial[44]. The LFSR connection is based on generating polynomial $g(x)$ is shown in Figure (2.15) and equation 2.17.

$$g(x) = x^m + x^{m-1} + x^{m-2} + \cdots + x^2 + 1 \qquad (2.17)$$

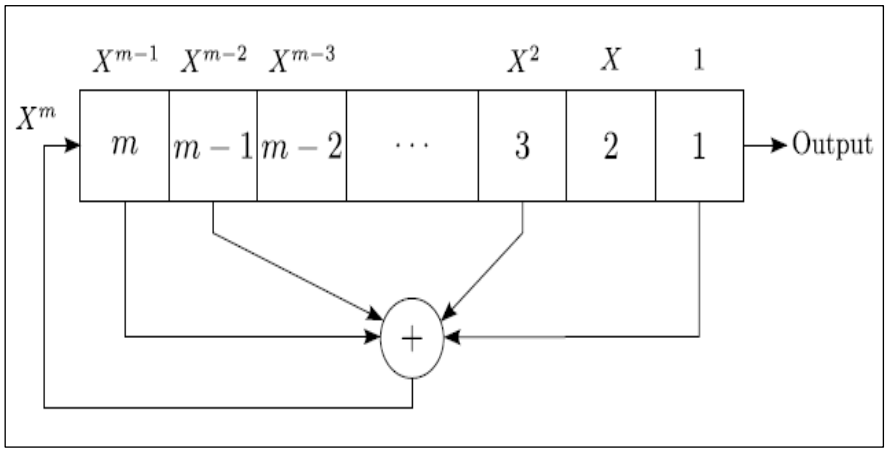

Figure (2.15): LFSR connected based on the generator polynomial g(x)[45].

2.8.2.2 Gold Codes

The Gold sequence set is one of the most well-known binary sequences with good correlation values. A set of Gold sequences is created from a preferred pair of m-sequences, x and y, with similar length Q, and the period of the Gold sequences generated by x and y is also Q. Every Gold sequence in a set is produced by cyclic shifts of y and a modulo-2 sum (XOR) of x. The m-sequences x and y are also included in the set. The whole collection of Gold sequences with a period of Q is given by.

$$Sg = \{x, y, x \oplus y, x \oplus T^{-1}y, x \oplus T^{-2}y, \ldots, x \oplus T^{-(Q-1)}y \qquad \ldots(2.18)$$

where $T^q y$ for $q=1, 2, \ldots..$ Q -1, represents a cyclic shift of y by q chip intervals; and the symbol $\oplus$ represents modulo-2 addition[Dr Osamah][46].

2.8.2.3 Kasami Sequences

Kasami sequences are constructed in the same way that Gold sequences are. The modulo-2 sum of an m-sequence and cyclic shifts of a sequence derived from the original m-sequence yields a Kasami code. The derived sequence is obtained by decimating and replicating the original m-sequence. Kasami codes provide cross-correlation lower than the gold codes [46].

2.8.2.4 Walsh-Hadamard Sequences

Orthogonal codes are easily generated by generating the so-called Walsh matrix. The Walsh Matrix is generated using a seed of zero where the seed is repeated horizontally and vertically, and the complement of the seed completes the diagonal as follows:

$$W_{2n} = \begin{bmatrix} w_n & w_n \\ w_n & \overline{w}_n \end{bmatrix} \quad \ldots(2.19)$$

beginning with w_1 = [0]. The logical complement matrix of w_n is $\overline{w}_n$. To create antipodal codes, simply replace all 0s against -1s.

The Walsh matrix is an M*M matrix (M is powers of 2). Each resulting matrix is treated as a seed, and the same previous generation steps are repeated to obtain other codes of different lengths. The rows of a Walsh matrix are orthogonal so that the dot product between any two codes (c_i and c_j) is zero, where each row can be set as a spreading code for a specific user [47]:

$$c_{i,n} . c_{i,n} = \sum_{n=1}^{N} c_{i,n}\ c_{j,n} = 0;\ \ i \neq j \quad \ldots(2.20)$$

2.8.2.5 Orthogonal variable spreading factor (OVSF)

Orthogonal variable spreading factor (OVSF) channel allocation codes are frequently utilized to support varied data rates in order to accommodate a variety of bandwidth requirements. An example of a code tree showing potential OVSF codes is provided in Figure (2.16). In the OVSF code tree, channelling codes have their unique description, written as $c_{SF,K}$ Where SF stands for the

code spreading element, and K represents the code number. All Channelization codes, whether equal in length or unequal, are orthogonal, provided that neither of them is a parent or offspring of the other[23].

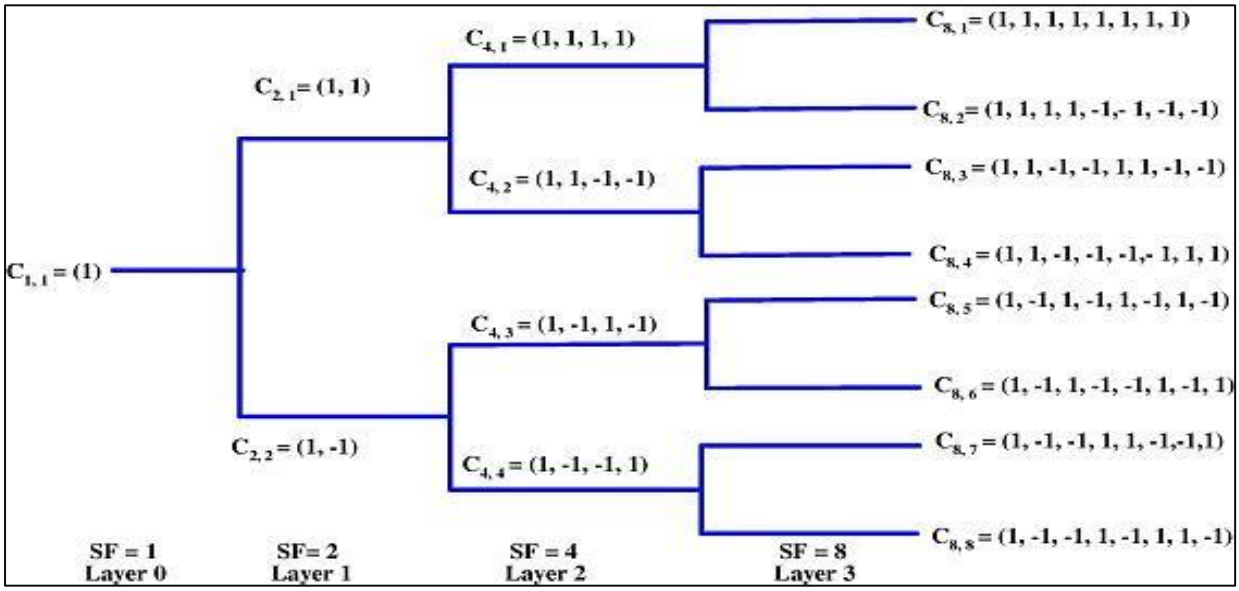

Figure (2.16): OVSF code-tree.

2.9 Peak to Average Power Ratio (PAPR)

The PAPR is the ratio of peak to average power. It is considered an essential factor in up-link transmission, typically measured for the transmitted signal. The peak signal-to-average ratio is regarded as one of the crucial topics that attracted researchers because of its impact on the transmitter power efficiency. The higher value of the peak-to-average ratio leads to lower transmitter efficiency, increasing the data error rate. The following expression can describe the theoretical relation between PAPR (in dB) and transmit power efficiency.

$$\eta = \eta_{max} \cdot 10^{-\frac{PAPR}{20}} \quad \ldots(2.21)$$

Where η refers to power efficiency and η_{max} to maximum power efficiency. From the relation shown in eq.2.21, it's clear that when the PAPR increases, the transmit power efficiency decreases [4]. The peak-to-average ratio for the transmitted signal x(t) can be shown in equation (2.22):

$$PAPR = \frac{peak\ power\ of\ x(t)}{average\ power\ of\ x(t)} = \frac{Max_{0\le t\le NT}|x(t)|^2}{(\frac{1}{NT})\int_0^{NT}|x(t)|^2 dt} \quad \ldots(2.22)$$

The PAPR Without pulse shaping, symbol rate sampling will give the same PAPR as the continuous. Thus, it can express the PAPR in decibel (dB) without a pulse shaping with the symbol rate sampling as follows [34]:

$$PAPR = 10\log_{10}\frac{max|x(n)|^2}{E\{|x(n)|^2\}} \quad \ldots(2.23)$$

where E {.} represents the mean value of the signal. Furthermore, a popular method for determining PAPR output is the CCDF (Complementary Cumulative Distribution Function). The CCDF based on PAPR denotes the probability that the PAPR value exceeds a certain threshold (PAPR0) [12].

$$P_r(PAPR > PAPR_0) = 1 - \ (1 - \exp(-PAPR_0))^N \quad \ldots(2.24)$$

Where N is the total subcarriers used to transmitted the OFDMA symbols.

The performance of the entire system and the difficulty and expense of installing the transmitter are all impacted by a high PAPR. Signals are sent to the base station during the uplink from all of the regional devices. That calls for an access method that guarantees the device's transmitting power is high enough to send a signal to the base station. The device needs a vast power amplifier with a large linear area if the value of PAPR is high. It has been discovered that reduced PAPR results in improved power efficiency, which boosts battery consumption for a longer time[48].

OFDMA employs several carriers, each transmitting data at a low bit rate. Thus, it effectively utilizes the spectrum, interference, and selective fading. The PAPR is high in OFDM due to the linear combination of many modulated symbols in the IFFT operation[15]. When the number of modulated symbols (i.e., total subcarriers) connected to the IFFT process increases, this leads to an increase in the value of the PAPR, as shown in Figure (2.17).

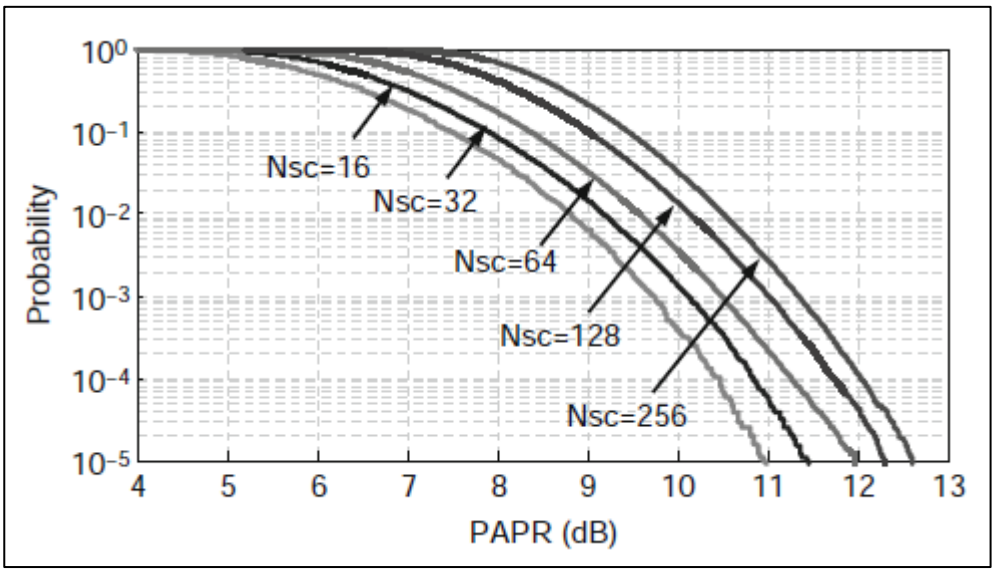

Figure (2.17): the CCDF curves of the OFDMA PAPR under many number of subcarriers.

One of the essential solutions to get rid of the problem of PAPR is presented by 3GPP. This solution suggests applying the Discrete Fourier Transform (DFT) to spread the baseband signal prior to applying the OFDMA modulator, resulting in a reduction in the envelope fluctuation compared to OFDMA. The method provided by 3GPP is named SC-FDMA. SC-FDMA transmissions have a lower PAPR than the typical OFDMA, which is a significant advantage. Because of this, SC-FDMA is used for 4G uplink transmission[49].

As said previously, the value of the PAPR is calculated in the transmission part. Figure (2.18) shows the diagram of the PAPR calculation of the OFDMA and SC-FDMA systems.

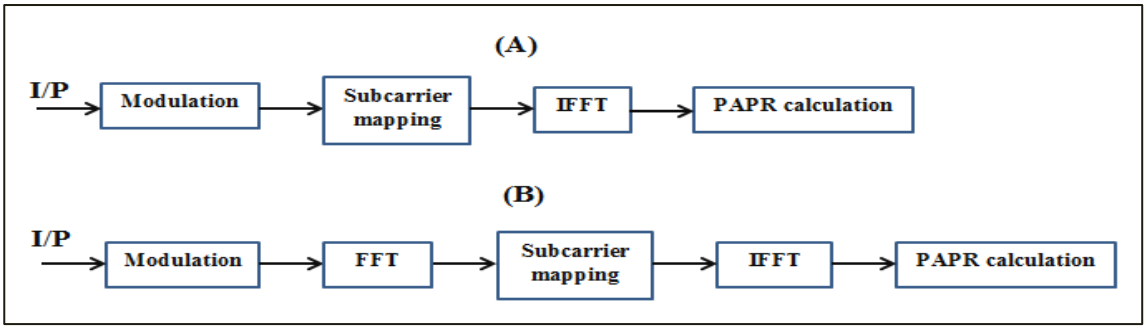

Figure (2.18): PAPR calculation diagram, (A) OFDMA, (B) SC-FDMA

Table (2.3) gives a detailed illustration of how SC-FDMA lowers PAPR values. In terms of calculating the PAPR performance using eq.2.23, the detailed example is like a comparison between OFDMA and SC-FDMA. The detailed example factors taken into account are: four symbols for ease, QPSK modulation, localized subcarrier mapping, and 8 total subcarriers.

Table (2.3): PAPR calculation of OFDMA and SC-FDMA systems

OFDMA system	
Input Data	1001
QPSK	-0.0000 - 1.0000i, 0.0000 + 1.0000i
Localized Mapping	-0.0000 - 1.0000i, 0.0000 + 1.0000i,0,0,0,0,0,0
IFFT	0.0000 + 0.0000i , -0.0884 - 0.0366i, -0.1250 - 0.1250i, -0.0884 - 0.2134i, 0.0000 - 0.2500i ,0.0884 - 0.2134i, 0.1250 - 0.1250i, 0.0884 - 0.0366i
PAPR (dB)	3.0103
SC-FDMA system	
Input Data	1001
QPSK	-0.0000 - 1.0000i, 0.0000 + 1.0000i
FFT	-0.0000 + 0.0000i, -0.0000 - 2.0000i
Localized Mapping	-0.0000 + 0.0000i, -0.0000 - 2.0000i,0,0,0,0,0,0
IFFT	0.0000 - 0.2500i , 0.1768 - 0.1768i, 0.2500 + 0.0000i , 0.1768 + 0.1768i, 0.0000 + 0.2500i , -0.1768 + 0.1768i, -0.2500 + 0.0000i , -0.1768 - 0.1768i
PAPR (dB)	0 (because Peak=Mean)

2.10 Digital Modulation Techniques

There are three primary classes of digital modulation techniques used to transmit digitally encoded data: ASK, PSK, and FSK. The base signal's amplitude, frequency, or phase is changed to modulate the data in reaction to the information signal. The phase of the base signal is changed to express the data signal in PSK[50].

A constellation diagram is a simple way to illustrate PSK schemes, as it displays the points in the complex plane where the real and imaginary axes are

referred to as the in-phase and quadrature axes due to their 90° difference, as shown in Figure(2.19).

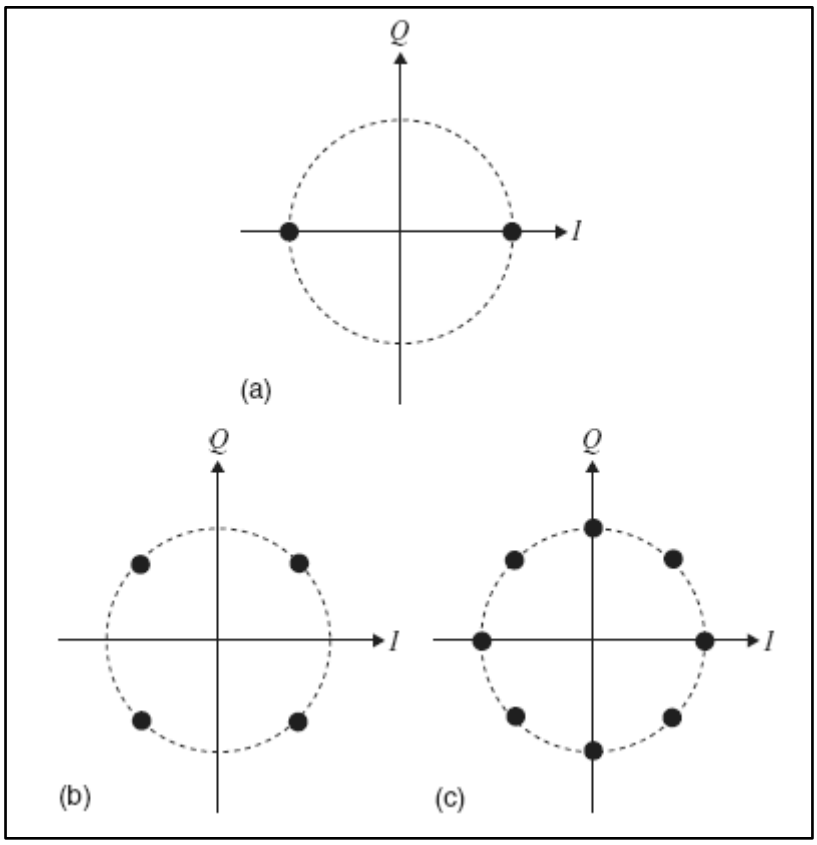

Figure (2.19): PSK constellations. (a) BPSK M = 2, (b) QPSK M = 4 and (c) 8PSK M = 8.

In PSK, the constellation points are often arranged with uniform angular spacing around a circle, which provides the greatest phase difference between neighbouring points and, hence, the most resistance to corruption. Since the data to be conveyed are usually binary, the PSK scheme is usually designed with the number of constellation points being a power of two[50].

The basic form of phase shift keying is known as Binary Phase Shift Keying (BPSK), or it is occasionally called Phase Reversal Keying (PRK). A digital signal alternating between +1 and -1 (or 1 and 0) will create 180-degree phase shifts as the data shifts state, as shown in Figure (2.20).

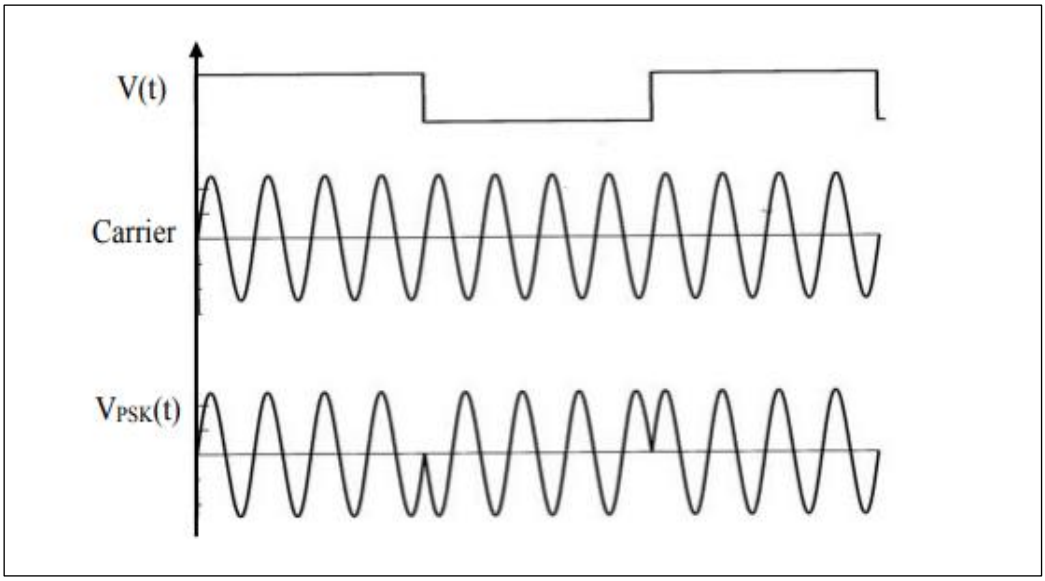

Figure (2.20): BPSK modulation.

In the proposed work, QPSK and 16 PSK are used as digital modulation techniques. QPSK modulation consists of two BPSK modulations on in-phase and quadrature components of the signal and the BER equation for QPSK modulation is given by:

$$BER_{QPSK} = Q\left(\sqrt{\frac{2E_b}{N_0}}\right) \quad \ldots(2.25)$$

Where $Q \approx \frac{1}{x\sqrt{2\pi}} \exp(\frac{-x^2}{2})$ is the complementary error function of a normal distribution, E_b is the signal energy per binary symbol, and N_0 is a single-sided noise power spectral density.

CHAPTER THREE

SC-FDMA-DSCDMA PROPOSED SYSTEM

CHAPTER THREE

SC-FDMA-DSCDMA PROPOSED SYSTEM

3.1 Introduction

This chapter is divided into three main sections. A simulation of the OFDMA system is shown in the first section. The second is a simulation of the SC-FDMA system, while the third is a simulation of the SC-FDMA-DSCDMA system. The simulation of these algorithms is carried out using the Matlab program.

Each simulation employed two modulation schemes (QPSK, 16PSK) with two kinds of sub-carrier mapping (localized and interleaved). Also, two models of the communication channel have been implemented (AWGN, Rayleigh), with multiple types of code sequences (Walsh-Hadamard sequences, OVSF codes, Maximum-length sequences "m-sequences", and Gold codes). Simulations are done upon multiple users, up to 128 users.

3.2 OFDMA System

The OFDMA block diagram is shown in Figure (3.1). At the OFDMA transmitter, PSK mapping maps the binary information into the constellation. After that, The complex symbols resulting from the modulating process are converted from serial to parallel form. Next, the data is mapped on the subcarriers using localized or interleaved subcarrier mapping. Then, using a fast inverse Fourier transform will be converted the mapped symbols into the time domain. After then, the last portion of the data is appended to the beginning, known as the cyclic prefix (CP), which combats ISI. Last, The data is turned to the serial form and passed via the channel. After receiving the signal from the channel in the receiving section, the same previous procedures are done reverse, in addition to the presence of frequency domain equalization.

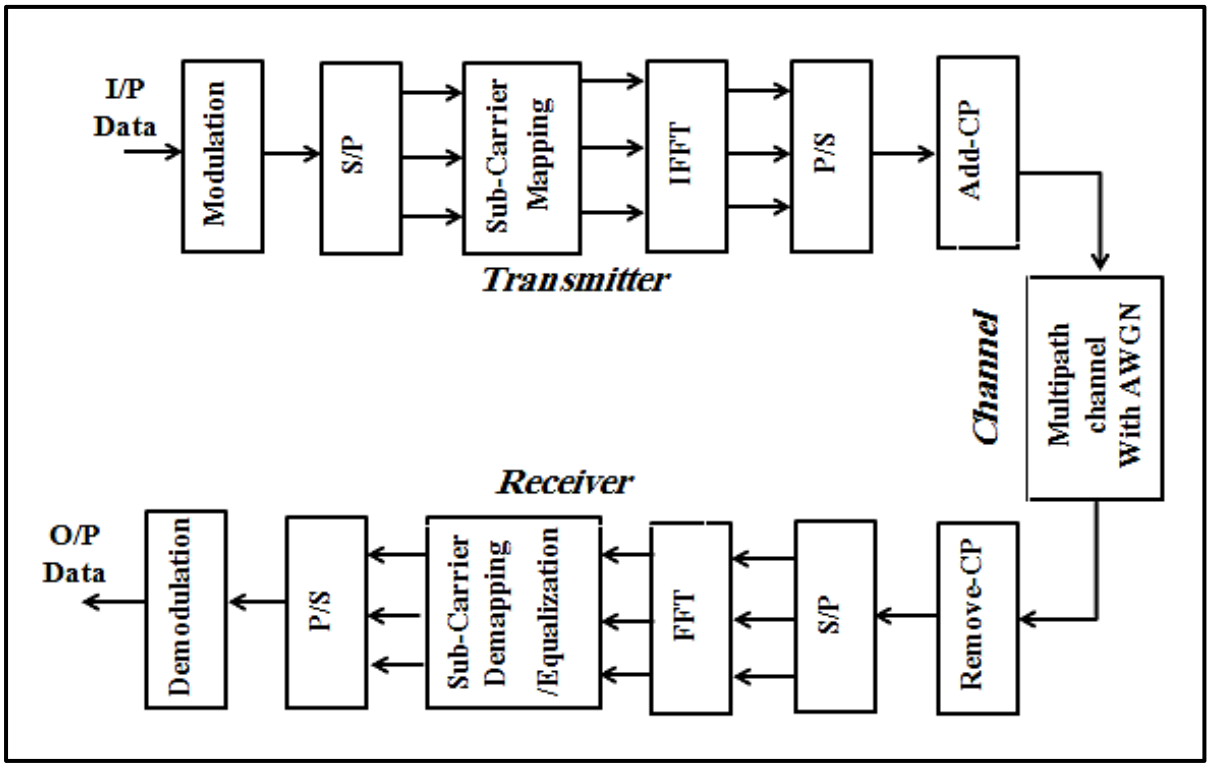

Figure (3.1): The OFDMA system block diagram.

3.2.1 The OFDMA Transmitter Section

As shown in Figure (3.1), OFDMA's transmission section consists of seven operations that will be explained how implemented in MATLAB program. There will also be an illustrative example on which all operations are based.

I. Input data (I/P)

Generally, to determine the performance of a communication system, a type of data is transmitted, and after receiving it, the system's performance is evaluated. In the Matlab program, data can be generated in several ways, whether it is digital or analog data.

In the simulation, random binary data is generated using the random function provided by the Matlab environment. The rand function generates random numbers with uniformly distributed elements.

Here is the beginning of the illustration example. Assuming 16000 bits of binary data is wanted to transmitting, the data can generate as follows.

```
data = randi([0 1],16000,1);                                    …(3.1)
```

The generated random data is a 16000-by-1 column vector of uniformly distributed samples from the interval [0,1], and as follows.

$$input\ data = \begin{bmatrix} bit_1 \\ \vdots \\ bit_{16000} \end{bmatrix}_{16000\times 1}$$

II. Modulation

Matlab provides a communications toolbox containing many specialized communication technologies, including all modulation types. In the simulation, QPSK and 16PSK were used as modulation methods. The process of modulation programmatically takes place in two steps. The first is to create an M-PSK Modulator object, which is in the following format:

hMod = comm.PSKModulator(M,'BitInput',true, 'PhaseOffset',pi/M); …(3.2)

M represents the modulation level, *BitInput* represents the input data type, and the *PhaseOffset* represents the phase shift between the complex symbols in the constellation. After creating the PSK modulation object, it can be called in the modulation process as follows:

txSigg=step(hMod,TX); …(3.3)

The step function represents the modulation step where *hMod* represents the M-PSK modulation object and *TX* represents the information to be modulated.

Let back to the illustrative example from the previous section. The previous process generated 16000 bits of binary data. Now the generated bits can be modulated using a QPSK modulation object, so the number of symbols produced after the modulating process is *16000/K*, where *K* represents the number of bits per symbol; therefore, *K =log2(M) = 2* bits per symbol. Finally, produced complex modulation symbols are 8000, as follows.

$$modulated\ data = \begin{bmatrix} symbol_1 \\ \vdots \\ symbol_{8000} \end{bmatrix}_{8000\times1}$$

III. Serial to Parallel conversion (S/P)

This operation is done using the matrix reshaping function. The reshaping function reshapes the array from one shape to another, ensuring that it contains the same elements and starts the process from the columns. The reshaping function form that is used is as follows.

y= reshape(A, B, C) …(3.4)

Where A represents the matrix to be reshaped, B and C indicate the number of rows and columns in the resulting matrix, y.

From the previous section, the modulation process produced 8000 symbols. Now, using the reshaping function, symbols can be converted from serial to parallel form with rows equaling the number of subcarriers specified for the user, and columns ensure the presence of the rest elements. Suppose there are 128 subcarriers, and 16 of them are assigned to the user, so the data array size after the symbols conversion process is 16-by-500. This process is considered a conversion of symbols from serial to parallel, and at the same time, it is symbols blocked process as follows.

Block 1 ⋯ Block 500

$$\text{S/P}=\begin{bmatrix} symbol1 & \cdots & symbol1 \\ \vdots & \vdots & \vdots \\ symbol\ 16 & \cdots & symbol16 \end{bmatrix}_{16\times500}$$

IV. **Subcarriers mapping**

The subcarriers mapping is the process of assigning subcarriers for users. Two types of subcarrier mapping are used: localized and interleaved subcarrier mapping. The subcarrier mapping is implemented using array operations and will be illustrated by continuing the illustrative example from the previous step.

The symbols conversion process (or symbols blocked process) produced a data array of 16-by-500, where 16 denotes block size and 500 represents the total number of blocks. The subcarriers mapping process is simulated through the following steps:

❖ Using for loops to enable us to deal with each block individually. Therefore, the loop's iteration equals the number of blocks.

❖ Generate a 128-by-1 array of zeroes, where 128 is the number of subcarriers.

❖ In the localized mapping, 16 block symbols are placed contiguously on the first 16 subcarriers of the total subcarriers. The rest subcarriers are allocated to other users or padded to zero. Because there is just one user in our illustrative example, the first 16 of the 128 subcarriers are assigned to this user, as illustrated in Table(3.1). In interleaved subcarrier mapping, each symbol is mapped on the subcarrier after Q, where Q indicates the spreading factor, 128 divided by 16.

V. Inverse Fast Fourier Transform (IFFT)

The ifft(x) function provided by the Matlab program is used to perform the IDFT. The ifft function uses the inverse fast Fourier transform algorithm to calculate the IDFT of the input. The inverse fourier transform is performed on each column separately if the algorithm's input is an array and the output array has exact dimensions as the input array.

Let's continue with the illustrative example from the previous section. After the subcarrier mapping operation, the result is a vector of length 128 containing 16 symbols representing the first block of the first iteration. Inside the same

loop and after the subcarrier mapping for the same vector, the ifft(x) function is performed, so the output is a vector with the same input length, 128 symbols.

In this step, i.e., before the signal passes through the transmission channel, PAPR is calculated using the equation (2.21).

Table (3.1): Subcarriers mapping process

Number of sub-carrier	Localized mapping	Interleaved mapping
1	Symbol 1	Symbol 1
2	Symbol 2	0
.	.	.
9	Symbol 9	Symbol 2
10	Symbol 10	0
.	.	.
16	Symbol 16	0
17	0	Symbol 3
.	.	.
121	0	Symbol 16
.	.	.
128	0	0

VI. Add Cyclic Prefix (CP)

The cyclic prefix is the last part of the signal copied and pasted at the start. In the simulation, The cyclic prefix is added through array operations by selecting the number of symbols needed, copying them from the frame's end, and inserting them at the start. As a cyclic prefix in the simulation, four symbols were used.

Let's keep going with the illustrative example. The IFFT operation on the previous section's output created a vector with a length of 128. This section will append a cyclic prefix of four symbols, resulting in a total of symbols in the vector equal to 132, as illustrated in Figure (3.2).

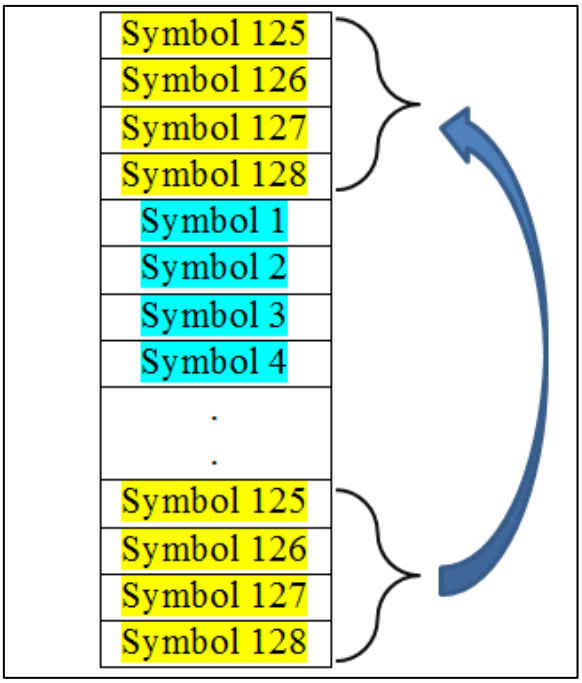

Figure (3.2): Appended the cyclic prefix

The final resuls can be shown as follows, so that, 132-by-500 matrix is obtained.

$$\text{data with CP} = \begin{matrix} \text{Block1} & \cdots\cdots & \text{Block 500} \\ \downarrow & & \downarrow \end{matrix} \begin{bmatrix} symbol_1 & \cdots & symbol_1 \\ \vdots & \vdots & \vdots \\ symbol_{132} & \cdots & symbol_{132} \end{bmatrix}_{132\times 500}$$

VII. Parallel to Serial conversion (P/S)

In the previous stage, the data array became 132-by-500, where 132 is the modified block size, and 500 is the total number of blocks. In this instance, the array of data is viewed as parallel blocks. The parallel blocks are turned into serial blocks using the reshape function, resulting in a data matrix of 132 × 500 symbols, or 66000-by-1, as follows.

$$serial\ blocks = \begin{bmatrix} block1_{132\times1} \\ block2_{132\times1} \\ \vdots \\ \vdots \\ block500_{132\times1} \end{bmatrix}_{66000\times1}$$

3.2.2 Channel Modelling

In order to test the system's performance under different transmission conditions, data being sent across two channels. The first is a Gaussian channel that augments the data with white Gaussian noise. Represented a Gaussian channel in the simulation using the Matlab function step(hAWGN, TX), where hAWGN represents the AWGN object through which the SNR and number of bits per symbol are set, and TX represents the signal to be transmitted. The second channel is the Rayleigh fading channel with three taps. The rand function randomly generated the three taps. After the taps are generated, the convolution function is used to implement the Rayleigh fading channel.

From the last process, the data arriving at the channel is a row matrix with a size of 66000×1. After passing through the channel, the resulting signal will be the same size, 66000×1.

3.2.3 The OFDMA Receiver Section

As shown in Figure (3.1), OFDMA's receiver section consists of seven operations that will be explained and implemented in MATLAB. The receiver processes will include completing the illustration example that started on the transmitter side.

I. Serial to parallel conversion (S/P)

The received data from the channel is an array of 66000-by-1. The received array was converted from its serial form to parallel form using reshape function,

then it became 132-by-500, where 132 represents the block size, and 500 is the total number of blocks, as follows.

$$\text{parallel data} = \begin{matrix} \text{Block1} & \ldots\ldots & \text{Block 500} \\ \downarrow & & \downarrow \end{matrix} \begin{bmatrix} symbol_1 & \cdots & symbol_1 \\ \vdots & \vdots & \vdots \\ symbol_{132} & \cdots & symbol_{132} \end{bmatrix}_{132\times500}$$

II. Removing Cyclic Prefix (CP)

Four symbols are added as a cyclic prefix in the transmission part, changing each block size from 128 to 132.

Here the first four symbols representing the cyclic prefix are easily removed through operations on the matrix, so the size of one block becomes 128 symbols, as follows.

$$\text{received data without CP} = \begin{matrix} \text{Block1} & \ldots\ldots & \text{Block 500} \\ \downarrow & & \downarrow \end{matrix} \begin{bmatrix} symbol_1 & \cdots & symbol_1 \\ \vdots & \vdots & \vdots \\ symbol_{128} & \cdots & symbol_{128} \end{bmatrix}_{128\times500}$$

III. Fast Fourier Transform (FFT)

After removing the cyclic prefix, the result is a vector of length 128, representing the first block of the first iteration. Inside the same loop, the fft function is performed, so the output is a vector with the same input length, 128 symbols.

IV. Subcarrier demapping

After converting the symbols to the frequency domain by the fft function, can be retrieved the data from the subcarriers according to the type of subcarrier mapping employed in the transmission part.

The coming vector from the previous process has a length of 128 symbols. The data can be retrieved from the subcarriers by operations on the matrix. In localized subcarrier demapping, data is retrieved from the first 16 subcarriers out of 128. In the case of interleaved subcarriers demapping, the first symbol is retrieved from the first subcarriers, and after each Q, another symbol is retrieved. Thus, 128 symbols have been reduced to 16 symbols.

As mentioned earlier, there are 500 blocks. After the subcarrier demapping process, the size of each block becomes 16 symbols, so the data matrix after the subcarrier demapping process becomes 16-by-500, as follows.

$$subcarriers\ demapping\ = [block1_{16\times1} \quad \dots \quad block500_{16\times1}]_{16\times500}$$

V. Parallel to serial conversion (P/S)

After the subcarriers demapping, the data matrix became 16-by-500, where 16 is the block size and 500 is the total number of blocks. The data array in this instance is regarded as parallel blocks. The parallel blocks are converted into serial blocks using reshape function, resulting in a data matrix of 8000-by-1, as follows.

$$P/S = \begin{bmatrix} symbol_1 \\ \vdots \\ symbol_{8000} \end{bmatrix}_{8000\times1}$$

VI. Demodulation

The demodulation process must first build the demodulation object before calling it during the demodulation process, just as it did during the modulation process. The M-PSK demodulation object utilized in the simulation has the following form:

hDemod = comm.PSKDemodulator(M,'BitOutput',true,'PhaseOffset', pi/M) …(3.5)

Where *M* denotes the modulation level, *BitOutput* represents the output data type, and the *PhaseOffset* indicates the phase shift between the complex symbols in the constellation. After the object is created, it is called in the demodulation process as follows:

rxSigg=step(hDemod, RX); …(3.6)

The *step* function represents the demodulation step, *hDemod* represents the M-PSK demodulation object, and *RX* means the data to be demodulated.

After converting the received data to serial form in the previous step, it became an 8000-by-1 array. In this step, the QPSK demodulation process is carried out so that the data became 16000-by-1, the same as the dimension of data sent, as follows.

$$demodulation = \begin{bmatrix} bit_1 \\ \vdots \\ bit_{16000} \end{bmatrix}_{16000\times 1}$$

After receiving the data, it is compared with the data sent to calculate the Bit Error Rate (BER). BER is the number of error bits in received data divided by the total number of bits sent.

3.3 SC-FDMA system

Figure (3.3) shows the SC-FDMA system structure built on the OFDMA system structure. Here the transmitting components of the SC-FDMA system, to some extent, has the same components as the transmitting part in the OFDMA system, but with one difference, which is the presence of an FFT block. As for the receiver part, it will contain an IFFT block. The details of the shared blocks

between the SC-FDMA and the OFDMA system were explained in the previous section, specifically in the OFDMA system.

The main difference between the transmission part of SC-FDMA and OFDMA is the presence of the FFT process, which converts the modulation symbols of each block into the frequency domain before mapping them on the user-assigned subcarriers. On the receiving side, the IFFT process converts the arriving block symbols into the time domain before the demodulation process.

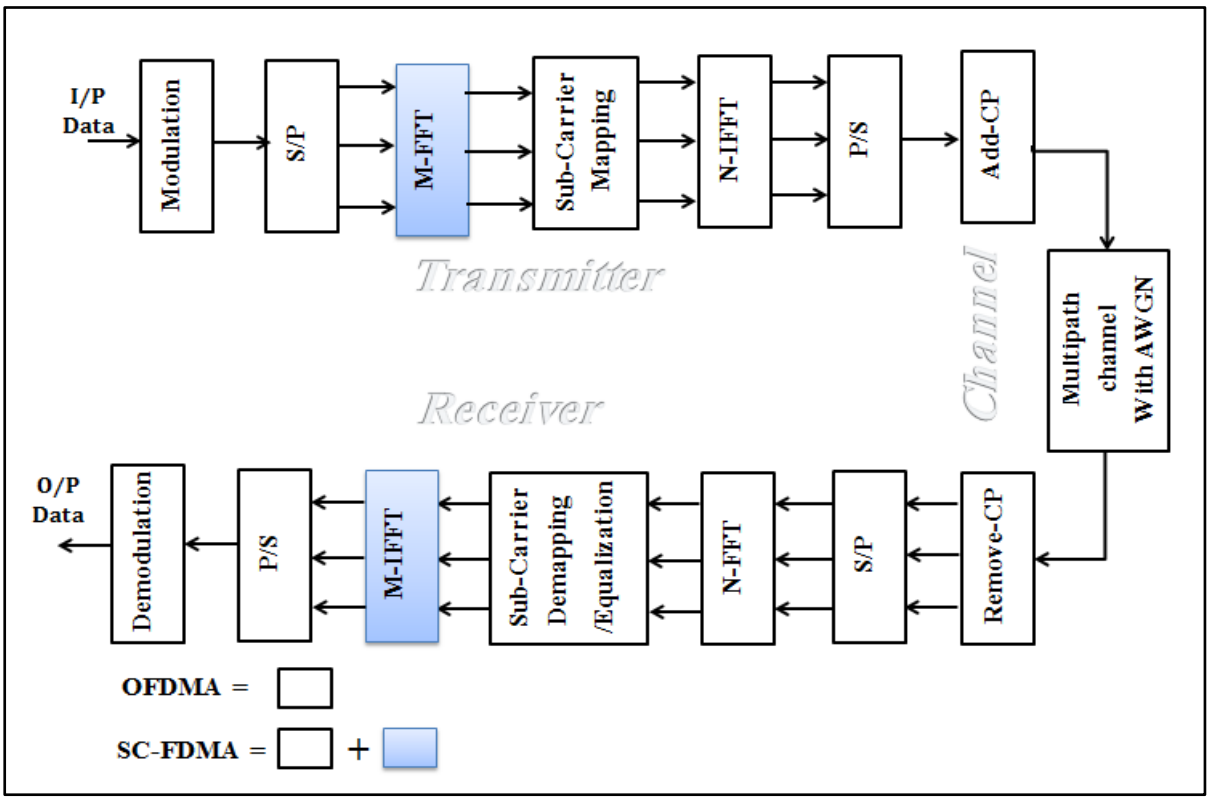

Figure (3.3): The SC-FDMA system

3.4 The SC-FDMA-DSCDMA Proposed System

Figure (3.4) shows the proposed system model built on the SC-FDMA system. Except for orange blocks, the SC-FDMA system can be reached. Firstly, the data is modulated on the proposed system's transmitter side using QPSK or 16PSKmodulation. After that, the complex symbols resulting from the modulating process are converted from serial to parallel form. Next, the users' symbols are multiplied by the spreading code that is assigned to each user

The maximum length of the spreading code is the same M-FFT size and represents the maximum number of active users. After the spreading process, M-FFT is executed. Then the M-FFT output is mapped on the user-specific subcarriers using one of the mapping types, either localized or interleaved subcarriers mapping. Then the symbols are converted to the time domain, and the cyclic prefix is added. Thus, the data is ready to be transmitted through the channel. After receiving the signal from the channel on the receiving side, the same previous procedures are done in reverse, in addition to the presence of frequency domain equalization.

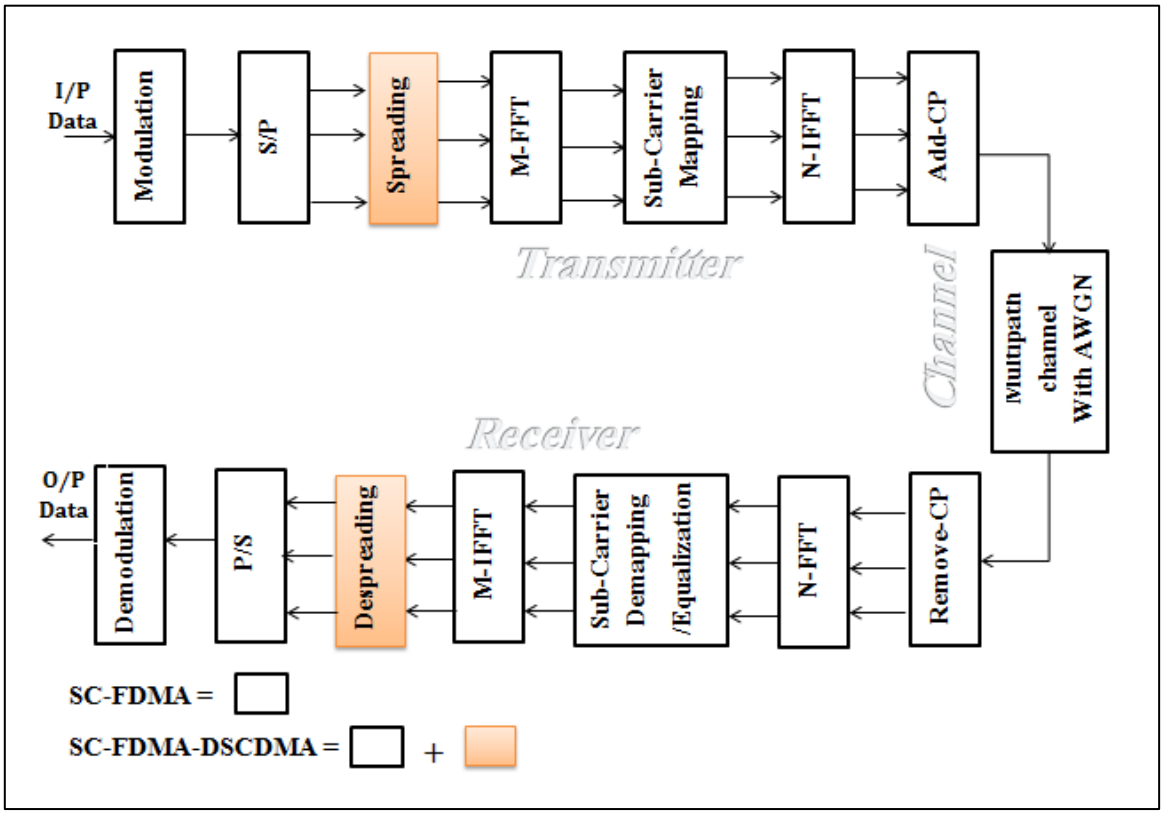

Figure (3.4): SC-FDMA-DSCDMA proposed system

3.4. 1 The SC-FDMA-DSCDMA Transmitter Section

The transmitter section of the proposed system, as shown in Figure (3.4), consists of the following processes: input data, modulation, serial to parallel conversion, spreading, FFT, subcarrier mapping, IFFT, and adding the cyclic prefix. All these processes will be explained in detail, including how they are

constructed in simulation. As well, there is an illustrative example that will accompany each process.

I. Input Data (I/P)

The rand() function supplied by the Matlab program is used to generate random numbers with uniformly distributed elements.

Here is the beginning of the illustration example that will be presented in all sending-related procedures. Assume that 16 users intend to send 6400 bits of (0,1) on the proposed system. To generate data for these users, proceed as follows:

Data= randi([0,1],6400,16); …(3.7)

The data for 16 users have been generated; thus, the data matrix is 6400-by-16, as follows.

$$\mathrm{I/P} = \begin{bmatrix} bit_{1,1} & bit_{2,1} & \cdots & bit_{16,1} \\ bit_{1,2} & bit_{2,2} & \cdots & bit_{16,2} \\ \vdots & \vdots & \cdots & \vdots \\ bit_{1,6400} & bit_{2,6400} & & bit_{16,6400} \end{bmatrix}_{6400\times16}$$

$bit_{i,k}$: Where i denote the user number and K represent the number of bit.

II. Modulation

the same procedure that seen in section 3.2.1 is done on the input data with the same function, so that, users' data is modulated by using the PSK object. With QPSK modulation, the modulated data array size is 3200-by-16, as follows.

$$\mathrm{modulation} = \begin{bmatrix} symbol_{1,1} & symbol_{2,1} & \cdots & symbol_{16,1} \\ symbol_{1,2} & symbol_{2,2} & \cdots & symbol_{16,2} \\ \vdots & \vdots & \cdots & \vdots \\ symbol_{1,3200} & symbol_{2,3200} & & symbol_{16,3200} \end{bmatrix}_{3200\times16}$$

$symbol_{i,k}$: Where i denote the user number and K represent the number of modulated symbol.

III. Serial to Parallel conversion(S/P)

From the previous step, the modulated data matrix is 3200-by-16. That is, there are 16 users, each with 3200 symbols. The modulated users' data will now arrange as blocking using the reshaping function. Each block consists of 16 complex symbols, so the total number of blocks is 200. Therefore, the users' data matrix will be in the form of 16-by-200-by-16. The first dimension represents the number of complex symbols in one block, the second dimension represents the total number of blocks, and the third dimension represents the users, as follows.

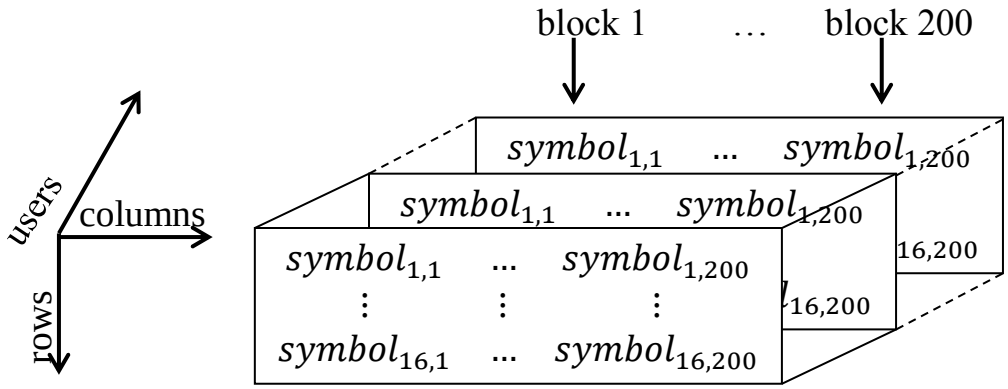

IV. Spreading

After converting the complex symbols from serial form to blocks, the spreading process is performed. The direct sequence spread spectrum multiplies each complex symbol with the user-specific spreading code. The maximum length of the spreading code refers to the maximum number of users and must be with a size equal to the FFT points. The simulation used many spreading codes, including Walsh code, m-sequences, OVSF, and gold sequences.

Back to the illustrative example, the users' data matrix is 16-by-200-by-16. Therefore, there are 16 users; each of them has 200 blocks, and each block contains 16 complex symbols. The first step in the spreading process is generating the spreading codes, and since there are 16 users, the process requires 16 spreading codes. In the illustrated example, the Walsh Hadamard

codes are used. The Walsh code is generated using the hadamard(n) function, where n is the size of the resulting square array in which each row is a spread code, which is orthogonal with the rest of the rows. After the codes are generated, it is assigned to users. With the help of iterative loops, the first complex symbol can be reached for each user and then multiply it by the user-specific code. Because the spreading code is 1-by-16 in length, each symbol after the spreading process will be 1-by-16 as well, as follows.

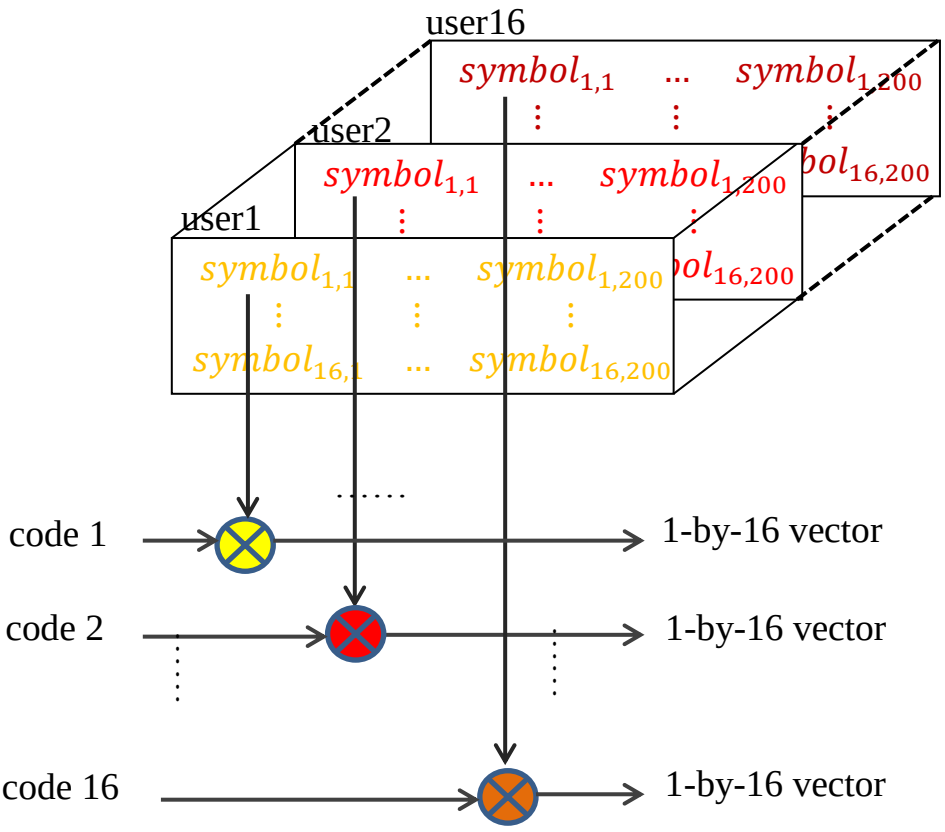

V. FFT

The fft function provided by the Matlab program is used to perform the discrete fourier transform. When the algorithm is given an array as input, the Fourier transform is applied to each column individually, and the output array has the exact dimensions as the original array.

Now, after spreading the first complex symbol for every user, the output is a vector of length 1-by-16 for each user. Then the discrete Fourier transform is performed on each vector using the fft function.

VI. Subcarrier mapping

From the previous step, after applying the fast Fourier transform, the vector size for each user is 1-by-16. Since there are 16 users, the subcarrier mapping process requires 256 subcarriers to transmit users' data. When employing local mapping, the first 16 sub-carriers are designated for the first user, the second 16 sub-carriers are reserved for the second user, and so on. The interleaved mapping assigns the first subcarrier to the first user, the second subcarrier to the second user, and so on until the first user receives the second subcarrier after all users have received the first subcarrier, as shown in Table (3.2).

Table (3.2): Assigning subcarriers to users

N. of subcarriers	Localized mapping		N. of subcarriers	Interleaved mapping
1-16	User1		1	User1
17-32	User2		2	User2
33-48	User3		3	User3
49-64	User4		.	.
65-80	User5		16	User 16
81-96	User6		17	User1
97-112	User7		18	User2
113-128	.		19	User3
129-144	.		.	.
145-160	.		32	User16
161-176	.		33	User1
177-192	.		34	User2
193-208	.		35	User3
209-224	.		.	.
225-240	.		255	User15
241-256	User 16		256	User16

VII. IFFT

In the previous process, after assigning the subcarriers to the users, the data array became 1-by-256. Now, using the ifft( ) function, the fast inverse Fourier transform for the data array is performed.

In this step, i.e., before the signal passes through the transmission channel, the PAPR value is calculated using the equation (2.21).

VIII. Add cyclic prefix

Let's continue with the illustrative example. After applying the inverse Fourier transform in the previous step, the data array became 1×256 symbols. In this step, 8 symbols will be added as a cyclic prefix so that the data size will be 1×264.

3.4. 2 Channel Models

Data is sent across two channels to test the system's performance under different transmission conditions. The first is a Gaussian channel that augments the data with white Gaussian noise. Represented a Gaussian channel in the proposed system using the Matlab function *step(hAWGN, TX)*, where *hAWGN* represents the AWGN object through which the SNR and modulation level are set, and *TX* represents the signal to be transmitted.

In the second channel, data is transmitted through a Rayleigh channel. The implementation of the Rayleigh channel assumed three taps with random delay and gain. The rand function randomly generated the three taps. After the taps are generated, the convolution function is used to implement the Rayleigh fading channel.

From the last process, the data arriving at the channel is a matrix with a size of 1×264. After passing through the channel, the resulting signal will be the same size, 1×264.

3.4. 3 The SC-FDMA-DSCDMA Receiver Section

As shown in Figure (3.4), the receiver section of the proposed system consists of the following processes: removing the cyclic prefix, FFT, subcarriers demapping and equalization, IFFT, Despreading, parallel to serial conversion, and demodulation. All these processes will be explained in detail, including how they are constructed in simulation with the help of the Matlab program environment.

I. Remove CP

From the previous process, the received signal is 1-by-264. The first eight symbols representing the cyclic prefix are easily removed through operations on the matrix, so the size of the matrix becomes 1-by-256 symbols.

II. FFT

In the previous step, after removing the cyclic prefix, the data array became 1-by-256. Now, using the fft function, the fast fourier transform for the received array is performed.

III. Subcarriers Demapping and Equalization

After converting the symbols to the frequency domain using the FFT function, it is possible to recover data from subcarriers based on the subcarrier mapping applied in the transmission section. Before performing a sub-carrier demapping, the equalization is performed by knowing the channel's frequency response and cancelling its effect by dividing the received data on the channel's frequency response.

From the previous process and after the equalization process, the size of the received data vector is 1-by-256. The data is retrieved from the sub-carriers through operations on the arrays and according to the type of mapping used in the transmitter.

In the localized demapping, the data is retrieved from the subcarriers as follows, the data of the first 16 subcarriers from 256 subcarriers are retrieved as

the first user' data, the second 16 of the 256 subcarriers as the second user's data, and so on for the rest of the users.

In the interleaved demapping, the data for users is retrieved by taking the data of the first subcarrier for the first user and the second subcarrier for the second user, and so on. Thus, each user will get 1-by-16 data by demapping the subcarriers.

IV. IFFT

After subcarriers are demapping, each user gets a data vector of length 1-by-16. The ifft function is executed on the data vector, converting them from frequency domain to time domain with length 1-by-16.

V. Despreading

After converting the received data into the time domain, the despreading process is performed by multiplying the received data by the same specific user spreading code used in the transmitter side.

Each user has a 1-by-16 array as received data from the previous step. The received data multiplying by the same Walsh code used in the transmitter side, and since the length of the Walsh code is 16-by-1, the users' received data will be 1-by-1. That means one symbol results after performing the despreading process.

VI. Parallel to serial conversion

In the transmission section, specifically in converting symbols from serial to parallel, the complex symbols are grouped into blocks where the number of blocks is 200, and each block consisted of 16 symbols. In the transmission process, one symbol is sent and received from each user, which is apparent through the previous operations. After receiving all the users' symbols, they are arranged and stored similarly to their previous shape to be ready for the demodulation process.

Let us complete the illustration example. Following the despreading process, each user received one symbol due to the transmission mechanism: sending and receiving one symbol via each user. After receiving all symbols, they are arranged in a 3200-by-16 matrix, as follows.

$$s/p = \begin{bmatrix} symbol_{1,1} & symbol_{2,1} & \cdots & symbol_{16,1} \\ symbol_{1,2} & symbol_{2,2} & \cdots & symbol_{16,2} \\ \vdots & \vdots & \cdots & \vdots \\ symbol_{1,3200} & symbol_{2,3200} & & symbol_{16,3200} \end{bmatrix}_{3200\times16}$$

$symbol_{i,k}$: Where i denote the user number and K represent the number of received symbol.

VII. Demodulation

In the process of converting symbols to serial form, the data array had a size of 3200-by-16, meaning there are 16 users, and each has 3200 symbols. Using the QPSK demodulation object, the size of the data becomes 6400-by-16 which is the same size as the original data, as follows.

$$\mathrm{O/P} = \begin{bmatrix} bit_{1,1} & bit_{2,1} & \cdots & bit_{16,1} \\ bit_{1,2} & bit_{2,2} & \cdots & bit_{16,2} \\ \vdots & \vdots & \cdots & \vdots \\ bit_{1,6400} & bit_{2,6400} & & bit_{16,6400} \end{bmatrix}_{6400\times16}$$

$bit_{i,k}$: Where i denote the user number and K represent the number of

After receiving the data, it is compared with the data sent to calculate the Bit Error Rate (BER). BER is the number of error bits in received data divided by the total number of bits sent.

3.5 Spreading Sequences

In the spread spectrum scheme, the data signal is multiplied by the spreading sequences in the transmitting part. After receiving the signal, it is multiplied by the same spreading sequence used in the transmitter. The simulation used four spreading sequences: m-sequences, gold sequences, Walsh

codes, and OVSF codes. This section will explain how the sequences are generated and how they are introduced into the simulation.

i. m-sequences

In the simulation, the m-sequences are generated using the LFSR(x,y) and cirshift(x) function. The LFSR(x,y) function performs the linear feedback shift register operation, x represents the generator polynomial, and y represents the initial condition. The generated sequence using the LFSR function has a period of 2^m-1, where m represents the highest degree of the generator polynomial. After obtaining the first sequence, it circularly shifts using the cirshift(x) function to get the maximum number of sequences which are 2^m-1.

ii. Gold Sequences

In the simulation, generating gold sequences requires the generation of two m-sequences called preferred pairs. The preferred pairs are generated similarly as m-sequences using the LFSR(x,y) and cirshift(x) function. The preferred pairs are the first two gold sequences. Up to N additional sequences can be generated for gold sequences of length $N = 2^m - 1$ by calculating the sum of modulo-2 of the first m sequence and the cyclic shift of the second m-sequence.

iii. Walsh Codes

The Walsh codes are generated using the simulation's hadamard(n) function. Hadamard function produces a square matrix. Each row in the Hadamard matrix represents spreading code orthogonal to other rows.

iv. OVSF Codes

The OVSF codes are generated using the OVSFCode object in the simulation. The OVSFCode object generates an orthogonal variable spreading factor (OVSF) code from a set of orthogonal codes.

Chapter Four

Results and Discussion

Chapter Four

Results and Discussion

4.1 Introduction

This chapter presents and discusses simulation results of OFDMA, SC-FDMA, and SC-FDMA-DSCDMA techniques implemented using the MATLAB program. This chapter is divided into six sections through which simulation results are presented in terms of PAPR and BER performance. After its introduction in the first section, the results of the OFDMA system performance are presented in the second section. In the third section, the results of the SC-FDMA system's performance are presented and compared with the OFDMA system's performance. In the fourth section, the performance results of the SC-FDMA-DSCDMA system are presented and compared to those of the conventional SC-FDMA system. The fifth shows the SC-FDMA-DSCDMA performance under different code sequences. The last section presents a comparison with related works.

4.2 OFDMA System Simulation Results

This section has two parts that show the simulation results for the OFDMA system shown in Figure (3.1). The first part represents the simulation results in terms of PAPR and the second in terms of BER. Random binary data and two forms of modulation (QPSK and 16PSK) are employed in the simulation. Also, two types of subcarrier mapping are used: localized and interleaved mapping. In addition, 16 subcarriers are assigned to the user out of 128 subcarriers. Two types of channel models are also used, AWGN and Rayleigh channel. The simulation is carried out using Matlab's script files and function files in addition to the communication toolbox functions.

4.2.1 OFDMA PAPR Results

This part presents the PAPR simulation results of the OFDMA system. The results are obtained using QPSK and 16PSK as modulation techniques, and

the localized and interleaved are used as subcarrier mapping. The data sent in the simulation is 16000 random bits, and 16 out of 128 subcarriers are assigned to the user. The PAPR values are calculated through equation (2.23) and presented in the graphics as Complementry Cumulative Distribution Function (CCDF) curves. The CCDF means the probability that the PAPR is greater than a specific value (PAPR0) which is calculated through equation (2.24) . Therefore, the X-axis in the results curves represents the threshold value (PAPR0), and the Y-axis represents the CCDF.

The PAPR performance comparison between the localized and interleaved subcarrier mapping of an OFDMA system is presented in Figure (4.1).

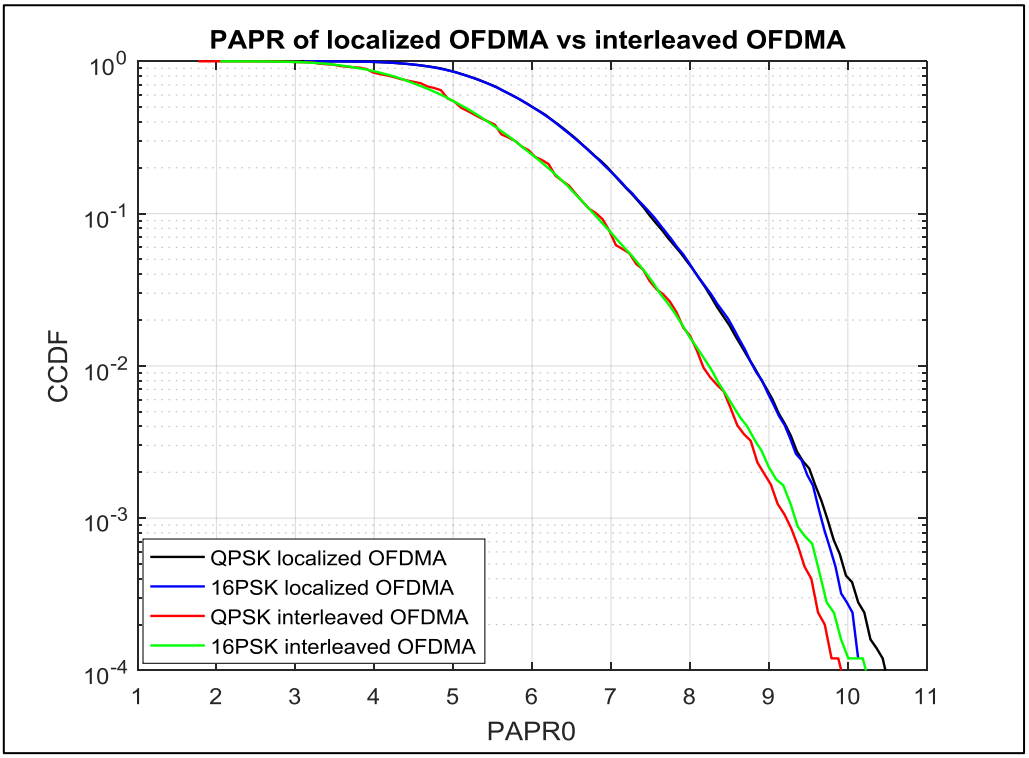

Figure (4.1): OFDMA PAPR simulation result.

Section 4.2.1 presented OFDMA simulation results regarding PAPR performance. Based on PAPR simulation results shown in Fig.4.1, it is evident that The performance of PAPR is not affected by the change in the modulation level, and it is almost identical when using QPSK and 16PSK and this is because the constellation points of the M-PSK modulation which are arranged

with uniform angular spacing around a circle, which provides the greatest phase difference between neighboring points and, hence, the peak amplitude of the complex modulated symbols is equal to the length of the vector from the origin to any constellation point. As for the subcarrier mapping methods, the PAPR behavior is better with interleaved than that with localized because the interleaved mapping provides more diversity through which the modulated symbols spread across the entire channel bandwidth.

4.2.2 OFDMA BER Results

In this part, The BER simulation results of the OFDMA system are obtained using QPSK and 16PSK as modulation techniques, and the localized and interleaved are used as subcarrier mapping. The data sent in the simulation is 16000 random bits, and 16 out of 128 subcarriers are assigned to the user.

Figure (4.2) shows the BER simulation results of the OFDMA system using the AWGN channel while Figure (4.3) shows the BER result with the Rayleigh channel. the Rayleigh fading channel is simulated with three paths. the BER is calculated by dividing the error bits by the total number of bits.

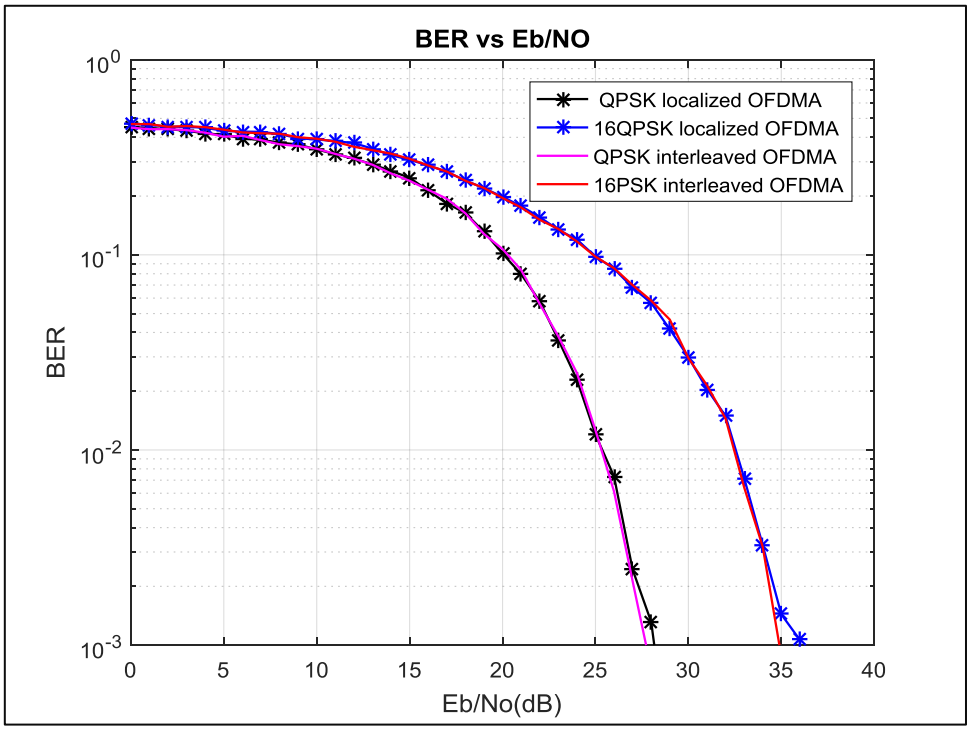

Figure (4.2): OFDMA BER results with AWGN channel.

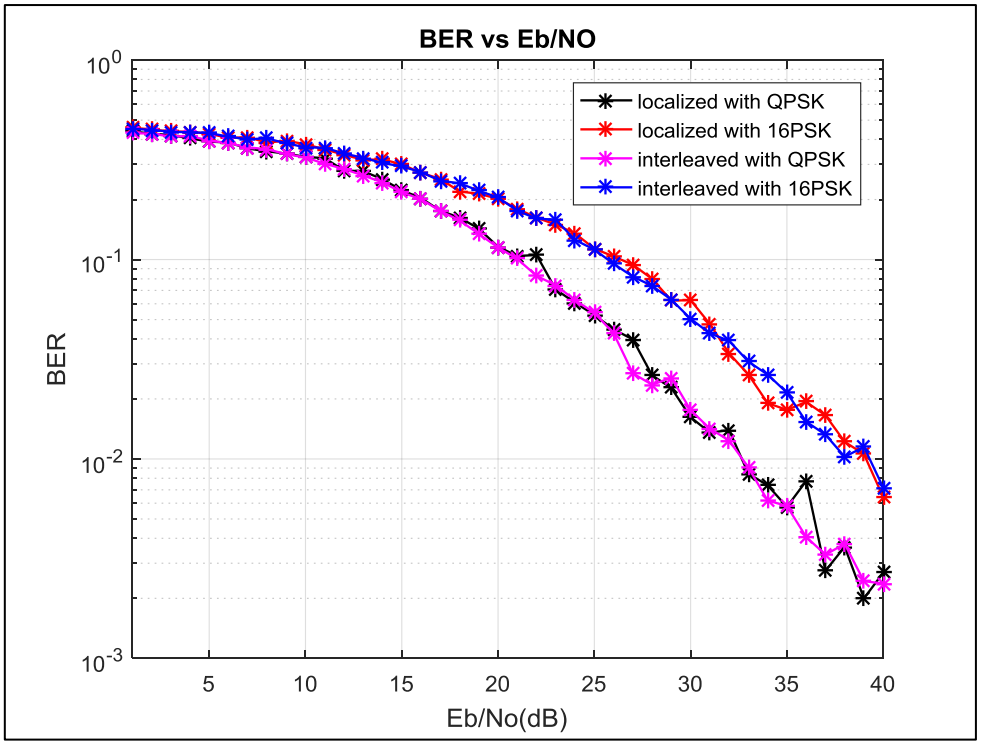

Figure (4.3): OFDMA BER results with Rayleigh channel.

Section 4.2.2 presented OFDMA simulation results regarding BER performance. From the simulation result of the BER shown in Figure (4.2-3), it is clear that the system performance with using the interleaved subcarrier mapping is the same as when using localized mapping. Also, the BER performance with QPSK modulation is better than that with 16PSK. QPSK is considered to be a robust modulation scheme compared to the 16 PSK as it is easy for the receiver to receive the original bits. After passing both QPSK and 16PSK through channel and noise, in the QPSK demodulator, only four decision points are required to retrieve the original binary information. while in 16PSK, sixteen decision points are required to retrieve the original binary information. Therefore 16PSK modulation is more susceptible to error than QPSK modulation. When observing the results in Figure (4.2-3), it becomes clear that the results in the presence of the fading channel worsened, and this is due to the fact that the fading channel is more realistic and influential than the Gaussian channel.

4.3 SC-FDMA System Simulation Results

The results of the simulations performed on the SC-FDMA system depicted in Figure (3.3) are presented in two parts. The first part displays the outcomes in terms of PAPR, while the second section displays the outcomes in terms of BER. The simulation results are obtained using QPSK and 16PSK as modulation techniques, and the localized and interleaved are used as subcarrier mapping. The data sent in the simulation is 16000 bits, and 16 out of 128 subcarriers are assigned to the user. Two types of channel models are also used, AWGN and Rayleigh channel. The simulation is carried out using Matlab's script files and function files in addition to the communication toolbox functions.

4.3. 1 SC-FDMA PAPR Results

This part presents the PAPR simulation results of the SC-FDMA system. The results are obtained using QPSK and 16PSK as modulation techniques, and the localized and interleaved are used as subcarrier mapping. The data sent in the simulation is 16000 random bits, and 16 out of 128 subcarriers are assigned to the user. The PAPR values are calculated through Eq (2.23) and presented in the graphics as CCDF curves.

Figure (4.4) show the PAPR simulation result for the SC-FDMA system by using localized and interleaved subcarrier mapping, and QPSK and 16 PSK modulation type.

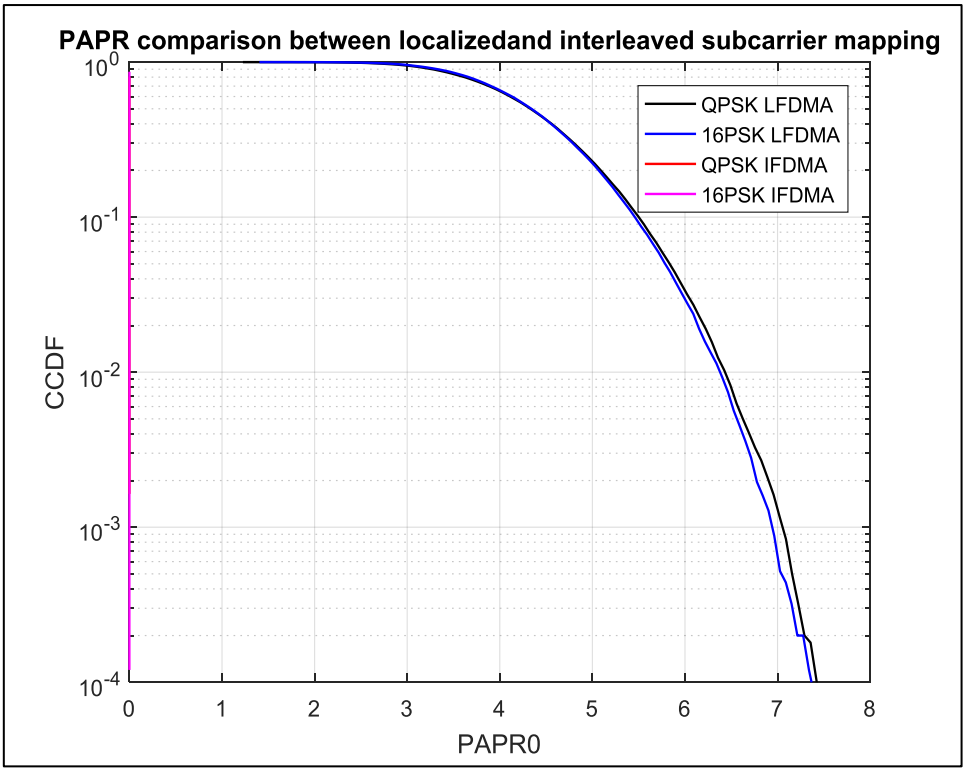

Figure (4.4): SC-FDMA PAPR simulation results.

Based on the PAPR simulation results shown in Fig.4.4, it is evident that The performance of PAPR is not affected by the change in the modulation level, and it is almost identical when using QPSK and 16PSK and this is because the constellation points of the M-PSK modulation which are arranged with uniform angular spacing around a circle, which provides the greatest phase difference between neighboring points and, hence, the peak amplitude of the complex modulated symbols is equal to the length of the vector from the origin to any constellation point. As for the subcarrier mapping methods, the PAPR behavior is better with interleaved than that with localized because the interleaved mapping provides more diversity through which the modulated symbols spread across the entire channel bandwidth.

4.3. 2 SC-FDMA BER Results

In this part, The BER simulation results of the SC-FDMA system are obtained using QPSK and 16PSK as modulation techniques, and the localized and interleaved are used as subcarrier mapping. The AWGN and Rayleigh

channels are used as channel models. The data sent in the simulation is 16000 bits, and 16 out of 128 subcarriers are assigned to the user. The results of this part are presented depending on the type of channel model used.

Figure (4.5) shows the BER simulation results of the SC-FDMA system using the AWGN channel while Figure (4.6) shows the BER result with the Rayleigh channel. the Rayleigh fading channel is simulated with three paths. the BER is calculated by dividing the error bits by the total number of bits.

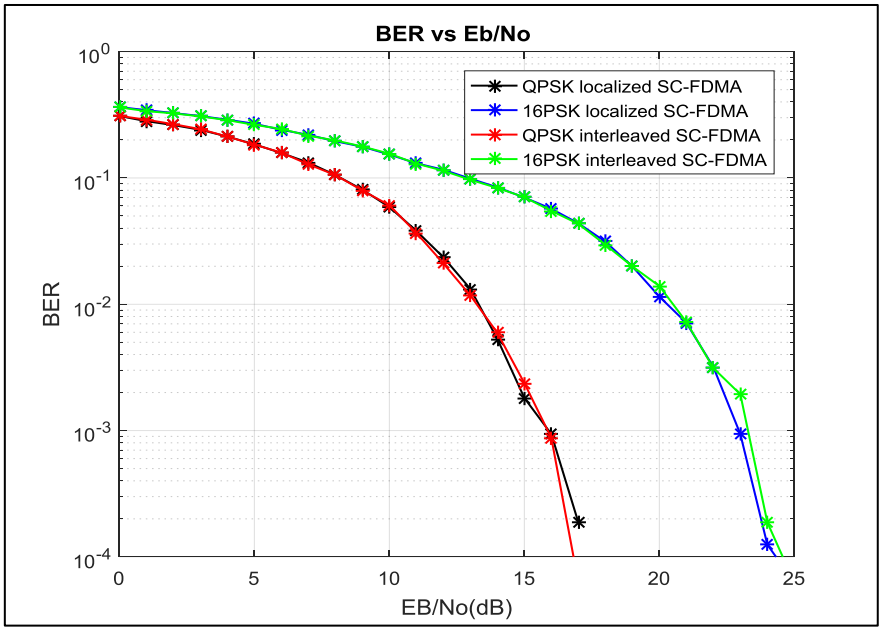

Figure (4.5): SC-FDMA BER simulation result with AWGN.

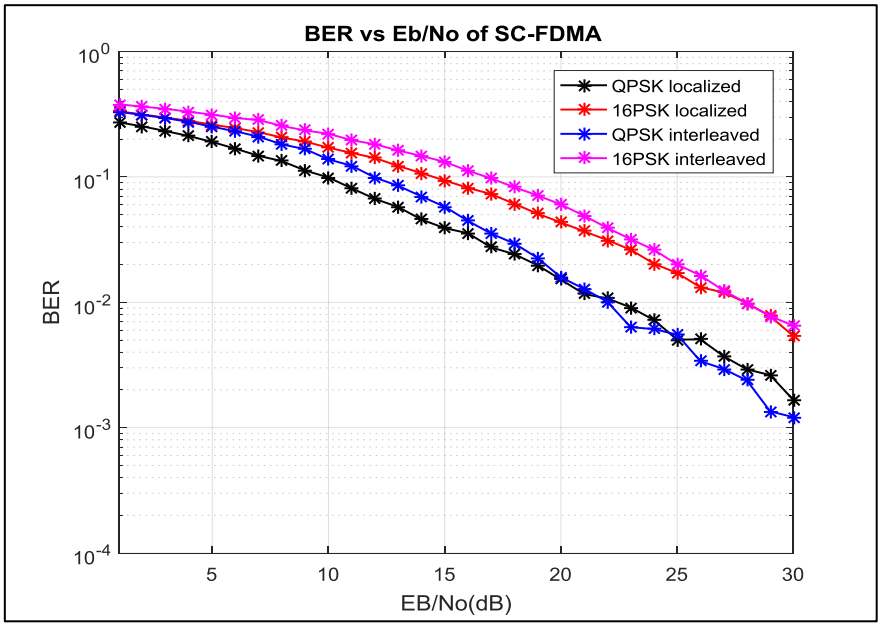

Figure (4.6): SC-FDMA BER simulation result with the Rayleigh channel.

Part 4.3.1 and part 4.3.2 presented SC-FDMA simulation results regarding PAPR and BER performance. The PAPR results show that the system performs better with interleaved sub-carrier mapping than with localized sub-carrier mapping. Based on the BER simulation results, it is clear that the system performance with the interleaved subcarrier mapping is approximately the same as when using localized mapping. Also, the BER performance with QPSK modulation is better than that with 16PSK.

4.3. 3 Comparison of SC-FDMA and OFDMA

The Performance results of OFDMA and SC-FDMA in terms of PAPR and BER are compared in this part. Figure(4.7) presents the PAPR comparison, and Figure (4.8) presents the BER comparison.

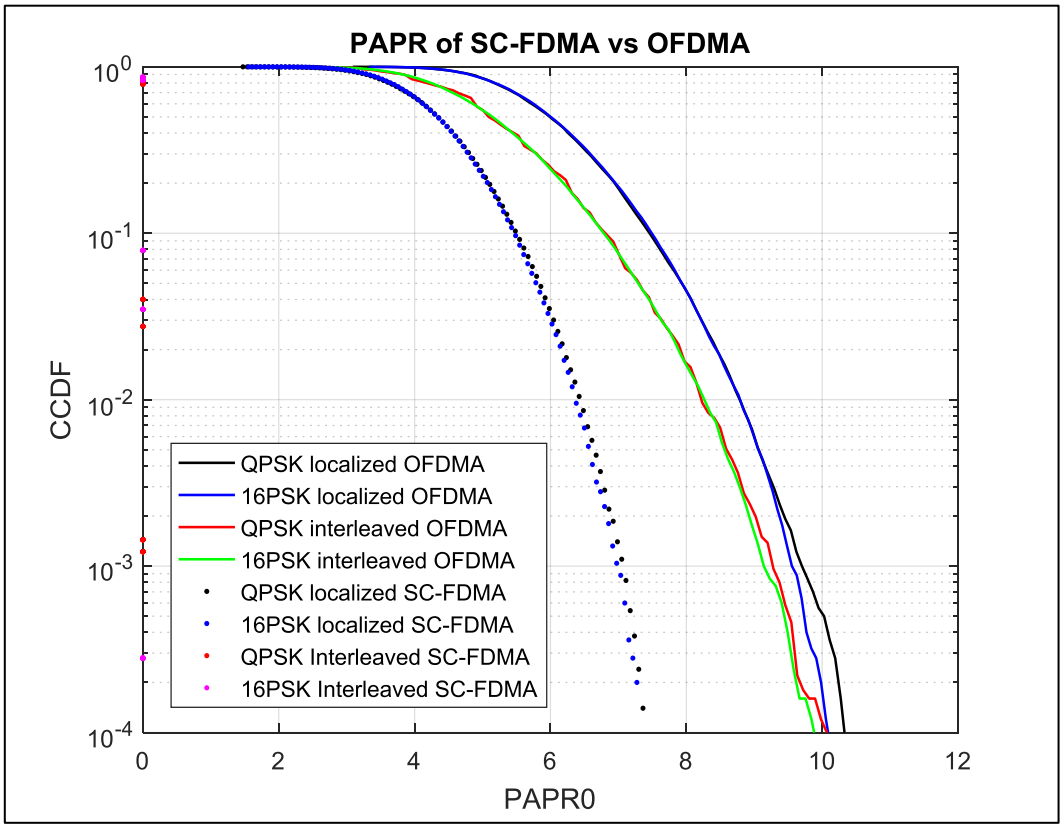

Figure (4.7) : PAPR comparison of SC-FDMA and OFDMA system.

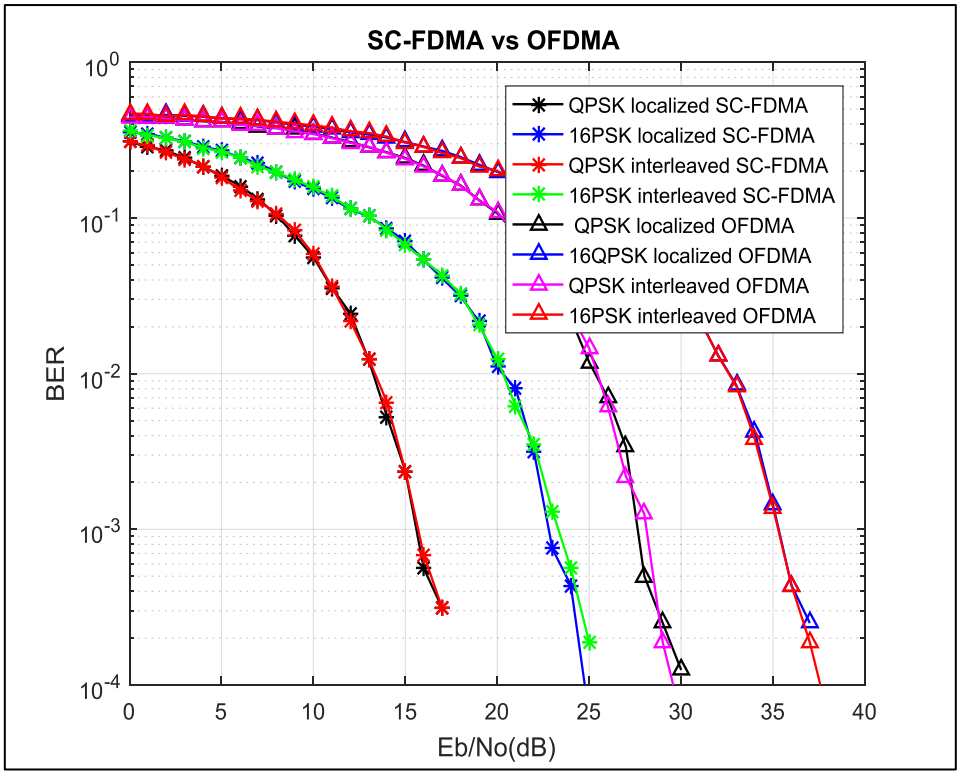

Figure (4.8): BER comparison of SC-FDMA and OFDMA system.

It can be seen from Fig.(4.7-8) that the SC-FDMA system performs better than the OFDMA system in terms of PAPR and BER. At a CCDF value is 10^{-3}, the PAPR of SC-FDMA is 7 dB, while the PAPR of OFDMA is 9.8 dB, thus SC-FDMA provides the best PAPR performance around 2.8 dB better than OFDMA system. SC-FDMA has a BER of 6.2×10^{-4} at an SNR of 17.5 dB, while OFDMA requires an SNR of 26.8 dB to achieve the same BER.

4.4 SC-FDMA-DSCDMA System Simulation Results

This section has two parts that show the simulation results for the suggested SC-FDMA-DSCDMA approach shown in Figure (3.4). The first part represents the results in terms of PAPR and the second in terms of BER. The simulation employed Walsh code as spreading code and two modulation schemes (QPSK, 16PSK) with two kinds of sub-carrier mapping (localized and interleaved). Also, two communication channel models have been implemented (AWGN, Rayleigh). The simulation is carried out on more than one user,

starting with 8 users and up to 128 users. The data sent in the simulation is 128Kbits. The simulation is performed using Matlab's script and function files, as well as the communication toolbox functions.

4.4.1 SC-FDMA-DSCDMA PAPR Results

In this part, the PAPR simulation results of the SC-FDMA-DSCDMA system are obtained. Here the results of localized and interleaved subcarrier mapping are presented in Figure (4.9) and (4.10). The simulation used the Walsh code as a spreading code with a length equal to the number of active users. Two modulation types are used (QPSK and 16PSK).

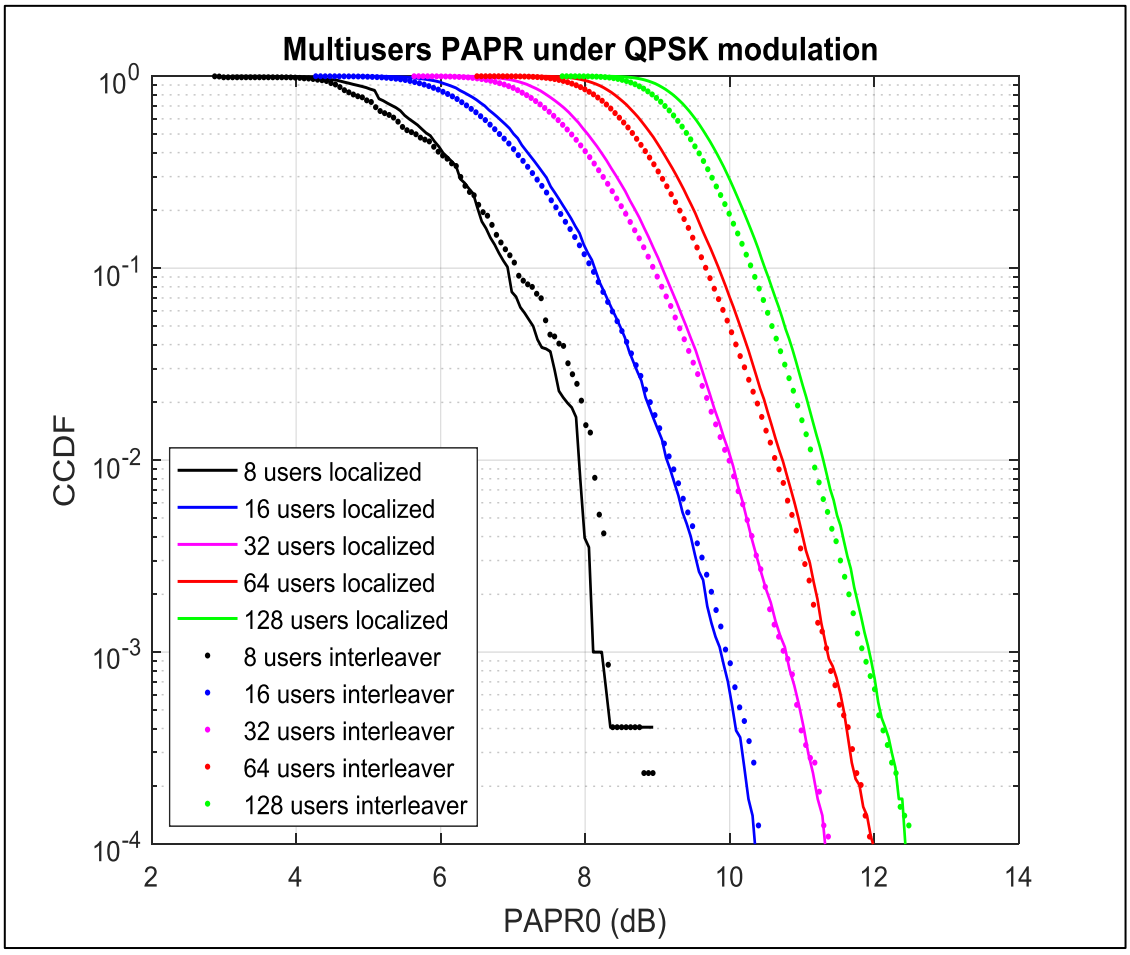

Figure (4.9): SC-FDMA-DSCDMA PAPR simulation result under QPSK.

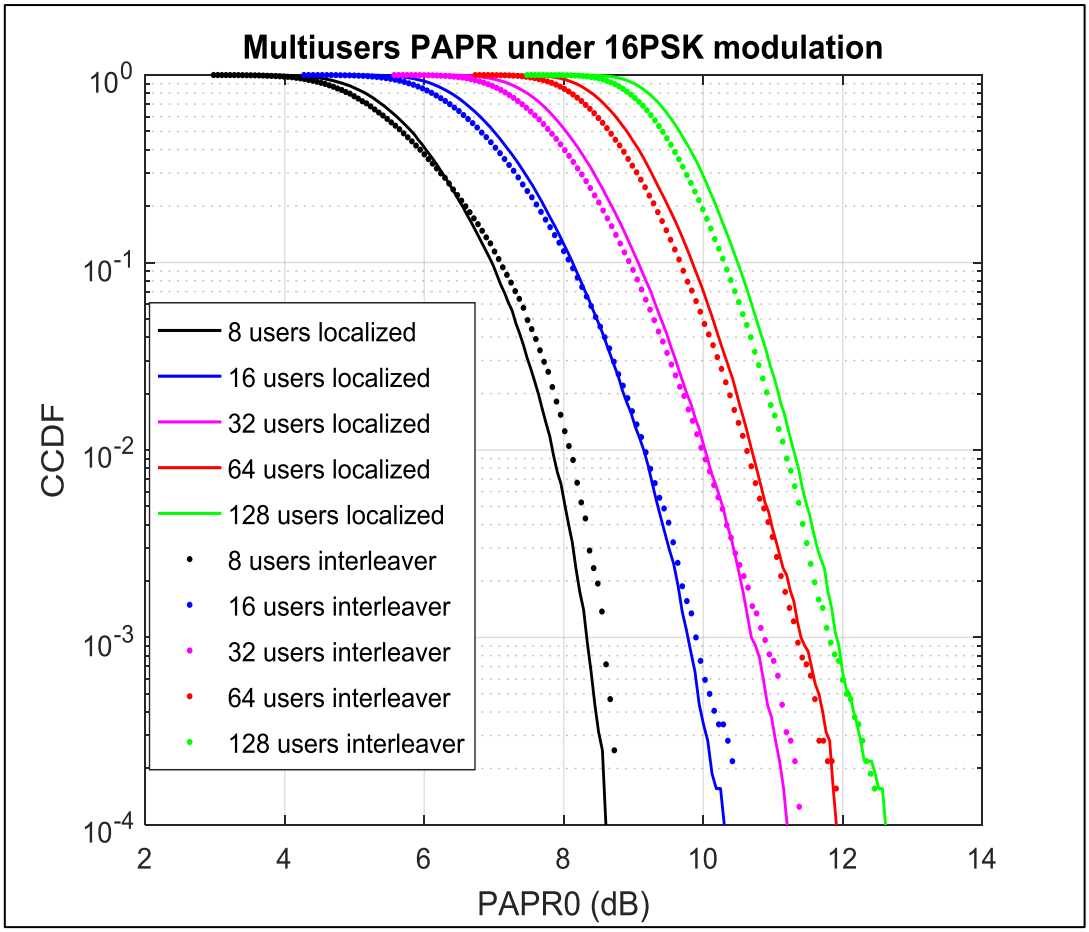

Figure (4.10): SC-FDMA-DSCDMA PAPR simulation result under 16 PSK.

It can be seen from Fig.(4.9-10) that the PAPR performance of the SC-FDMA-DSCDMA system is not affected by the change in the modulation level, and it is almost identical when using QPSK and 16PSK and this is because the constellation points of the M-PSK modulation which are arranged with uniform angular spacing around a circle, hence, the peak amplitude of the complex modulated symbols is equal to the length of the vector from the origin to any constellation point. As for the subcarrier mapping methods, the PAPR behavior is almost the same when employing localized or interleaved mapping.

4.4.2 SC-FDMA-DSCDMA BER Results

In this part, the BER simulation results of the suggested system are obtained using QPSK and 16PSK as modulation techniques, the localized and interleaved are used as subcarrier mapping, and the AWGN and Rayleigh are

used as channel models. The simulation is carried out on more than one user, starting with 8 users and up to 128 users. The data sent in the simulation is 10.24Kbits.

A. SC-FDMA-DSCDMA BER with AWGN Channel

Figure (4.11) and Figure(4.12) present the BER performance of the SC-FDMA-DSCDMA system under the AWGN channel. the simulation was carried out using localized and interleaved subcarrier mapping. The result is achieved through the employment of QPSK and 16PSK modulation techniques and multi-user start from 8 users up to 128 users.

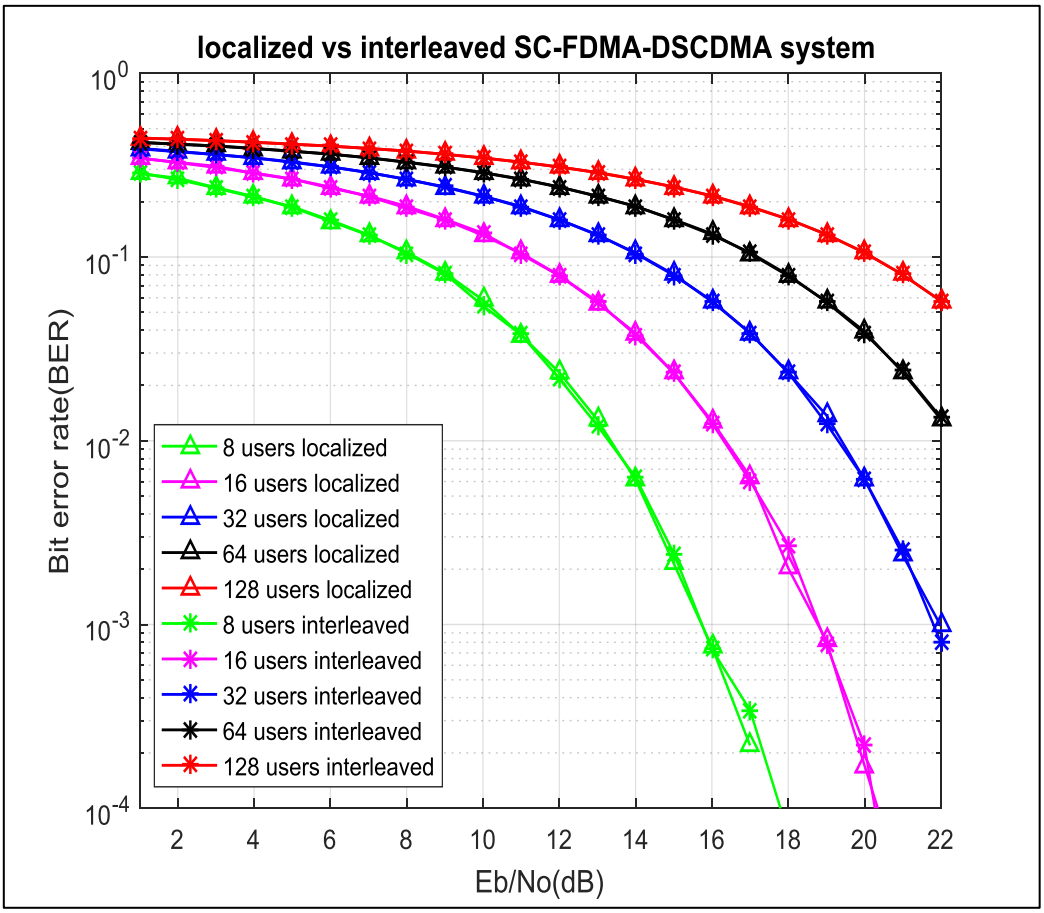

Figure (4.11): BER comparison of the localized and Interleaved proposed system with QPSK.

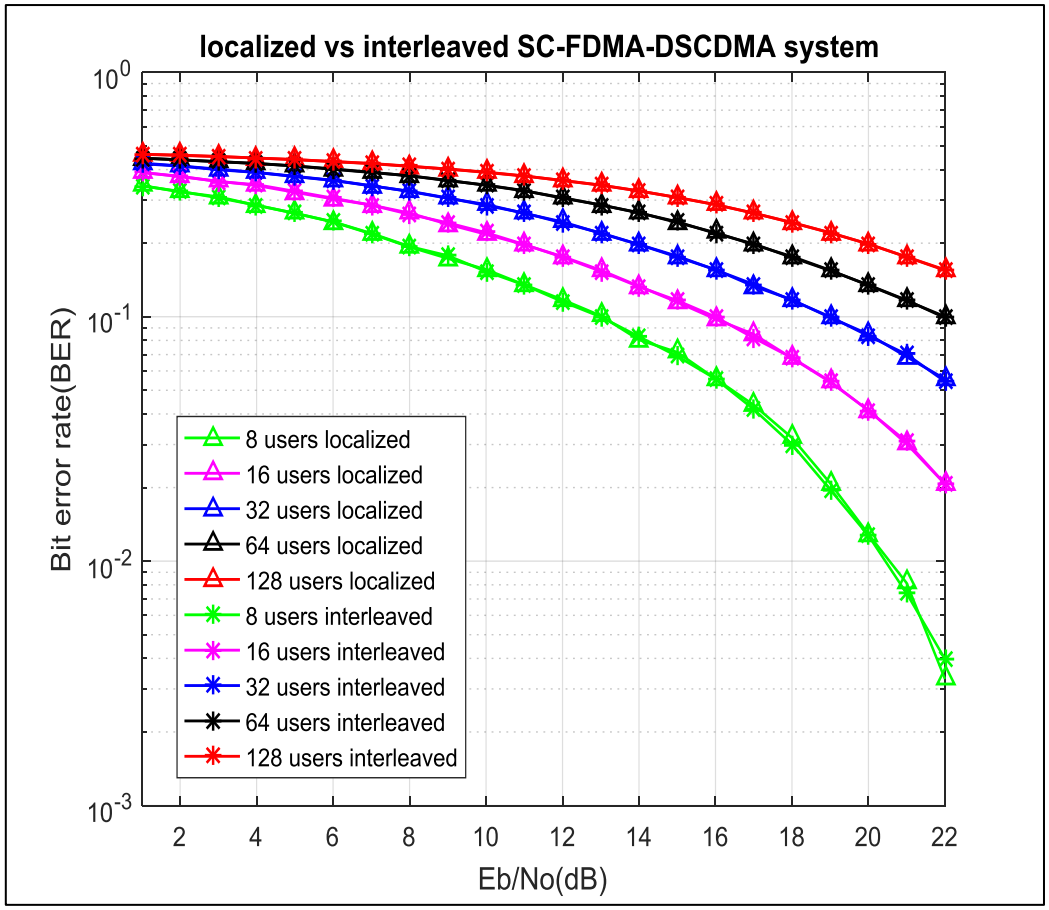

Figure (4.12): BER comparison of the localized and Interleaved proposed system with 16PSK.

It can be very clearly observed in Figure (4.11) that, at BER of 10^{-3} over the AWGN channel, the Eb/No requirement of the SC-FDMA-DS-CDMA system with 8 users is 15.9 dB, with 16 users is 18.9 dB, and with 32 is 22 dB, and so on. therefore the BER of the proposed system increased with the user's increment. Figure (4.12) show the same behavior illustrated by Figure (4.11) but the Eb/NO requirement increased due to the increment in the modulation level. As for the subcarrier mapping point of view, the BER curves are identically this means the BER is the same when employing localized or interleaved subcarrier mapping.

B. SC-FDMA-DSCDMA BER with Rayleigh

Figure (4.13) and Figure(4.14) present the BER performance of the SC-FDMA-DSCDMA system under the Rayleigh channel.

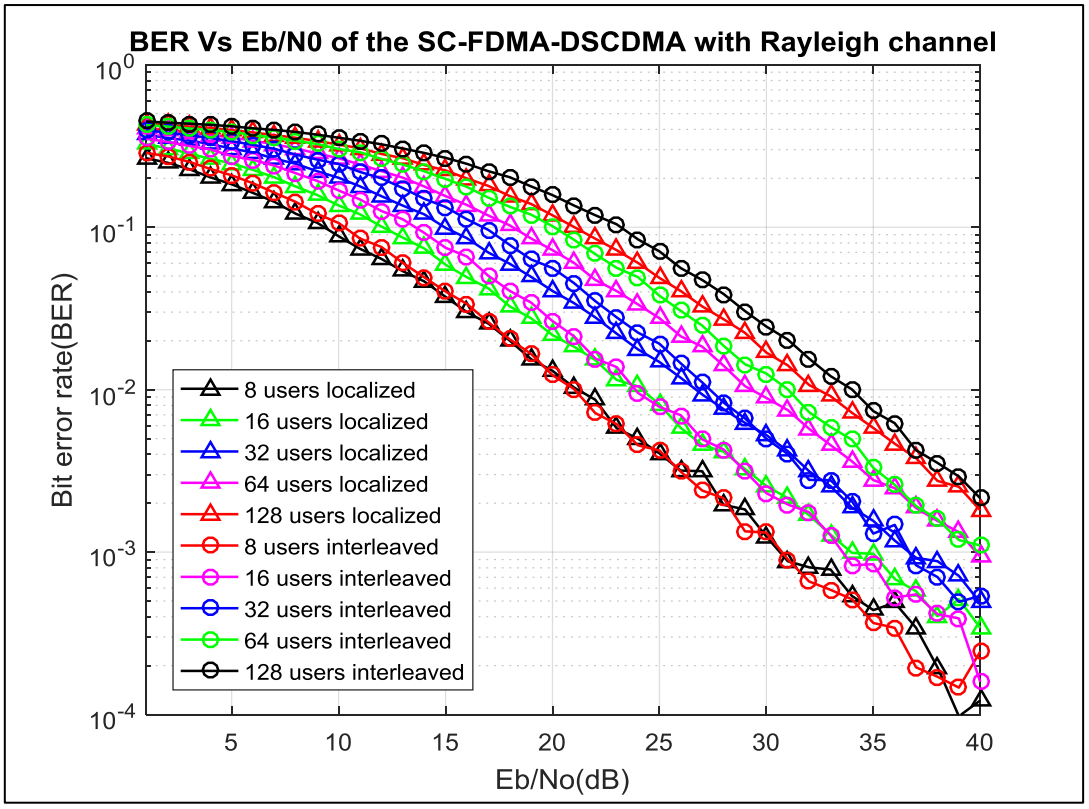

Figure (4.13): SC-FDMA-DSCDMA BER results withQPSK and Rayleigh channel.

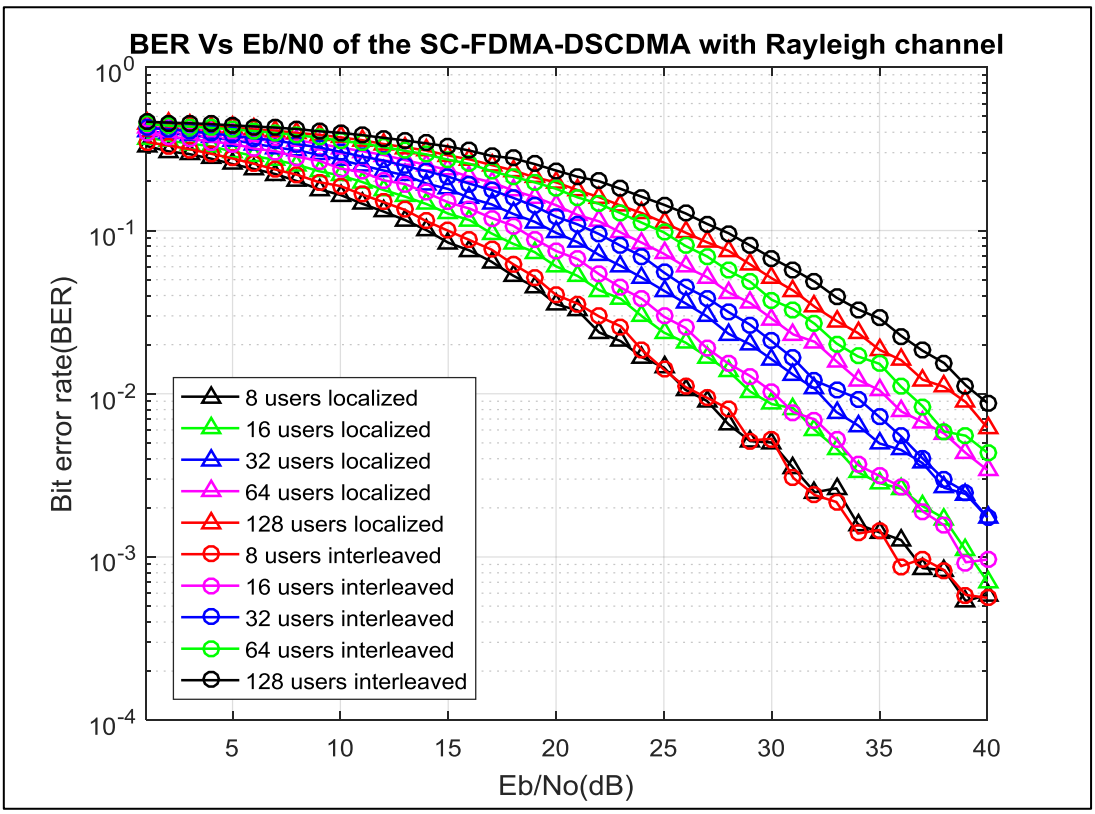

Figure (4.14): SC-FDMA-DSCDMA BER results with16PSK and Rayleigh channel.

It can be very clearly observed in Figure (4.13) that, at BER of 10^{-3} over the Rayleigh channel, the Eb/No requirement of the SC-FDMA-DS-CDMA system with 8 users is 30 dB, with 16 users is 33 dB, and with 32 is 36.2 dB, and so on. therefore the BER of the proposed system increased with the user's increment. Figure (4.14) show the same behavior illustrated by Figure (4.13) but the Eb/No requirement increased due to the increment in the modulation level. As for the subcarrier mapping point of view, the BER curves are almost identical this means the BER is the same when employing localized or interleaved subcarrier mapping.

4.4.3 SC-FDMA-DSCDMA system and SCFDMA System Comparison

This part compares the suggested SC-FDMA-DSCDMA approach to SC-FDMA in terms of PAPR and BER. The simulation results are obtained using the QPSK and 16PSK modulation approaches, as well as localized and interleaved subcarrier mapping. The simulation is performed on several users, beginning with 8 and progressing to 128. The simulation sends 128Kbits of data.

A. PAPR Comparison Results

The PAPR comparison results between the proposed system and the traditional SC-FDMA system with localized subcarrier mapping and using QPSK and 16PSK are presented in Figures (4.15) and (4.16), respectively.

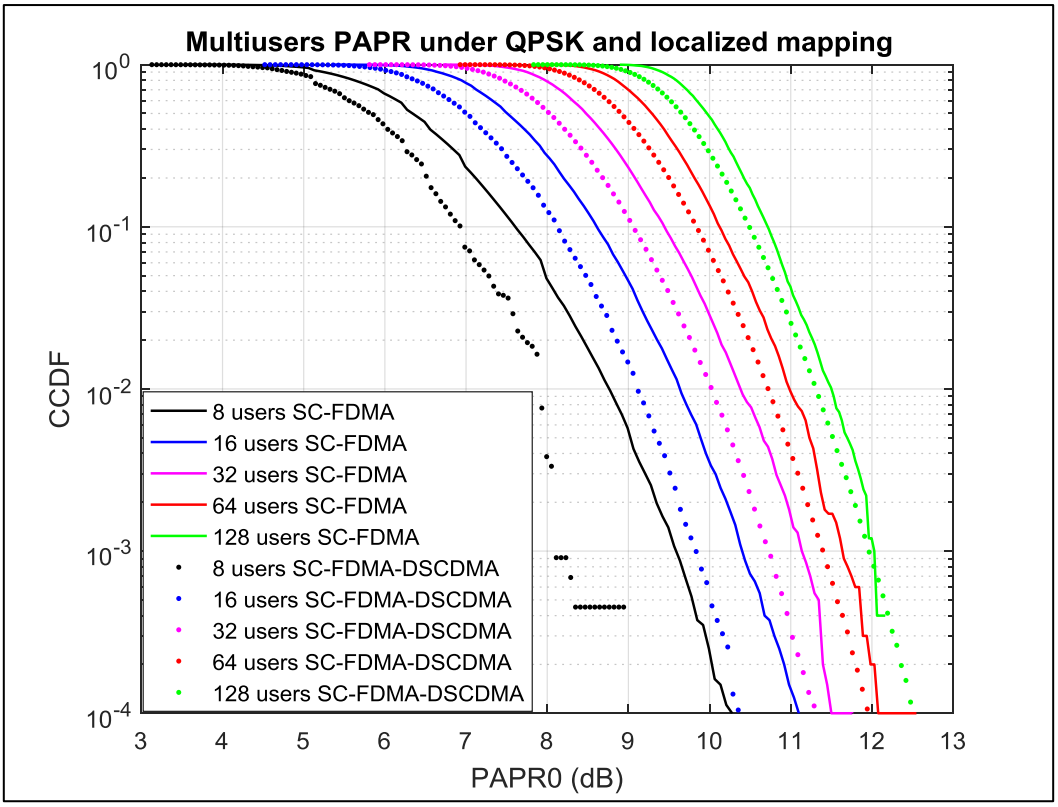

Figure (4.15): PAPR comparison between the proposed and SC-FDMA system with localized and QPSK mapping

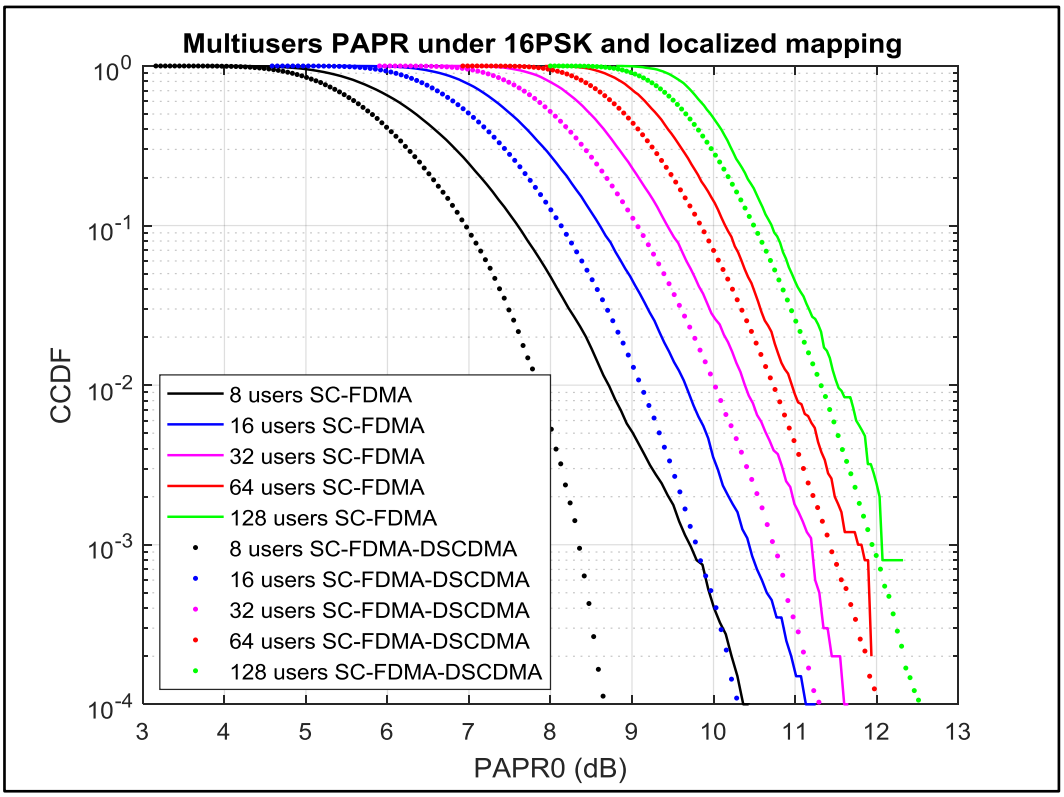

Figure (4.16): PAPR comparison between the suggested system and SC-FDMA under localized and 16PSK mapping

Figure (4.15) shows the CCDF curves of PAPR for SC-FDMA-DSCDMA and SC-FDMA systems while the modulation technique is QPSK and localized subcarrier mapping. This plot clearly shows that the proposed modified technique, that is, SC-FDMA-DSCDMA, provides the best PAPR performance than the SC-FDMA system. From the plot, it is observed that when the CCDF value is 10^{-3} and the number of a user is 8 the PAPR of the SC-FDMA-DS-CDMA is 8.1 dB while the SC-FDMA PAPR is 9.6 dB which means the proposed technique provides the best PAPR performance around 1.5 dB better than SC-FDMA. also when the number of users is 16 the PAPR of the proposed system is 9.8 dB while the SC-FDMA PAPR is 10.5 dB and so on. from Figure (4.16) it can be said the PAPR is not affected by the change in modulation level.

The PAPR comparison results between the proposed system and the traditional SC-FDMA system with interleaved subcarrier mapping are presented in Figures (4.17) and (4.18), respectively

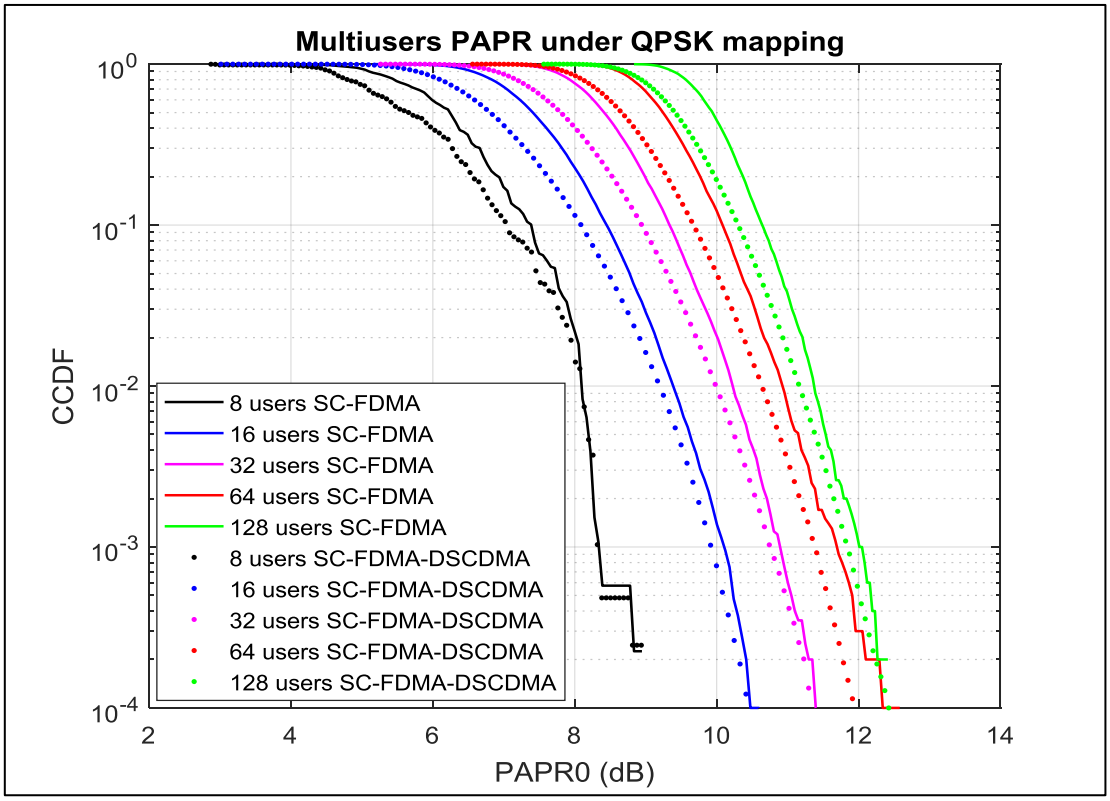

Figure (4.17): PAPR comparison between the suggested and SC-FDMA system under interleaved and QPSK mapping.

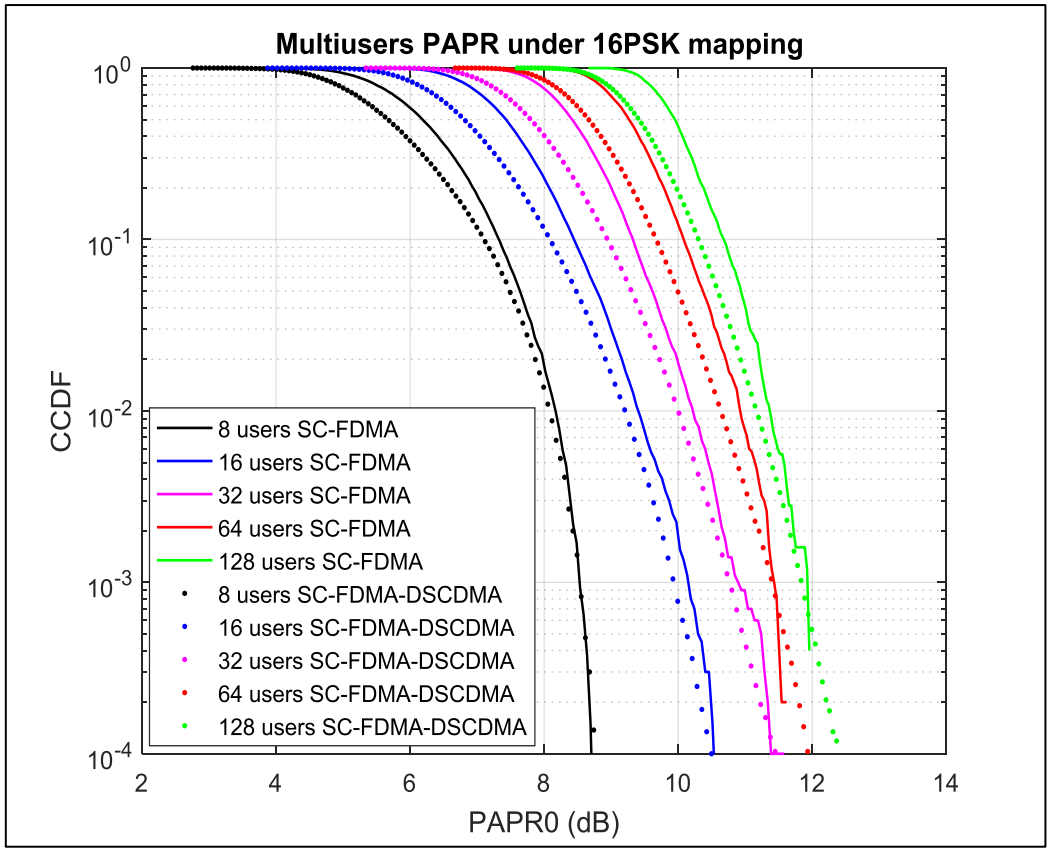

Figure (4.18): PAPR comparison between the suggested system and SC-FDMA under interleaved and 16PSK mapping.

Figure (4.17-18) shows the CCDF curves of PAPR for SC-FDMA-DSCDMA and SC-FDMA systems while the modulation technique is QPSK and interleaved subcarrier mapping. This plot clearly shows that the proposed modified technique, that is, SC-FDMA-DS-CDMA, provides PAPR performance that is almost identical to that in the SC-FDMA system at the CCDF value is 10^{-3}.

B. BER Comparison Results

The BER comparison results between the SC-FDMA-DSCDMA technique and the SC-FDMA technique are presented in this part.

i. BER Comparison with AWGN

The BER comparison results between the SC-FDMA-DSCDMA system and the traditional SC-FDMA system under the AWGN channel are presented

in this part. The parameters employed in the simulation are two modulation schemes (QPSK and 16 PSK), two kinds of subcarrier mapping (localized and interleaved), also Walsh code as spreading code. The simulation is carried out on multiple users, 8 up to 128 users.

The BER comparison results between the proposed system and the traditional SC-FDMA system with localized and interleaved subcarrier mapping are shown in Figure (4.19), Figure (4.20), Figure (4.21), and Figure (4.22), respectively.

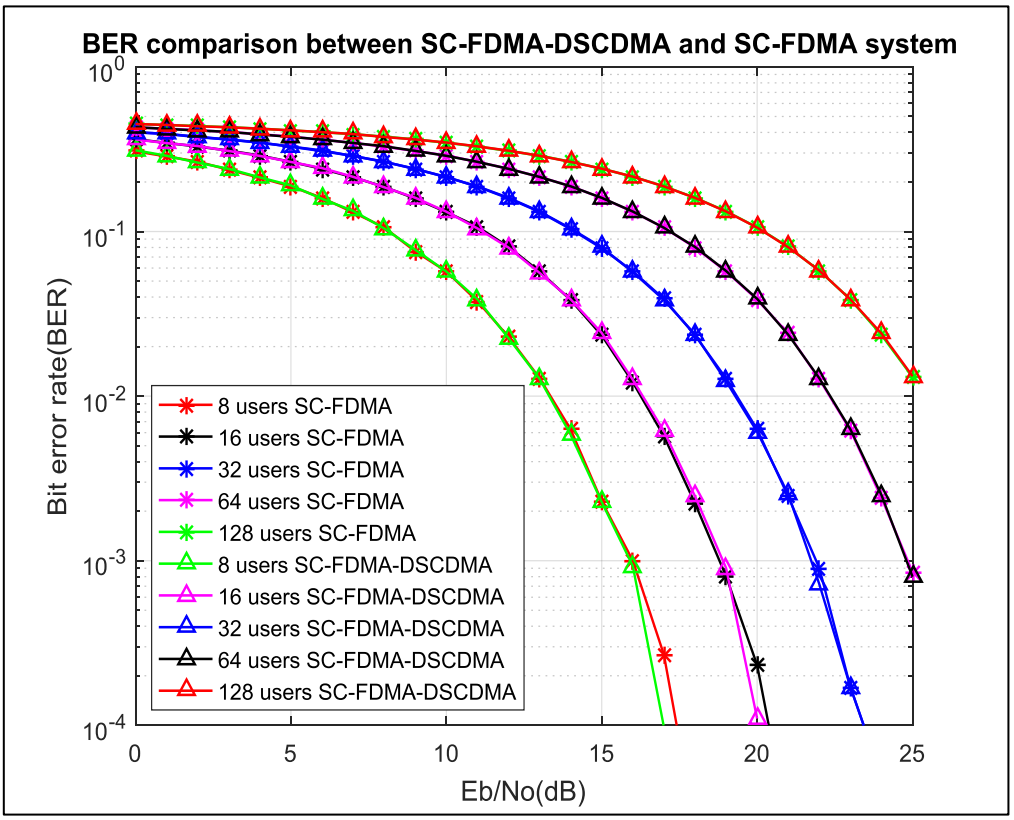

Figure (4.19): BER comparison between the proposed system and SC-FDMA with localized and QPSK under the AWGN channel.

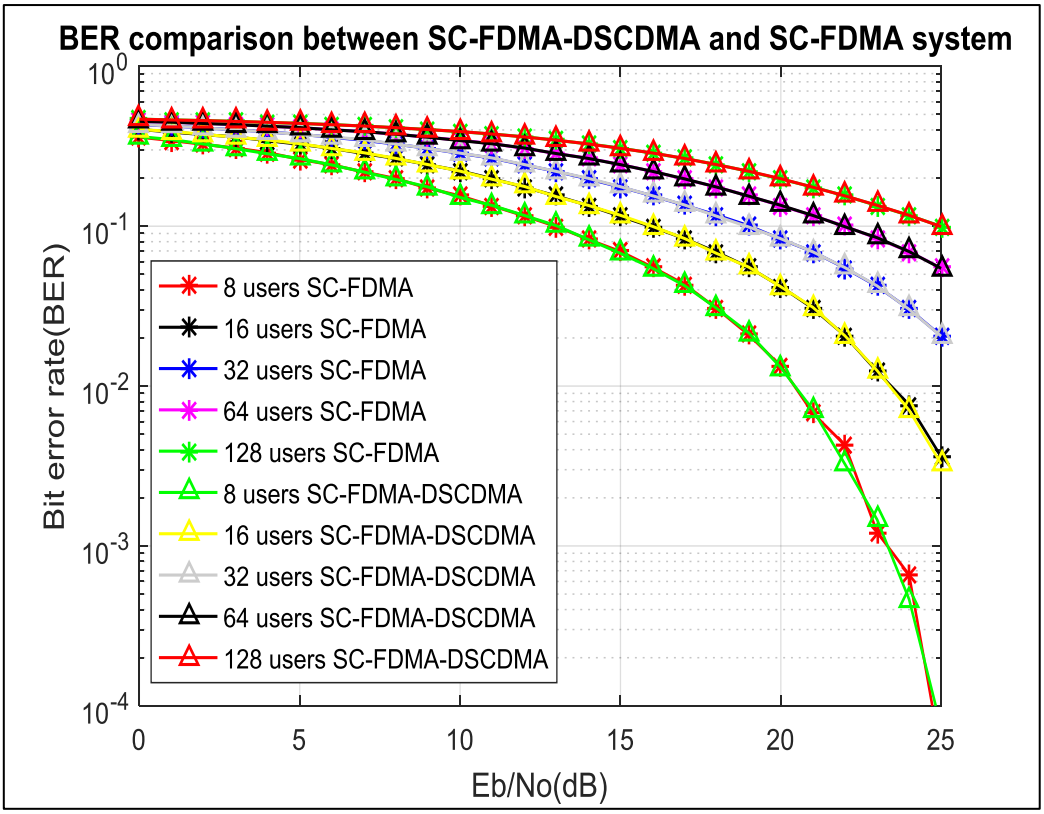

Figure (4.20): BER comparison of the suggested system and SC-FDMA under localized and 16PSK under the AWGN channel.

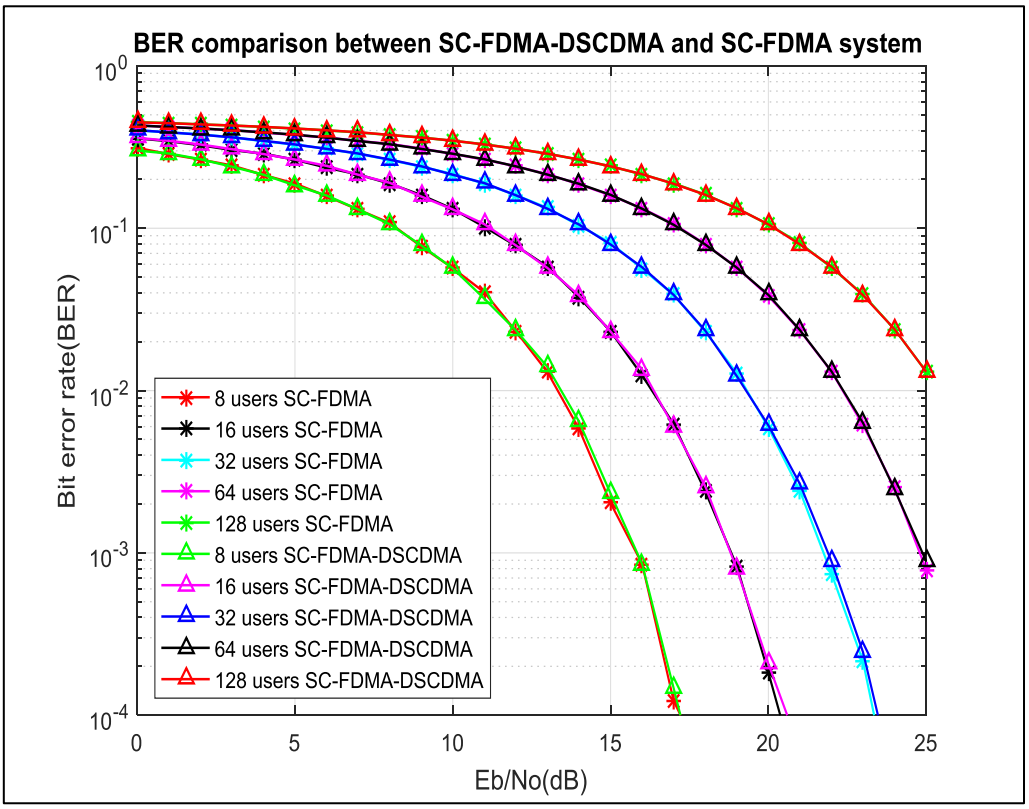

Figure (4.21): BER comparison between the suggested and SC-FDMA system under interleaved and QPSK mapping under the AWGN channel.

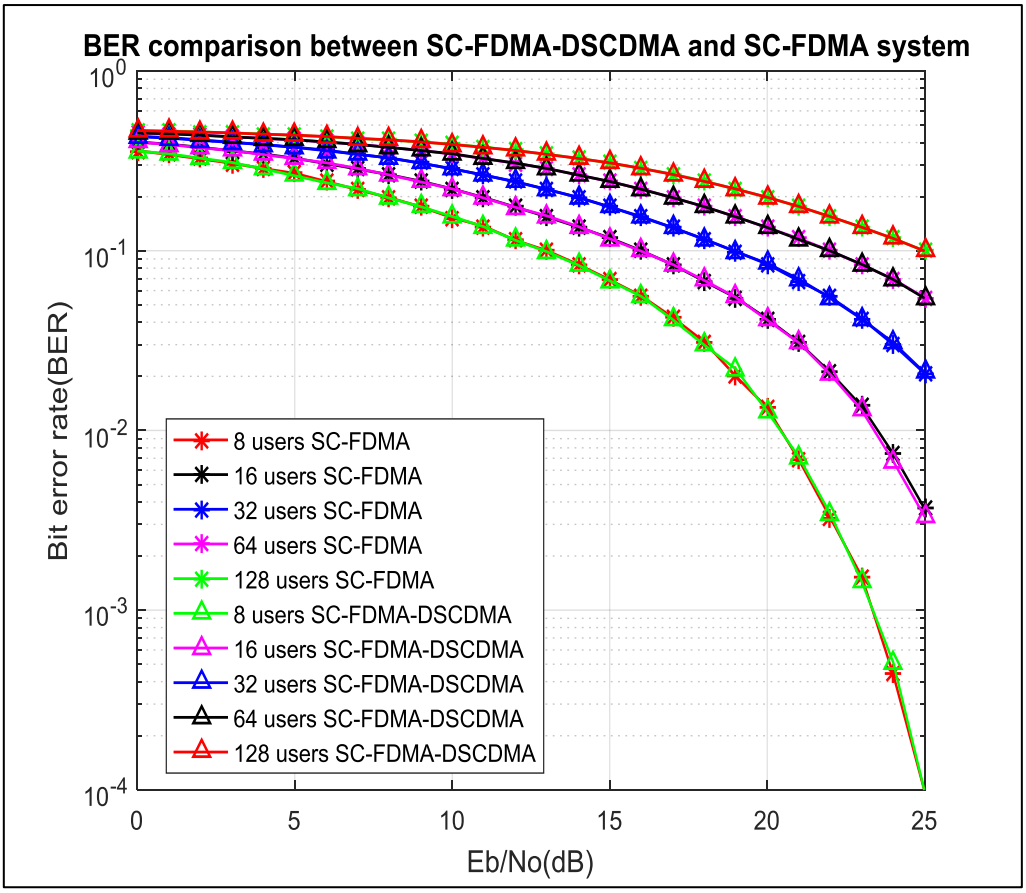

Figure (4.22): BER comparison between the suggested and SC-FDMA system under interleaved and 16PSK mapping under the AWGN channel.

It can be very clearly observed in Figures (4.19 - 20 - 21 - 22) that, the SC-FDMA-DS-CDMA BER curves are identical to the SC-FDMA BER curves. therefore the BER of the proposed system is the same as that in the traditional SC-FDMA system. when BER is 10^{-3} it can be seen that in Figures (4.19 - 21) the Eb/No required for both systems with 8 users is 16 dB which means the system behavior with localized mapping is the same when employing the interleaved mapping. In addition, by observing the figures, we notice that when the number of users increases, the Eb/No value needed by the system increases to obtain the same percentage of errors. For example, in Figure (4.19), the system needs an Eb/No value of 16 dB to reach an error rate of 10^{-3} when the number of users is 8, while it needs approximately 19 dB When the number of users is 16, and also to 22 dB, when the number of users is 32, and so on. Therefore, it can be said that when users increase, the percentage of errors

increases, and this is due to the reason that when the number of users increases, the size of the transmitted packet data increases, and therefore the percentage of errors increases.

ii. BER Comparison with The Rayleigh Channel

The BER comparison results between the SC-FDMA-DSCDMA system and the traditional SC-FDMA system under the Rayleigh channel are presented in this part. The parameters employed in the simulation are two modulation schemes (QPSK and 16 PSK), two kinds of subcarrier mapping (localized and interleaved), also Walsh code as spreading code.

The BER comparison results between the proposed system and the traditional SC-FDMA system with localized subcarrier mapping are presented in Figures (4.23) and (4.24), respectively. In contrast, the same results are presented using interleaved subcarrier mapping, as presented in Figures (4.25) and (4.26).

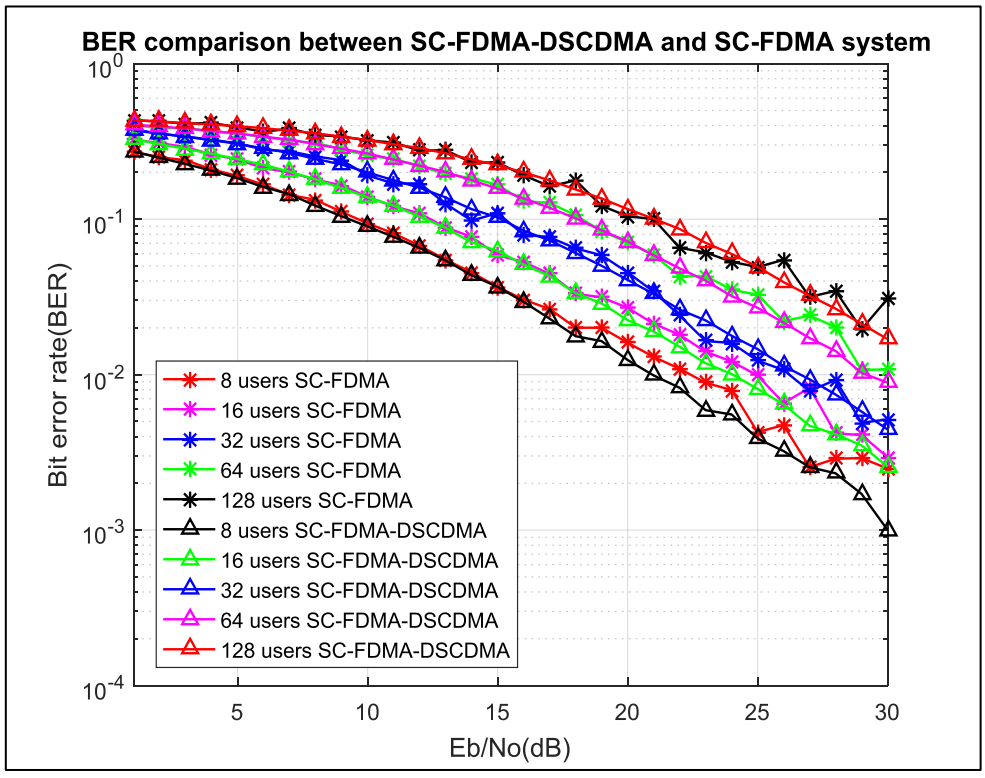

Figure (4.23): BER comparison between the proposed and SC-FDMA system with localized and QPSK mapping under the Rayleigh channel.

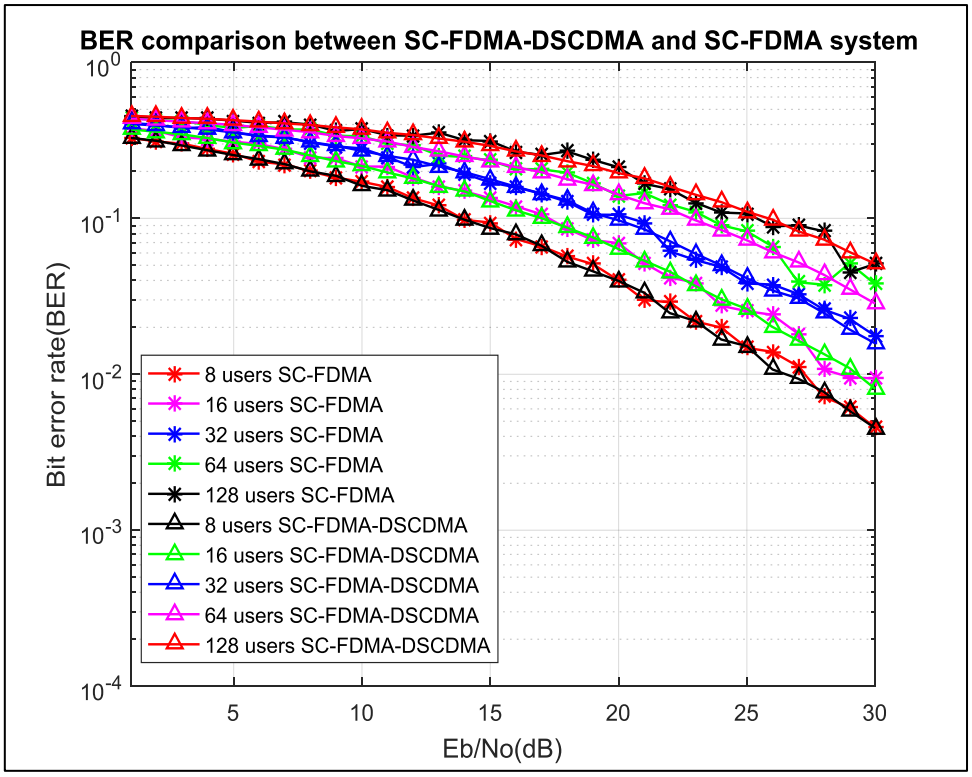

Figure (4.24): BER comparison between the suggested and SC-FDMA system under localized and 16PSK mapping under the Rayleigh channel.

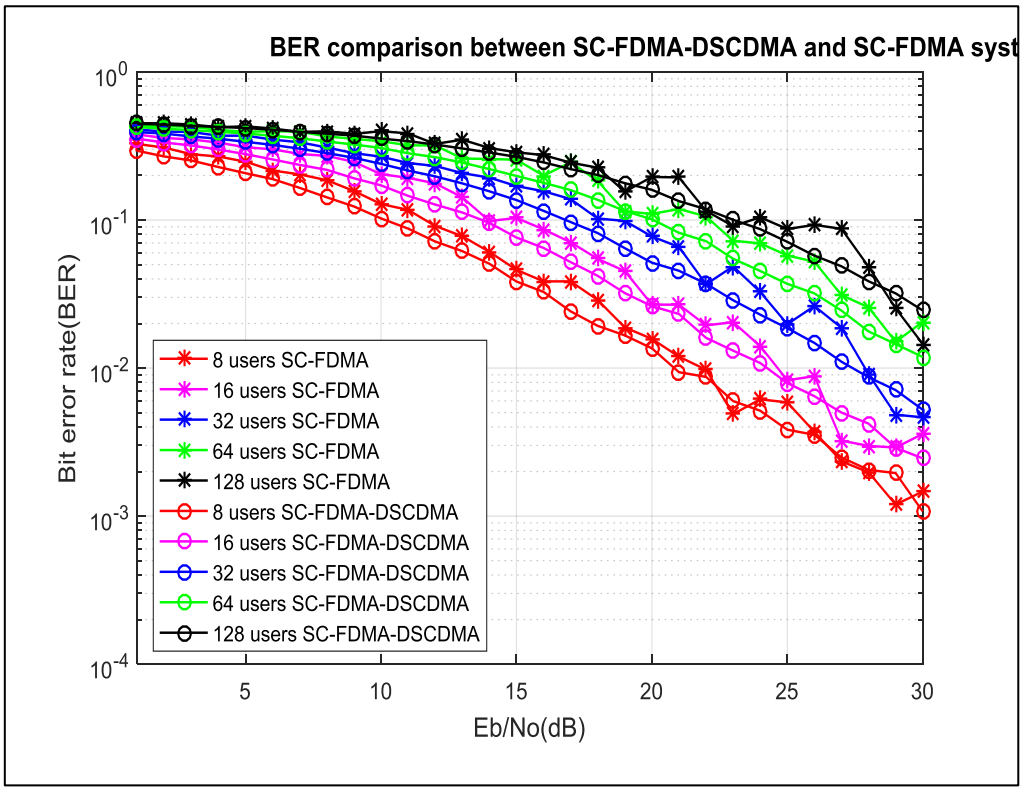

Figure (4.25): BER comparison between the suggested system and SC-FDMA under interleaved and QPSK through the Rayleigh channel.

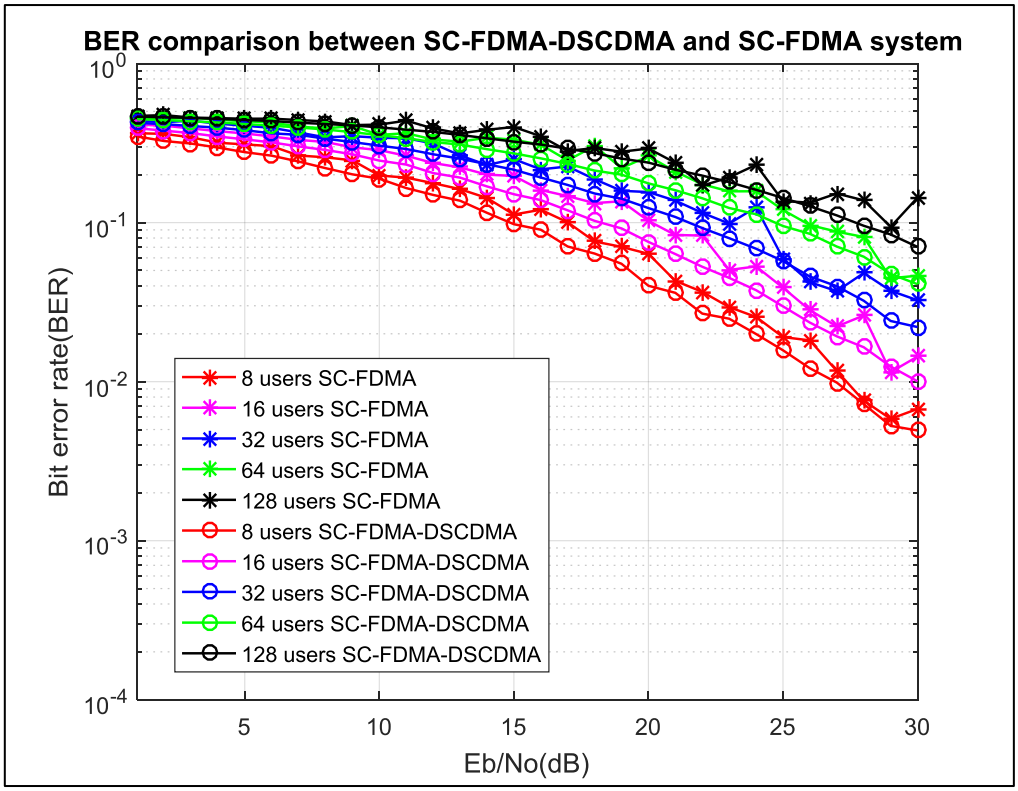

Figure (4.26): BER comparison between the suggested system and SC-FDMA under interleaved mapping, QPSK, and Rayleigh channel.

It can be very clearly observed in Figures (4.23 - 24 - 25 - 26) that, the SC-FDMA-DS-CDMA BER curves are almost approximated to the SC-FDMA BER curves. when BER is 10^{-2} it can be seen that in Figure (4.23) the Eb/No required for the SC-FDMA-DS-CDMA system with 8 users is 21.6 dB and in SC-FDMA is 22 dB while with 16 users the SC-FDMA-DS-CDMA system required 24.6 dB and SC-FDMA required 25 dB while with 32 users the Eb/No required for the SC-FDMA-DS-CDMA system is 27 dB and SC-FDMA required also 27 dB, therefore, there are slightly different in the behavior of the two systems and their performance start to be identical when the number of users increases.

4.5 Proposed System with Different Spreading Sequences

This section has two parts that show the simulation results of the proposed SC-FDMA-DSCDMA system using multiple types of code sequences (Walsh-Hadamard sequences, OVSF codes, Maximum-length sequences "m-

sequences", and Gold codes). The first part represents the results in terms of PAPR and the second in terms of BER. Because of the odd length of the sequences that are generated by LFSR and also because of the length of the preferred pairs that are used to generate gold sequences, the simulation is carried out on individual numbers of users starting from 31 to 127. The parameters employed in the simulation are two modulation schemes (QPSK and 16 PSK), two kinds of subcarrier mapping (localized and interleaved), and also two channel models (AWGN and Rayleigh).

4.5.1PAPR Results with Different Spreading Sequences

The PAPR results of simulating the proposed system using different spreading codes are presented in this part.

I. Localized Subcarriers Mapping

The simulation results of the SC-FDMA-DSCDMA under different spreading codes and using localized subcarrier mapping are presented in Figures (4.27), (4.28), (4.29), (4.30), (4.31), and (4.32).

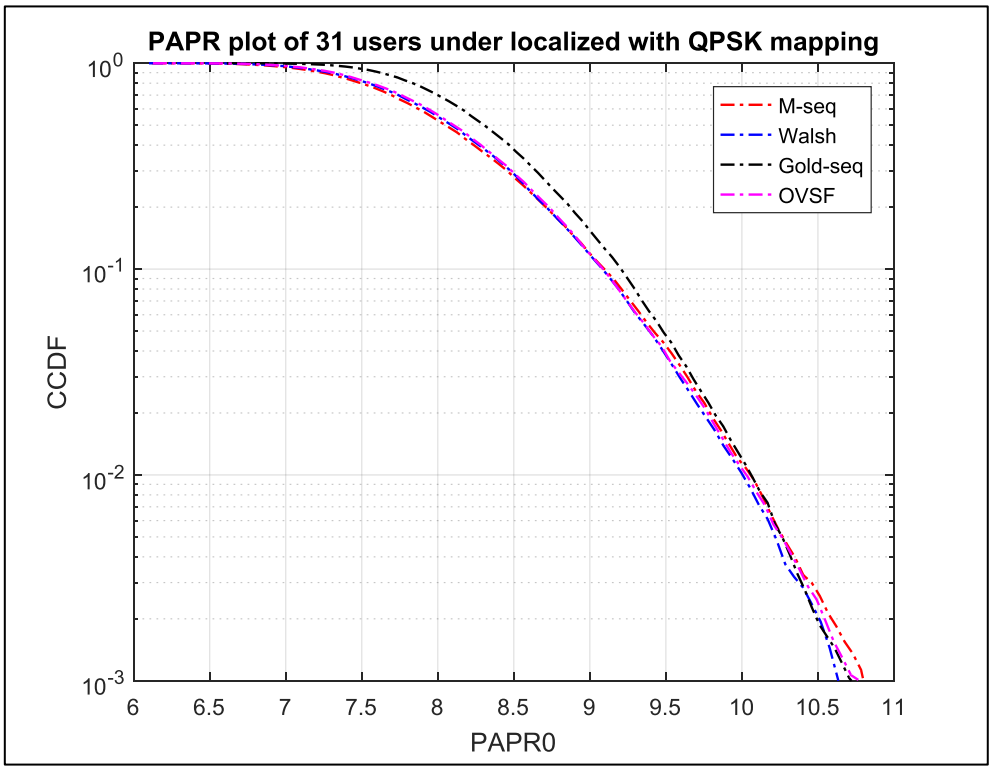

Figure (4.27): PAPR of the proposed system for 31 users with QPSK modulation and localized mapping.

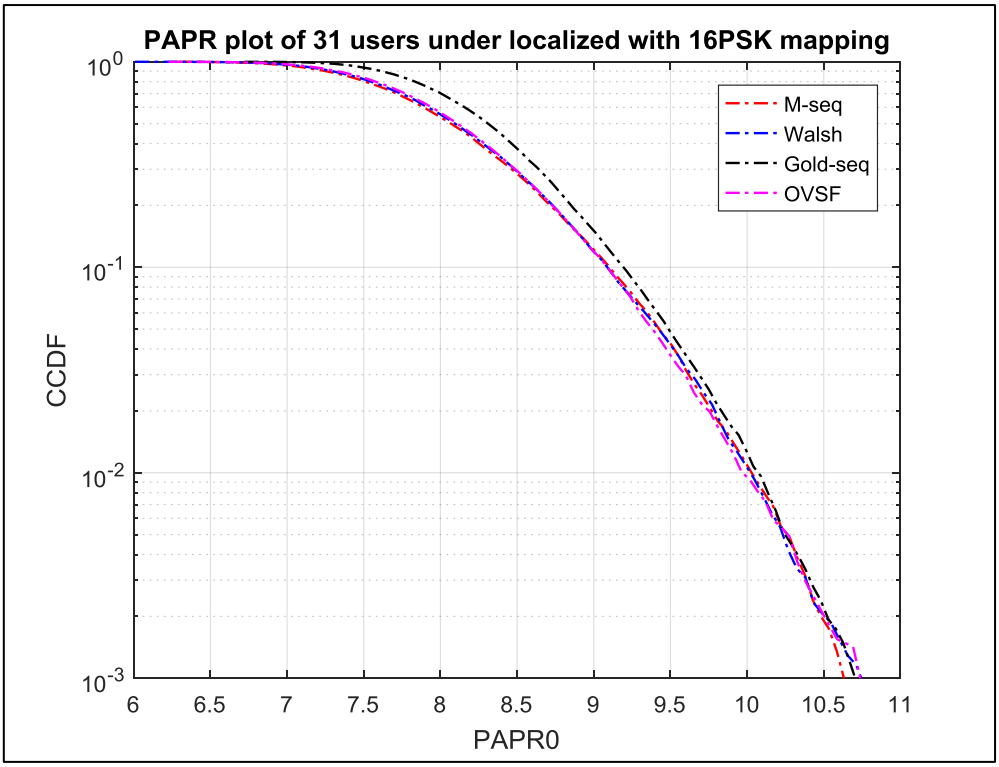

Figure (4.28): PAPR of the proposed system for 31 users with 16PSK modulation and localized mapping.

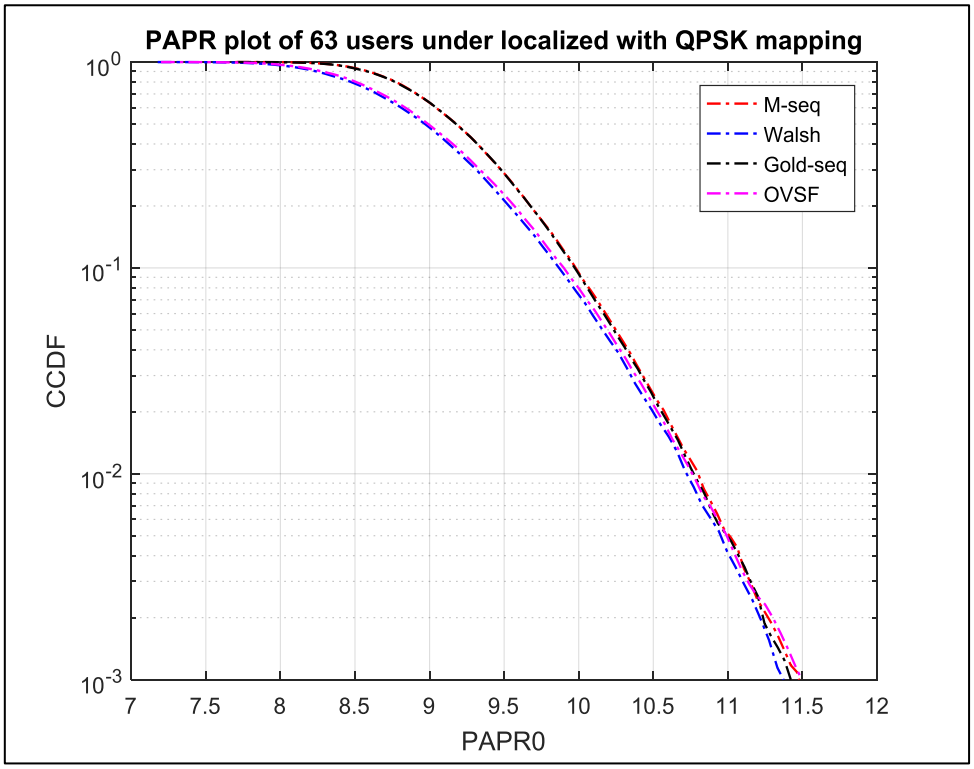

Figure (4.29): PAPR of the proposed system for 63 users with QPSK modulation and localized mapping.

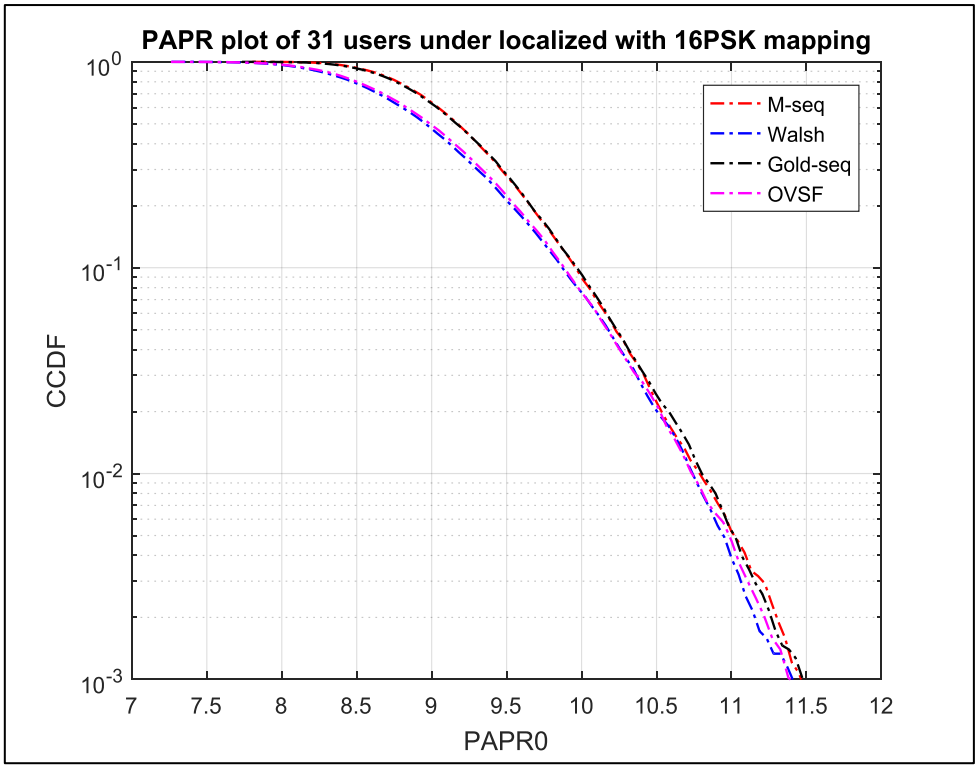

Figure (4.30): PAPR of the proposed system for 63 users with 16PSK modulation and localized mapping.

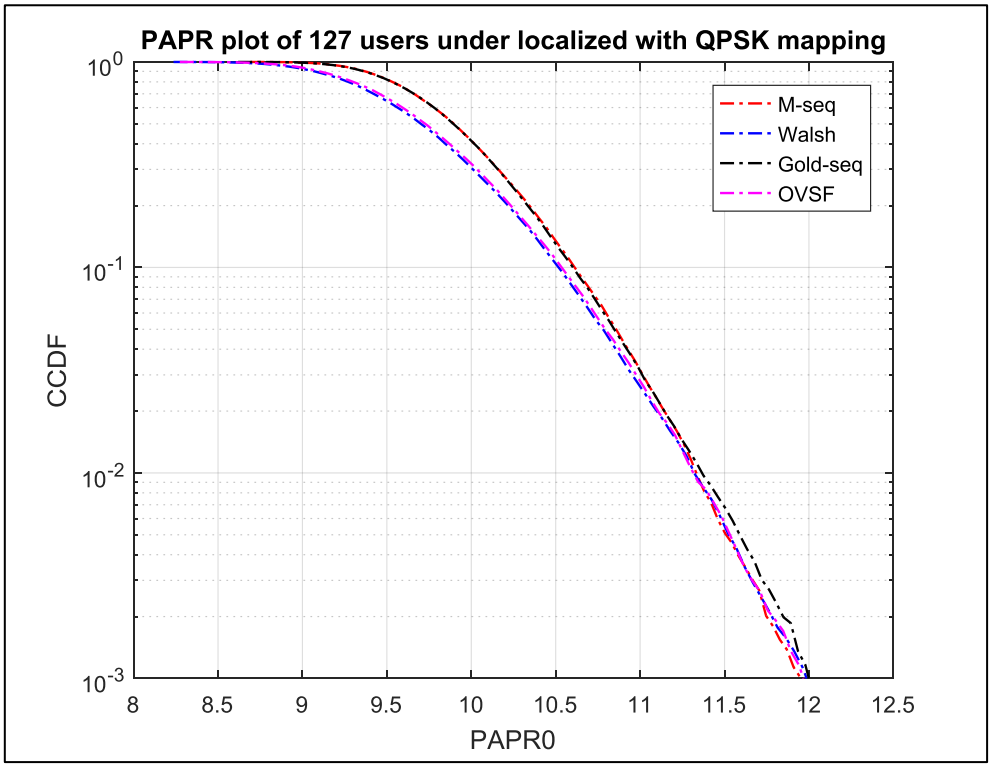

Figure (4.31): PAPR of the proposed system for 127 users with QPSK modulation and localized mapping.

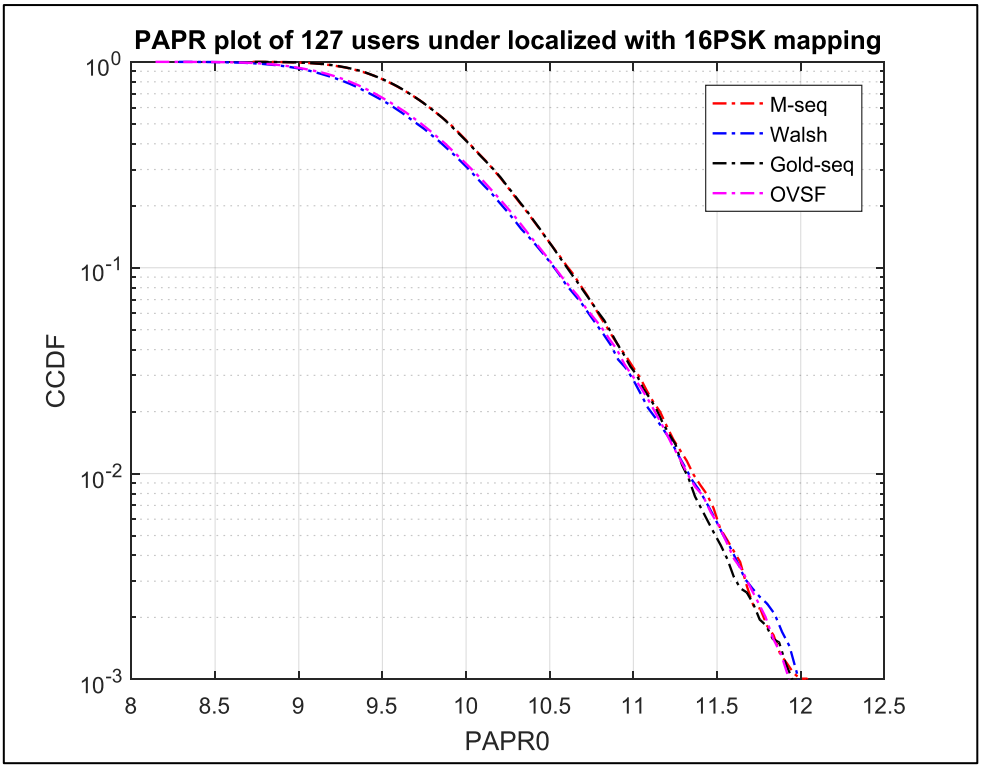

Figure (4.32): PAPR of the proposed system for 127 users with 16PSK modulation and localized mapping.

It can be very clearly observed in Figures (4.27 - 28 - 29 - 30 - 31- 32) that, the SC-FDMA-DS-CDMA PAPR result at a specific CCDF value are almost similar when employing multiple types of code sequences (Walsh-Hadamard sequences, OVSF codes, Maximum-length sequences "m-sequences", and Gold codes) for example when CCDF value is 10-2 the PAPR is ranged from 10 to 10.1 dB, therefore, this difference very small we can say that the PAPR of the proposed system under localized mapping and multiple users are the same when using Walsh-Hadamard sequences, OVSF codes, Maximum-length sequences "m-sequences", or Gold codes.

II. Interleaved Subcarriers Mapping

The simulation results of the SC-FDMA-DSCDMA under different spreading codes and using interleaved subcarrier mapping are presented in Figures (4.33), (4.34), (4.35), (4.36), (4.37), and (4.38).

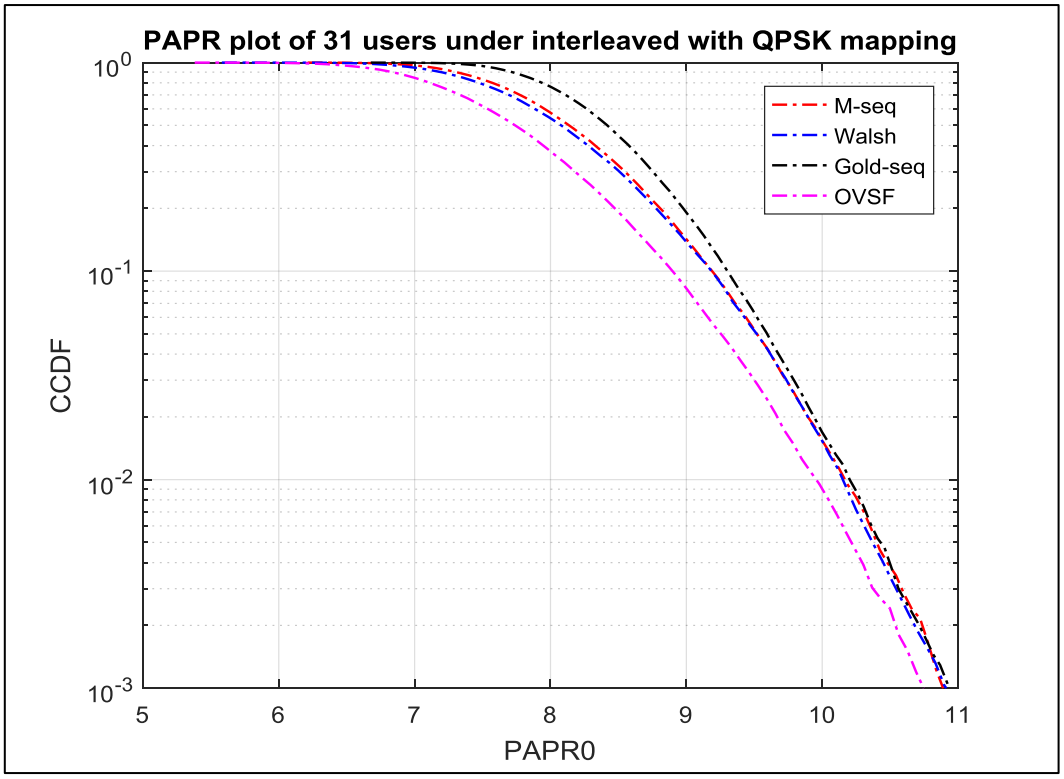

Figure (4.33): PAPR of the proposed system for 31 users with QPSK modulation and interleaved mapping.

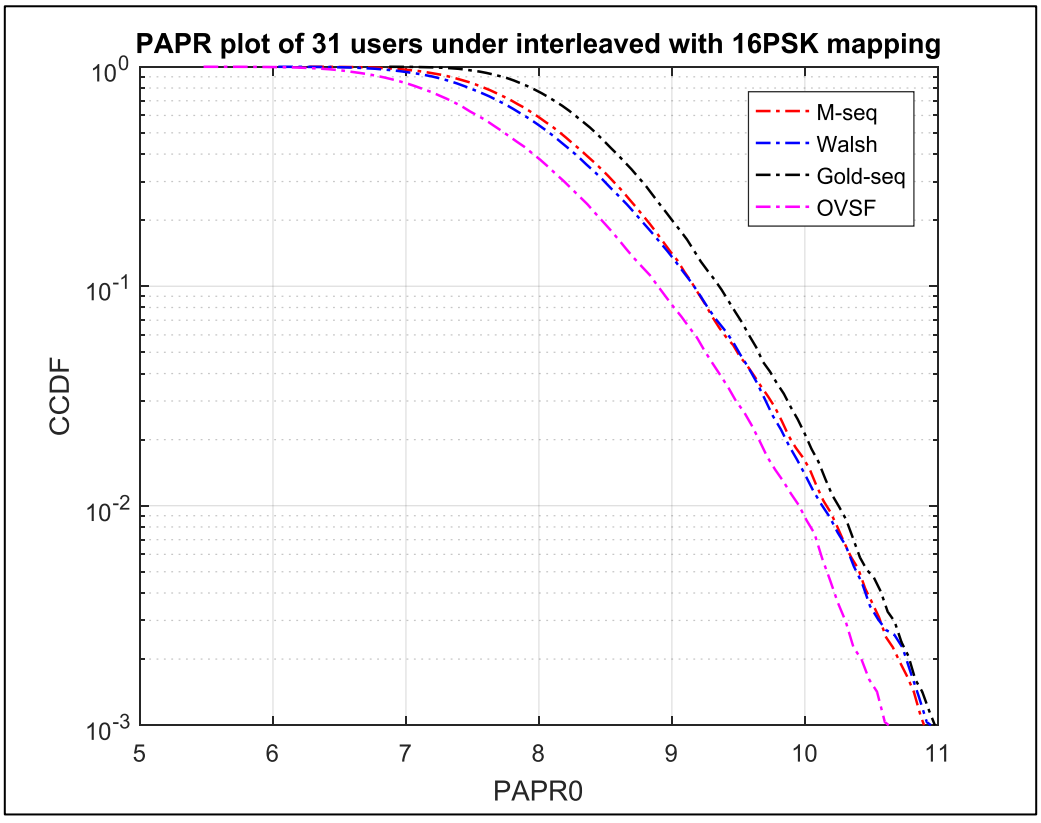

Figure (4.34): PAPR of the proposed system for 31 users with 16PSK modulation and interleaved mapping.

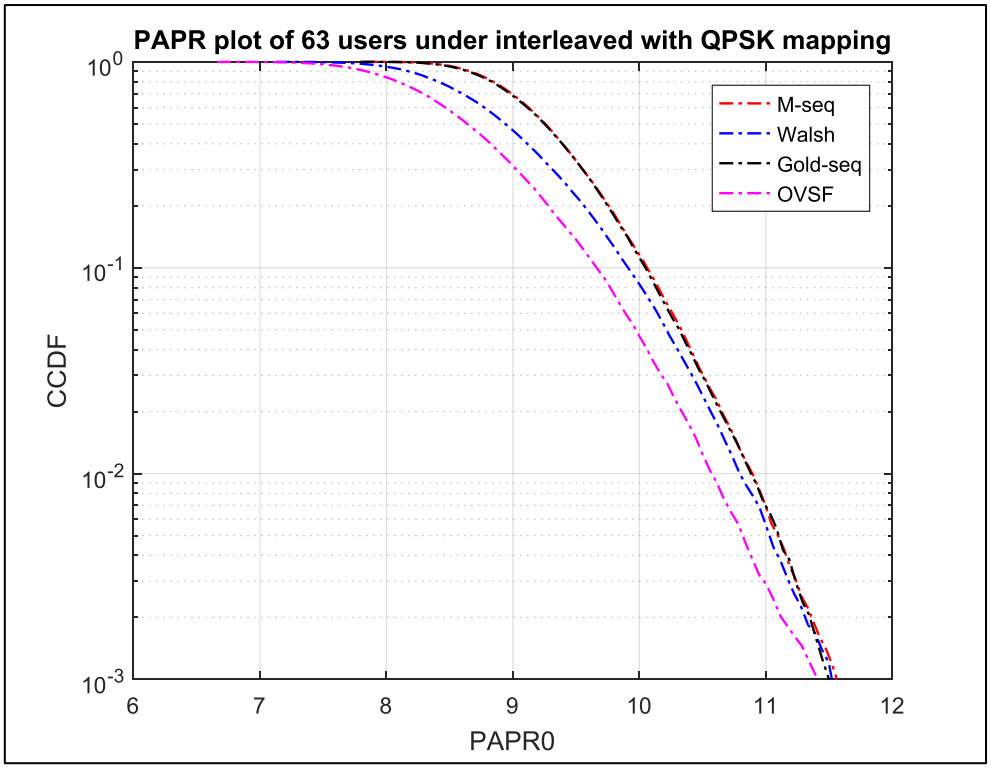

Figure (4.35): PAPR of the proposed system for 63 users with QPSK modulation and interleaved mapping.

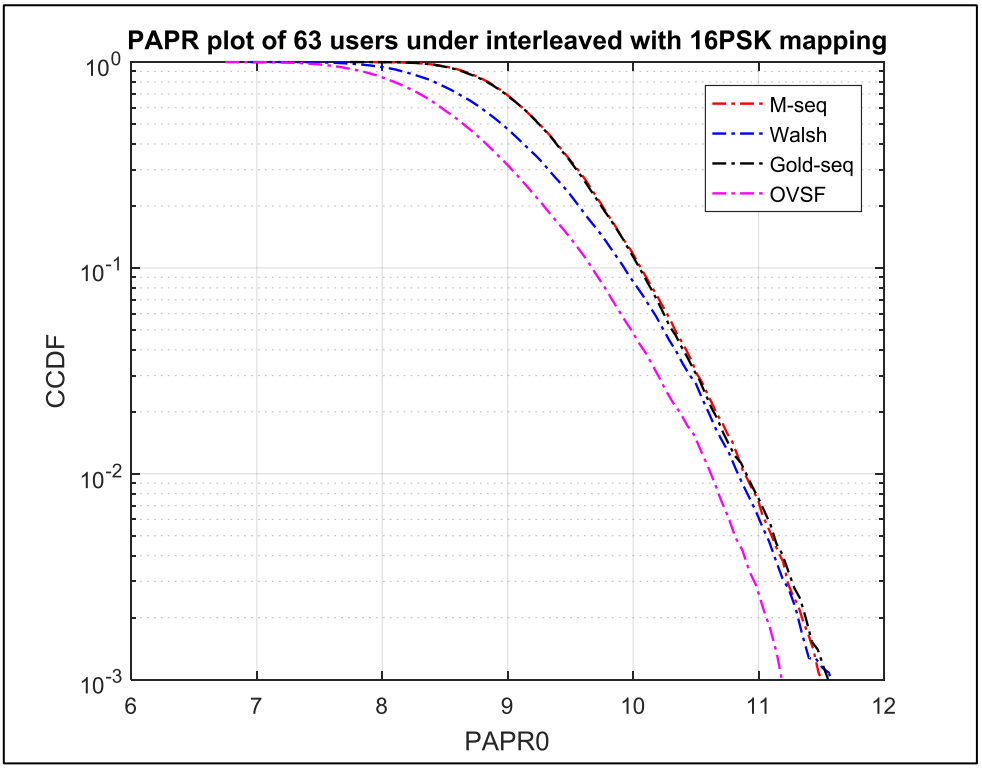

Figure (4.36): PAPR of the proposed system for 63 users with 16PSK modulation and interleaved mapping.

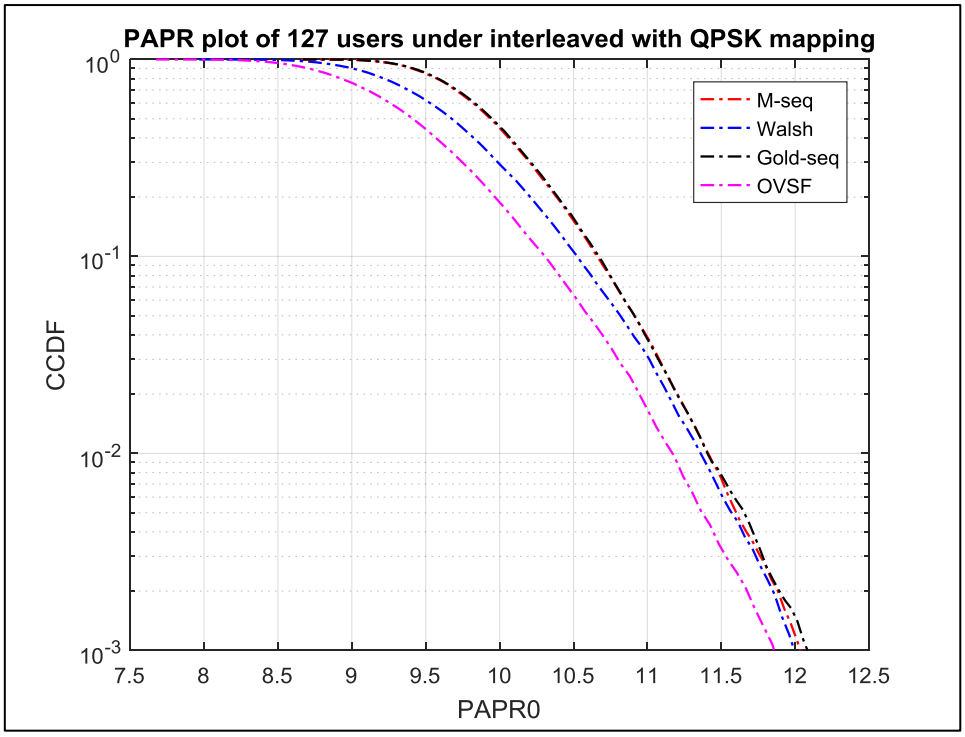

Figure (4.37): PAPR of the proposed system for 127 users with QPSK modulation and interleaved mapping.

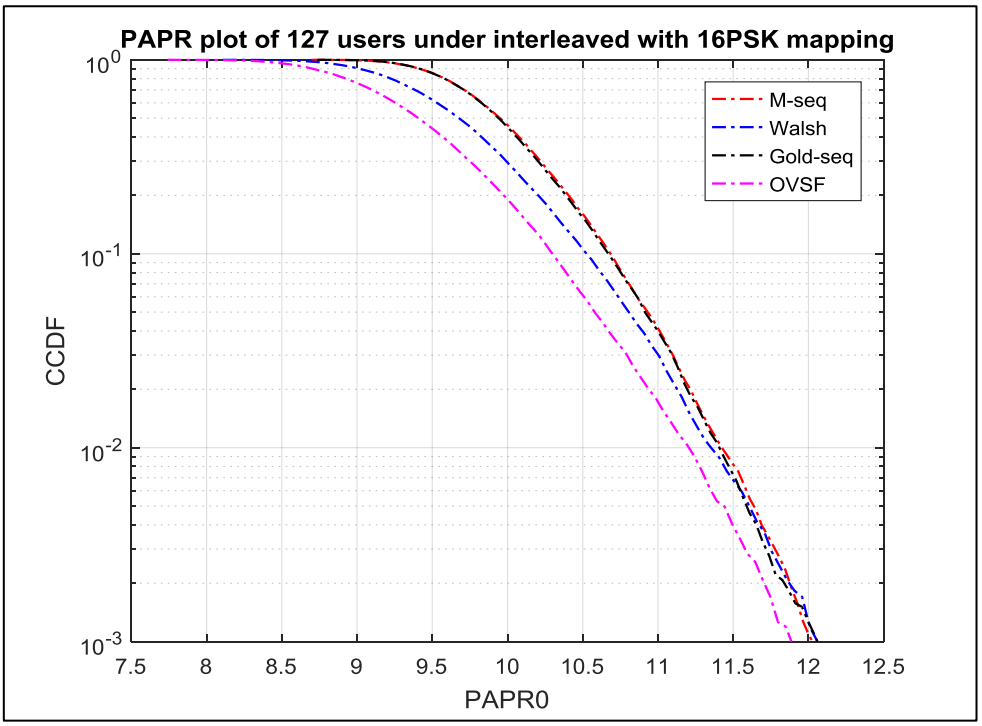

Figure (4.38): PAPR of the proposed system for 127 users with 16PSK modulation and interleaved mapping.

It can be very clearly observed in Figures (4.33 - 34 - 35 - 36 - 37- 38) that, the SC-FDMA-DS-CDMA PAPR is better with the OVSF code than the other

spreading code. it can be seen in Figure (4.33) at the CCDF value is 10^{-3} the PAPR with the OVSF code is 10.7 dB while the PAPR with the other spreading codes is approaching 11 dB. In addition, by observing the figures, we notice that when the number of users increases, the PAPR increases. For example, in Figure (4.33), at the CCDF value 10^{-3}, the PAPR of the proposed system with the OVSF code is 10.7 dB while as shown in Figure (4.35) the PAPR of the proposed system with 63 users is 11.1 dB and in Figure (4.37) the PAPR of the proposed system with 127 users is 11.8 dB. In fact, the PAPR increases with an increasing number of users due to the increase in the number of subcarriers which leads to an increase in the linear combination of the IDFT process.

4.5.2BER Results with Different Spreading Sequences

In this part, the proposed system's BER results are evaluated using the QPSK and 16PSK modulation techniques. Localized and interleaved are used for subcarrier mapping. The AWGN and Rayleigh models are utilized as channel models.

A. BER with AWGN Channel

The BER results of simulating the proposed system using different spreading codes and multiple users under the AWGN channel are presented in this part as follows.

I. Localized Subcarrier Mapping

The BER results of the proposed system with AWGN channel using localized subcarrier mapping and QPSK,16 PSK as a modulation method, are shown in Figures (4.39), (4.40), and (4.41).

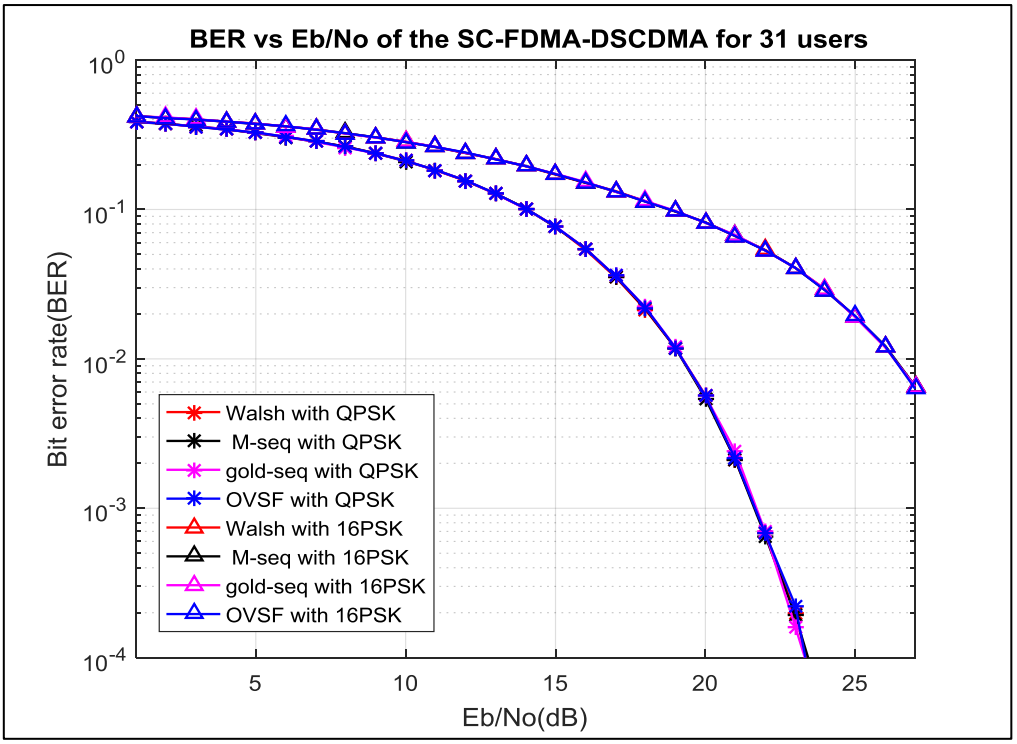

Figure (4.39): BER of the proposed system for 31 users with localized subcarriers mapping under the AWGN channel.

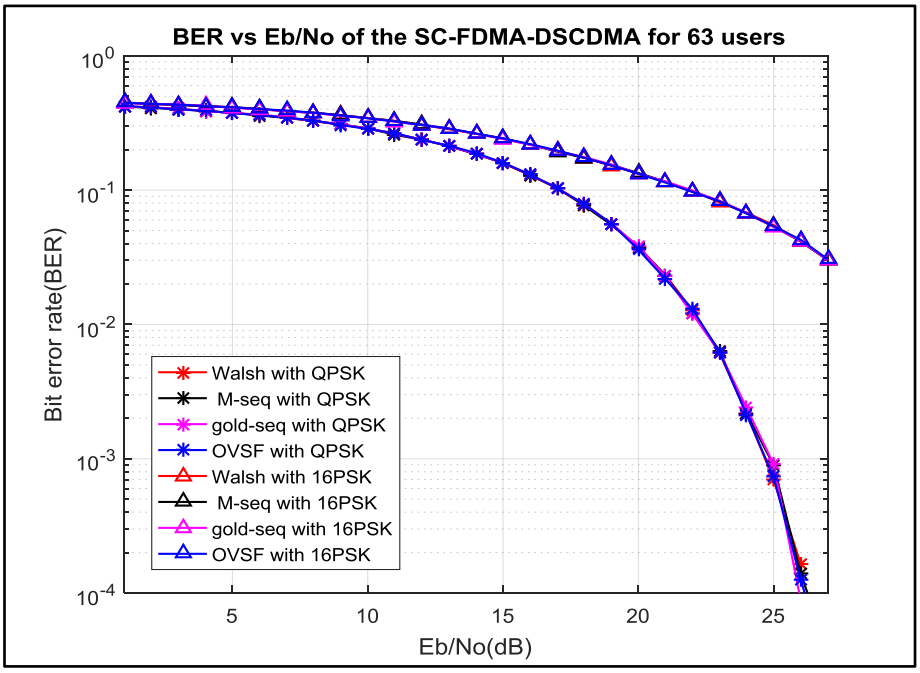

Figure (4.40): BER of the suggested system for 63 users with localized subcarriers mapping under the AWGN channel.

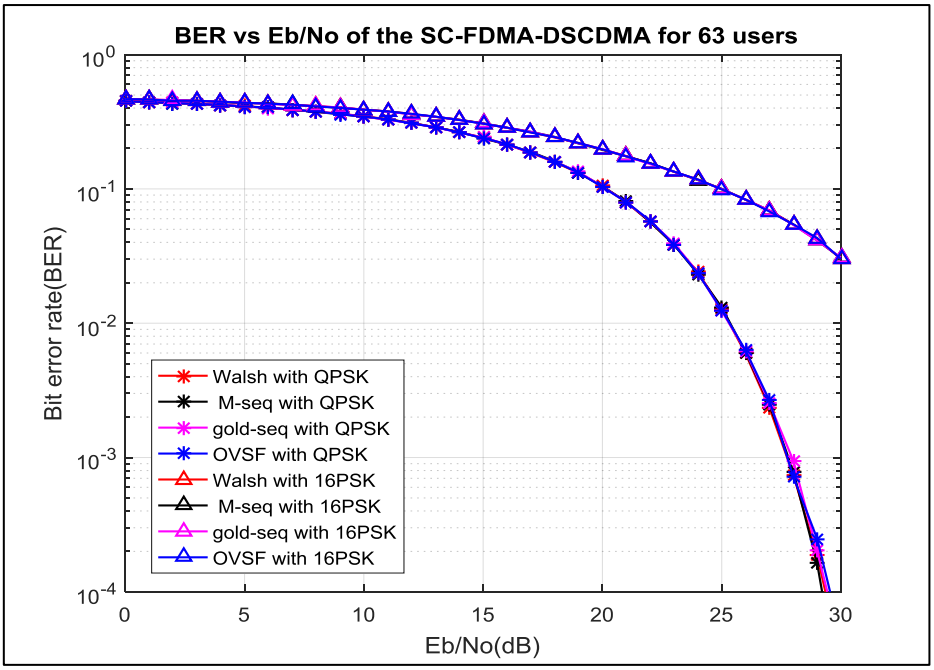

Figure (4.41): BER of the suggested system for 127 users with localized subcarriers mapping under the AWGN channel.

II. BER Interleaved Sub-carrier Mapping

The BER results of the proposed approach with AWGN channel using localized subcarrier mapping and QPSK,16 PSK as a modulation method, are shown in Figures (4.42), (4.43), and (4.44).

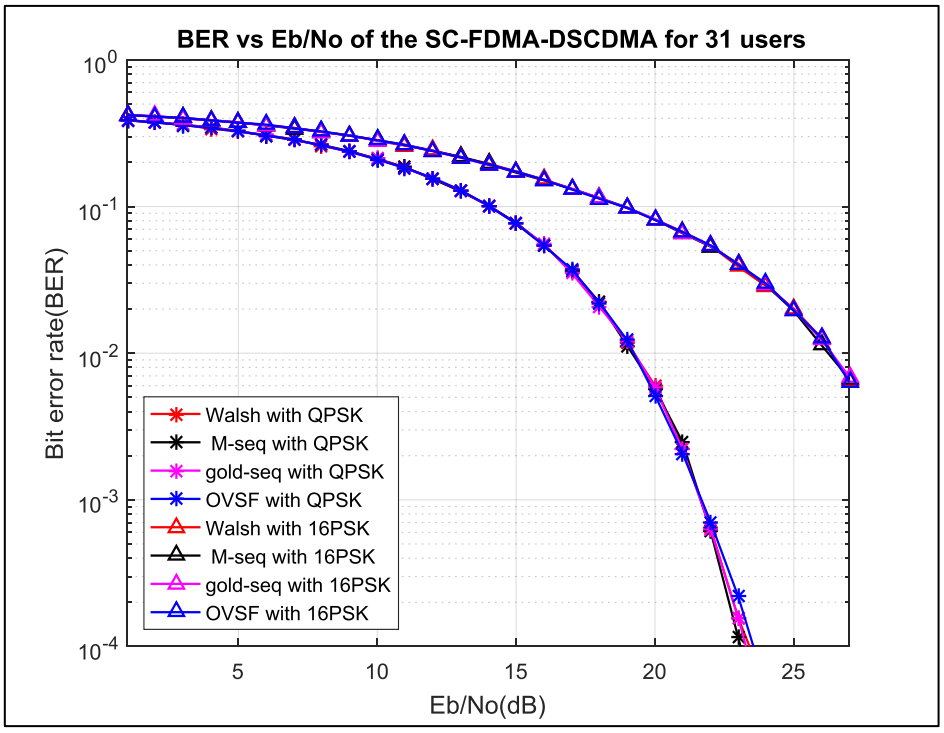

Figure (4.42): BER of the suggested system for 31 users with interleaved subcarriers mapping under the AWGN channel.

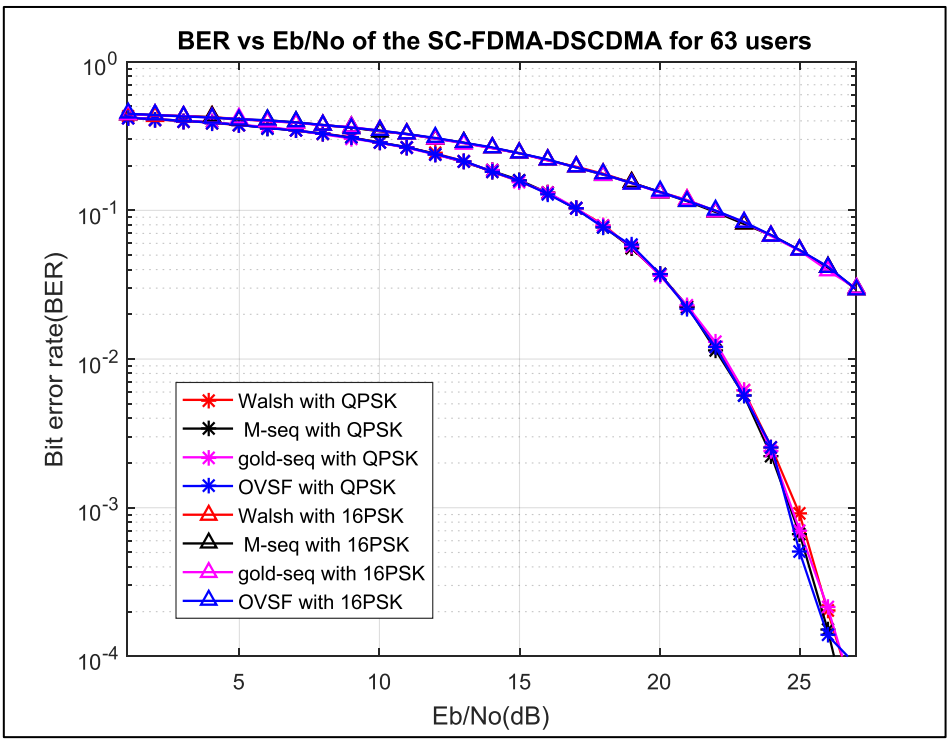

Figure (4.43): BER of the suggested system for 63 users with interleaved subcarriers mapping under the AWGN channel.

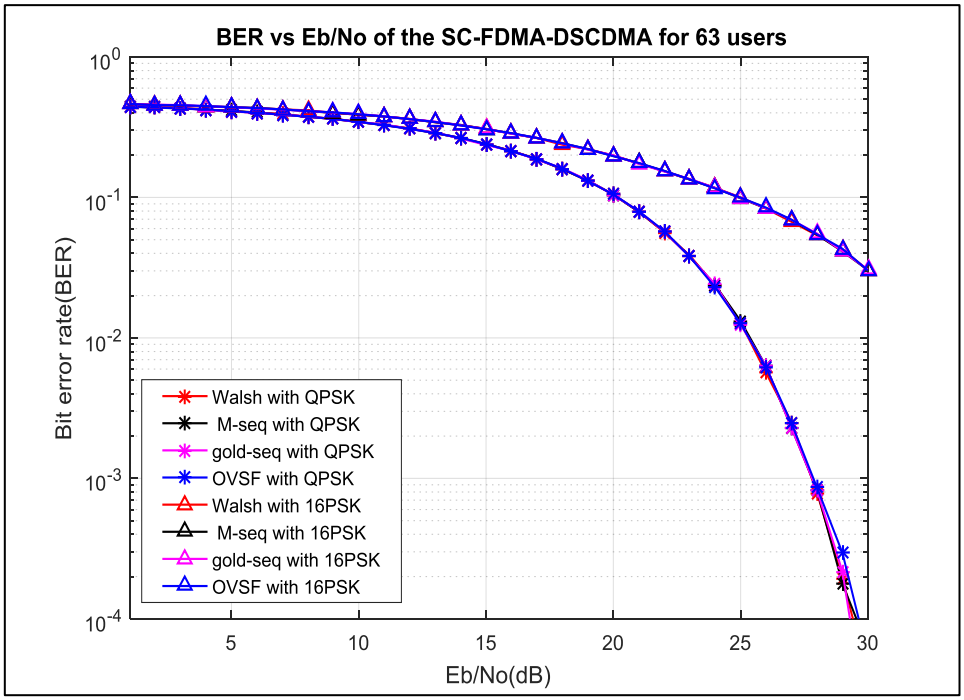

Figure (4.44): BER of the suggested system for 127 users with interleaved subcarriers mapping under AWGN.

B. BER with Rayleigh Channel

The BER results of simulating the proposed system using different spreading codes and multiple users under the Rayleigh fading channel are presented in this part as follows.

I. Localized subcarriers mapping

The BER results of the proposed system with Rayleigh channel using localized subcarrier mapping and QPSK,16 PSK as a modulation method, are shown in Figures (4.45), (4.46), and (4.47).

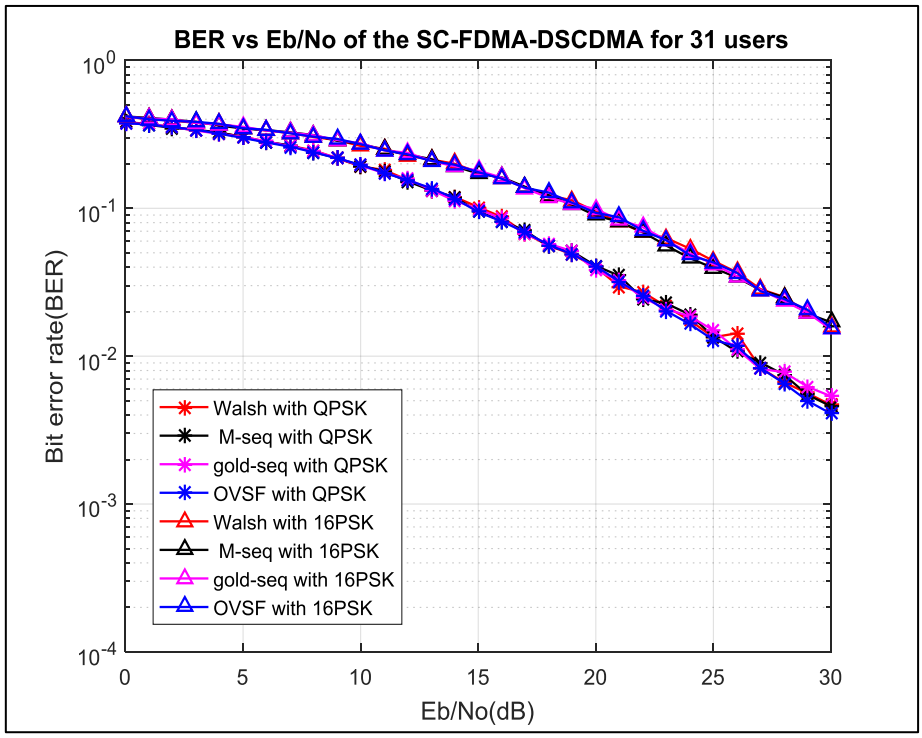

Figure (4.45): BER of the proposed system for 31 users with localized subcarriers mapping under the Rayleigh channel.

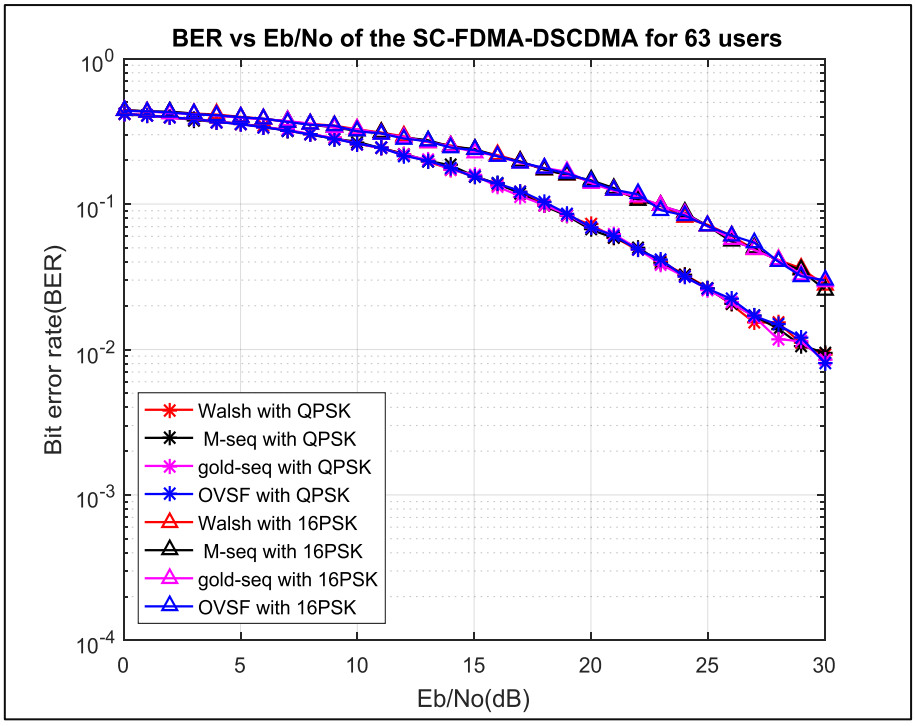

Figure (4.46): BER of the suggested system for 63 users with localized subcarriers mapping under the Rayleigh channel.

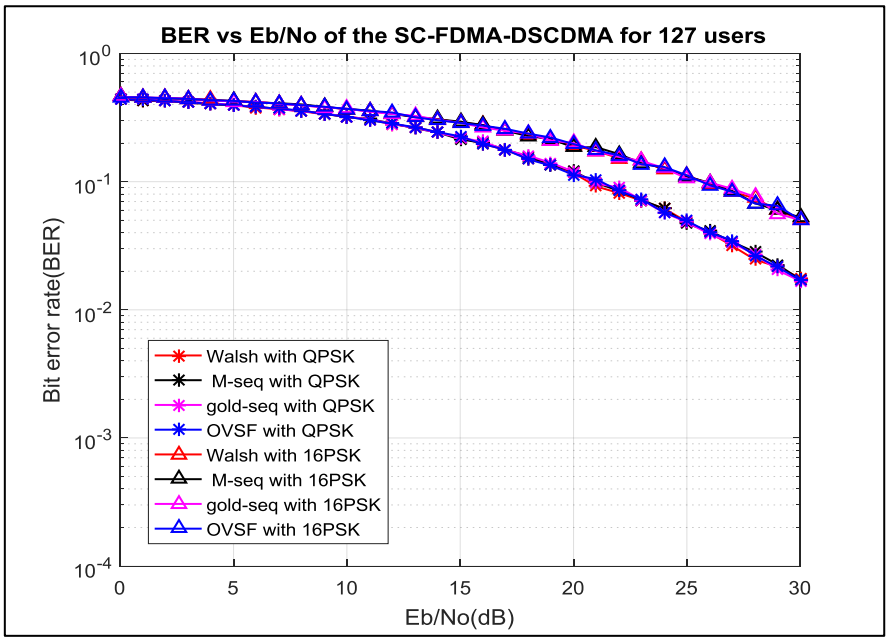

Figure (4.47): BER of the suggested system for 127 users with localized subcarriers mapping under the Rayleigh channel.

II. Interleaved subcarriers mapping

The BER results of the proposed system with Rayleigh channel using interleaved subcarrier mapping and QPSK,16 PSK as a modulation method, are shown in Figures (4.48), (4.49), and (4.50).

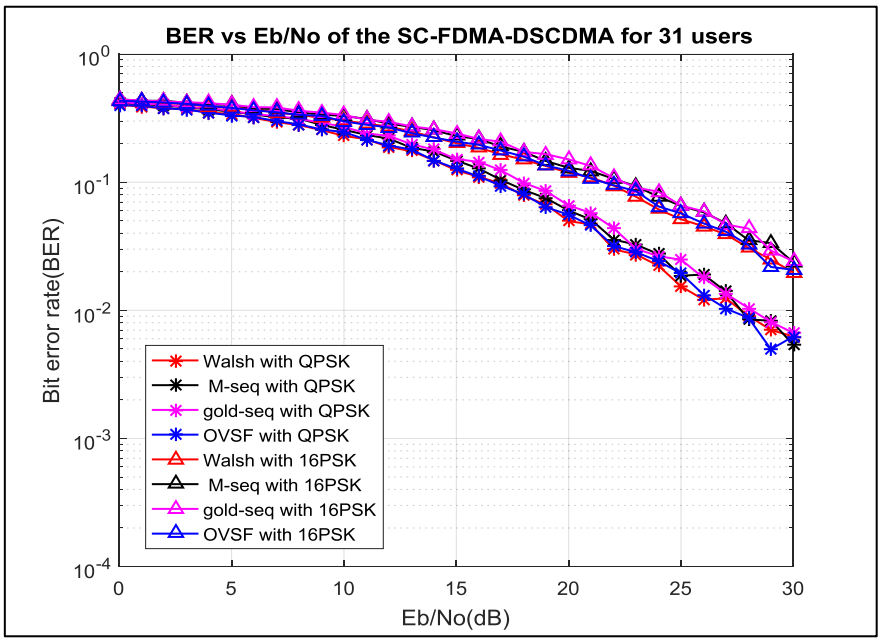

Figure (4.48): BER of the suggested system for 31 users with interleaved subcarriers mapping under the Rayleigh channel.

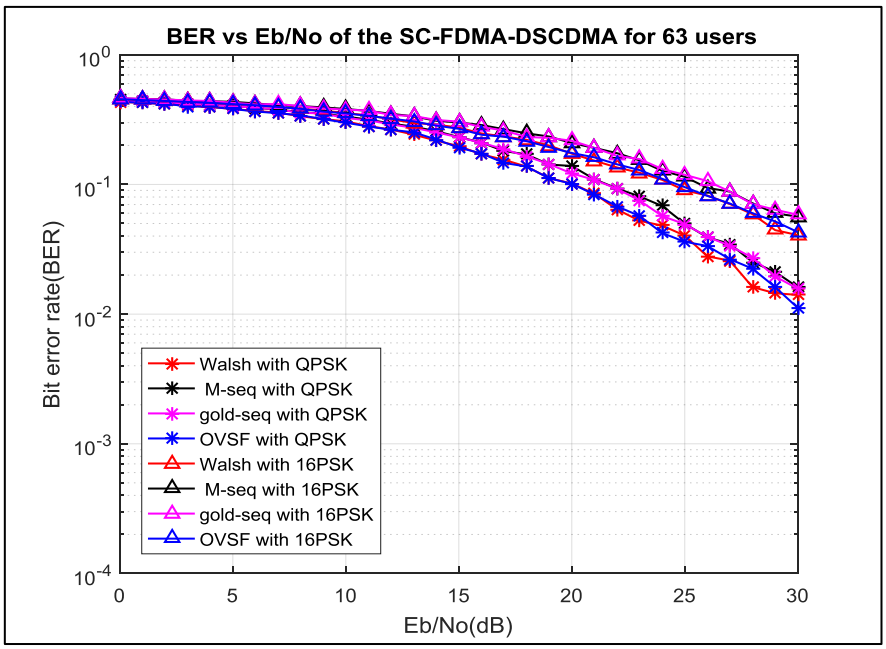

Figure (4.49): BER of the suggested system for 63 users with interleaved subcarriers mapping under the Rayleigh channel.

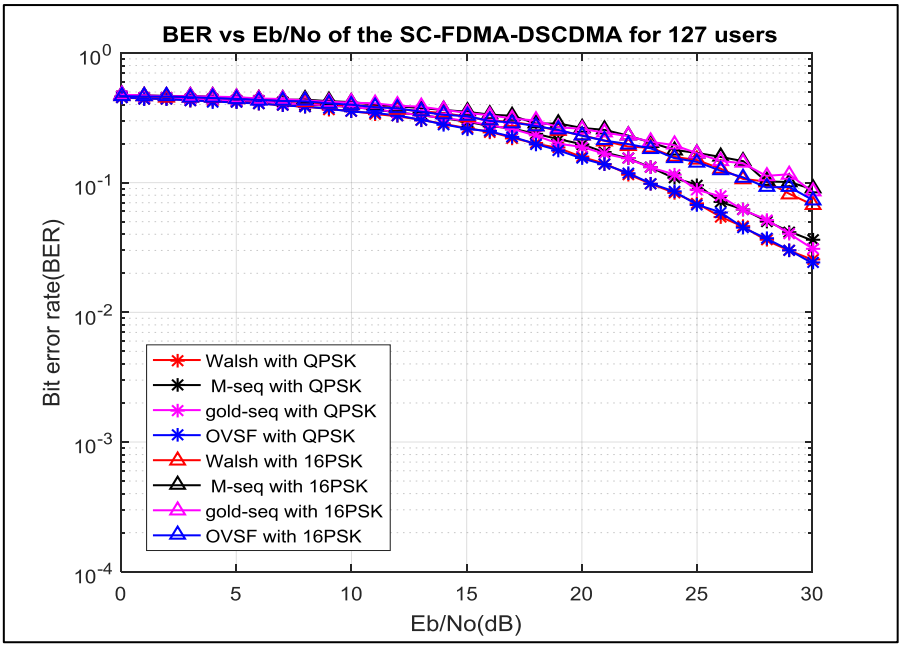

Figure (4.50): BER of the suggested system for 127 users with interleaved subcarriers mapping under the Rayleigh channel.

Section 4.5 presents simulation results of the proposed system in terms of PAPR and BER using different spreading codes. The PAPR performance results show that while utilizing the localized subcarrier mapping, the proposed system's performance using the various spreading codes seems to be approximately similar. Still, in the case of using the interleaved subcarriers mapping, the behaviour of the suggested system using the OVSF code is slightly better than the rest of the spreading codes. Regarding BER performance, The proposed system shows a very close performance for all the spreading codes.

4.6 Comparison with related works

Many works are employed to lower the PAPR value of the SC-FDMA system. These works are carried out using different types of spreading codes, transmission channels, and subcarrier mapping methods, in addition to the number of users.

To show how the proposed system is different from what has been done before, a comparison of the proposed system and the previous works is shown

in Table 4.1. The comparison considered various factors, including the number of users, the type of modulation, spreading code types, channel model, and channel estimation.

Table (4.1): comparison of the proposed system and the previous works.

Ref.	Mapping	No. of Users	Spreading code	Channel	Equalizer	Estimation	PAPR 8 user
Proposed System	QPSK, 16PSK	8,16,32 ,64,128	Walsh, M-sequences, gold, OVSF	AWGN and Rayleigh	Least square	Ideal	7.8 dB
[10]	QPSK	16	PN	AWGN and Rayleigh	Zero forcing	Ideal	8.1 dB
[7]	QPSK	16	Walsh	AWGN	---	---	10.3 dB
[6]	16QAM	1	---	AWGN	---	---	---

CHAPTER FIVE
Conclusion and Future Works

CHAPTER FIVE
Conclusion and Future Works

5.1 Conclusions

The following is a list of the conclusions that can be drawn from the results of testing numerous different situations.

- ❖ The OFDMA scheme with interleaved sub-carrier assignment has better PAPR than localized sub-carrier assignment. The OFDMA system has the same BER when employing interleaved and localized sub-carrier assignment.
- ❖ SC-FDMA PAPR with interleaved sub-carrier assignment is better than that with localized sub-carriers. The SC-FDMA system has nearly the same BER when employing the localized or interleaved sub-carrier assignment.
- ❖ SC-FDMA has better performance than OFDMA in terms of both PAPR and BER.
- ❖ The suggested SC-FDMA-DSCDMA system's PAPR is slightly better with interleaved sub-carrier mapping than with the localized subcarrier assignment. As for the BER, the proposed system performs similarly when employing localized or interleaved sub-carrier assignment.
- ❖ SC-FDMA-DSCDMA has a better PAPR than SC-FDMA. The proposed system's error rate is close to SC-FDMA. The suggested technique lowers PAPR without affecting BER.
- ❖ The performance of the suggested system in terms of PAPR when employing Walsh codes, m-sequence, gold, and OVSF code is similar in localized subcarrier mapping. Still, in interleaved, the OVSF code is somewhat better. The error rate of the suggested system using all four codes is similar.

5.2 Future works

Several proposed ideas could help to create a more robust SC-FDMA-DSCDMA system:

- ❖ Employing the Field Programmable Gate Array (FPGA) to implement the SC-FDMA-DSCDMA system.
- ❖ Utilizing the polar code as the channel coding in the SC-FDMA-DSCDMA system lowers the error rate and PAPR value.
- ❖ Implementing the SC-FDMA-DSCDMA system with pulse shaping to decreasing the PAPR value.
- ❖ Implement the hybrid subcarrier mapping for the SC-FDMA-DSCDMA system.

References

[1] K. Fazel and S. Kaiser, *Multi-Carrier and Spread Spectrum Systems*, Second Edition. Wiley, 2008. doi: 10.1002/9780470714249.

[2] S. Tripathi and R. Paulus, "Design and Analysis of OFDMA and SC-FDMA for LTE Uplink Enhancement," *Adv. Comput. Sci. Technol.*, vol. 10, no. 8, pp. 2675–2684, 2017.

[3] T. Jiang, D. Chen, C. Ni, and D. Qu, *OQAM/FBMC for future wireless communications: Principles, technologies and applications*. 2017. doi: 10.1016/C2016-0-05186-0.

[4] H. G. Myung and D. J. Goodman, *Single carrier FDMA: A new air interface for long term evolution*. John Wiley & Sons., 2008. doi: 10.1002/9780470758717.

[5] F. Adachi, D. Garg, A. Nakajima, K. Takeda, L. Liu, and H. Tomeba, "Fundamentals of single-carrier CDMA technologies," *Enhanc. Radio Access Technol. Next Gener. Mob. Commun.*, pp. 81–120, 2007, doi: 10.1007/1-4020-5532-3_3.

[6] J. Gazda, P. Drotár, P. Galajda, and D. Kocur, "Comparative evaluation of OFDMA and SC-FDMA based transmission systems," *SAMI 2010 - 8th Int. Symp. Appl. Mach. Intell. Informatics, Proc.*, pp. 177–181, 2010, doi: 10.1109/SAMI.2010.5423744.

[7] Z. Luo and X. Xiong, "Performance comparison of SC-FDMA-CDMA and OFDM-CDMA systems for uplink," *2011 Int. Conf. Consum. Electron. Commun. Networks, CECNet 2011 - Proc.*, pp. 1475–1479, 2011, doi: 10.1109/CECNET.2011.5768185.

[8] C. A. Azurdia-Meza, K. Lee, and K. Lee, "PAPR reduction in SC-FDMA by pulse shaping using parametric linear combination pulses," *IEEE Commun. Lett.*, vol. 16, no. 12, pp. 2008–2011, 2012, doi: 10.1109/LCOMM.2012.111612.121891.

[9] S. Shukla, S. Shukla, and N. Purohit, "PAPR Reduction in SC-FDMA Using NCT Technique," *Procedia Technol.*, vol. 10, pp. 927–934, 2013, doi: 10.1016/j.protcy.2013.12.439.

[10] D. Kedia and A. Modi, "Performance analysis of a modified SC-FDMA-DSCDMA technique for 4G wireless communication," *J. Comput. Networks Commun.*, vol. 2014, 2014, doi: 10.1155/2014/747824.

[11] F. S. Al-Kamal *et al.*, "An Efficient Transceiver Scheme for SC-FDMA Systems Based on Discrete Wavelet Transform and Discrete Cosine Transform," *Wirel. Pers. Commun.*, vol. 83, no. 4, pp. 3133–3155, 2015, doi: 10.1007/s11277-015-2587-8.

[12] R. F. Chisab, B. S. Hassen, and A. M. Al-A'assam, "Performance of Single Carrier Frequency Division Multiple Access Under Different Channel Cases," *Int. J. Eng. Adv. Technol.*, vol. 5, no. 6, pp. 94–98, 2016.

[13] S. Singh, M. Sharique, and A. A. Moinuddin, "PAPR reduction in SC-FDMA using transmit pulse shaping," *IMPACT 2017 - Int. Conf. Multimedia, Signal Process. Commun. Technol.*, pp. 275–279, 2018, doi: 10.1109/MSPCT.2017.8364020.

[14] K. S. Ramtej and S. Anuradha, "PAPR Reduction in LTE Uplink Communications by Airy Companding Transform," *2018 9th Int. Conf. Comput. Commun. Netw. Technol. ICCCNT 2018*, vol. 1, no. 3, pp. 1–5, 2018, doi: 10.1109/ICCCNT.2018.8494087.

[15] G. B. S. R. Naidu and V. M. Rao, "A Papr reduction of companded Sc-Fdma for 5g uplink communications," *Int. J. Innov. Technol. Explor. Eng.*, vol. 8, no. 7, pp. 135–139, 2019.

[16] K. S. Ramtej and S. Anuradha, "On companding techniques to mitigate PAPR in SC-FDMA systems," *Int. J. Wirel. Mob. Comput.*, vol. 18, no. 3, pp. 295–302, 2020, doi: 10.1504/IJWMC.2020.106778.

[17] P. Analysis, K. K. Vaigandla, and N. Venu, "BER , SNR and PAPR Analysis of OFDMA and SC-FDMA," *GIS Sci. J.*, vol. 8, no. 9, pp. 970–977, 2021.

[18] P. Miguel Rodrigues Cunha, D. Luis Bernardo, F. Doutor Rui Dinis, D. Rodolfo Oliveira Arguentes, D. João Oliveira Vogais, and D. Rui Dinis, "Implementing the SC-FDMA Transmission Technique Using the GNURadio Platform," Faculdade de Ciências e Tecnologia, 2014.

[19] L. Frenzel, *Principles of electronic communication systems*, Fourth Edition. New York: McGraw-Hill, Inc., 1982. doi: 10.1049/ep.1982.0354.

[20] A. Kukushkin, *Introduction to Mobile Network Engineering*, First Edit. wiley, 2018.

[21] T. T. Ha, *Theory and Design of Digital Communication Systems*, vol. 59. New York: Cambridge university press, 2010. doi: 10.1017/cbo9780511778681.

[22] G. E. Bottomley, *Channel Equalization for Wireless Communications: From Concepts to Detai. Mathematics*. WILEY and IEEE PRESS, 2011. doi: 10.1002/9781118105283.

[23] A. Ali and G. Hamza, "Design and Performance Analysis of Multi Carrier Code Division Multiple Access," university of Babylon, 2021.

[24] M. Golio, *The RF and Microwave Handbook*, Second Edition. Arizona, 2018.

[25] D. V. Sarwate, "Acquisition of Direct-Sequence Spread-Spectrum Signals," University of Tasmania Hobart, 1997. doi: 10.1007/978-1-4757-2604-6_6.

[26] A. Goldsmith, *Wireless Communicatinos*. New York: Cambridge university press, 2005.

[27] Fraidoon Mazda, Ed., *Telecommunications Engineer's Reference Book*. London: Elsevier Ltd, 2014. doi: https://doi.org/10.1016/C2013-0-06529-2.

[28] O. Q. J. Al-Thahab, "A Multi Carrier-Code Division Multiple Access System Using Multiwavelet and Radon Transforms," University of Technology, 2006.

[29] M. Schwartz, "Mobile Wireless Communications," *IEEE Signal Process. Mag.*, vol. 22, no. 4, pp. 110–111, 2005, doi: 10.1109/MSP.2005.1458312.

[30] J. Xinzhu, "Channel Estimation Techniques of SC-FDMA," Karlstad University, 2007.

[31] H. Holma and A. Toskala, *LTE for UMTS*, First Edition. both of Nokia Siemens Networks, Finland: John Wiley & Sons, Ltd, 2009. doi: 10.1002/9780470745489.

[32] M. Hua, B. Ren, M. Wang, J. Zou, C. Yang, and T. Liu, "Performance analysis of OFDMA and SC-FDMA multiple access techniques for next generation wireless communications," *IEEE Veh. Technol. Conf.*, 2013, doi: 10.1109/VTCSpring.2013.6692696.

[33] R. Grammenos and I. Darwazeh, "SC-FDMA and OFDMA : The two competing technologies for LTE," *4th Int. Symp. Broadband Commun.*, pp. 2–4, 2010.

[34] F. E. Abd El-Samie, F. S. Al-Kamali, A. Y. Al-Nahari, and M. I. Dessouky, *SC-FDMA for mobile communications*, First Edition. New York: Taylor & Francis, 2014.

[35] K. Takeda and F. Adachi, "Uplink capacity of single-carrier frequency-interleaved spread spectrum multiple access," *IEEE Veh. Technol. Conf.*, pp. 999–1003, 2007, doi: 10.1109/VETECF.2007.217.

[36] M. Al-Rawi, "Performance analysis of ofdma and SC-FDMA," *Int. Rev. Appl. Sci. Eng.*, vol. 8, no. 2, pp. 113–116, 2017, doi: 10.1556/1848.2017.8.2.2.

[37] C. Estevez, J. Molina, and C. A. Azurdia-Meza, "Subcarrier mapping distribution effect on single carrier FDMA transmissions," *2016 8th IEEE Latin-American Conf. Commun. LATINCOM 2016*, 2016, doi: 10.1109/LATINCOM.2016.7811611.

[38] R. Skaug and J. F. Hjelmstad, *Introduction to spread spectrum communications*, First edit. Colorado: McGraw-Hill, Inc., 2011. doi: 10.1049/pbte012e_ch1.

[39] A. Jeklin, "Principles of spread-spectrum communication systems," *Choice Reviews*. WILEY, New York, pp. 42-5295-42–5295, 2005. doi: 10.5860/choice.42-5295.

[40] J. M. Giron-Sierra, *Digital Signal Processing with Matlab Examples*. Singapore: Springer Singapore, 2017. doi: 10.1007/978-981-10-2540-2.

[41] J. Ravindrababu and E. V. K. Rao, "Performance comparison of spreading codes in linear multi-user detectors for DS-CDMA system," *WSEAS Trans. Commun.*, vol. 12, no. 2, pp. 52–62, 2013.

[42] M. Viswanathan, *Wireless Communication Systems in Matlab: Second Edition*, Second Edition. WILEY, New York, 2020.

[43] K. Fazel and S. Kaiser, *Multi-Carrier and Spread Spectrum Systems*, Second Edi. A John Wiley and Sons, Ltd, Publication, 2008.

[44] C. Engineering and M. T. Student, "Code Selection with Application to Spread Spectrum Systems Based on Correlation Properties," *Int. J. Adv. Res. Comput. Commun. Eng.*, vol. 4, no. 6, pp. 348–351, 2015, doi: 10.17148/IJARCCE.2015.4675.

[45] P. Franceschetti, V. Greco, G. Redaelli, and G. Coppola, “Analysis of single and multi carrier modulation schemes for 42 GHz broadband wireless systems,” *Conf. Rec. / IEEE Glob. Telecommun. Conf.*, vol. 4, pp. 1924–1929, 1998, doi: 10.1109/glocom.1998.775878.

[46] L. Vinet and A. Zhedanov, “A ‘missing’ family of classical orthogonal polynomials,” *J. Phys. A Math. Theor.*, vol. 44, no. 8, pp. 37–72, 2011, doi: 10.1088/1751-8113/44/8/085201.

[47] A. Kesteloot and C. L. Hutchinson, *the Arrl Spread Spectrum Sourcebook*, First Edit. Colorado: The American Radio Relay League, Inc, 1997.

[48] M. M. R. and S. B. Manir, “Performance Analysis of OFDMA in LTE Performance Analysis of OFDMA in LTE,” *Int. J. Comput. Appl.*, no. June 2014, 2018, doi: 10.5120/7090-9795.

[49] R. Saadia and N. M. Khan, “Single carrier-frequency division multiple access radar: Waveform design and analysis,” *IEEE Access*, vol. 8, pp. 35742–35751, 2020, doi: 10.1109/ACCESS.2020.2974935.

[50] E. McCune, *Practical digital wireless signals*, vol. 9780521516. New York: Cambridge university press, 2010. doi: 10.1017/CBO9780511674648.

الخلاصة

الوصول المتعدد بتقسيم التردد المتعامد (OFDMA) هو إصدار جديد من مضاعفة تقسيم التردد المتعامد (OFDM) الذي يسمح بوصول متعدد المستخدمين على أساس تقسيم التردد المتعامد من خلال تخصيص قنوات فرعية للتردد الزمني لمستخدمين متميزين ، مما يجعل من الممكن لعدة مستخدمين إرسال البيانات في وقت واحد. على الرغم من المزايا العديدة التي أدت إلى نشر تقنية OFDMA في العديد من التطبيقات ، إلا أن OFDMA بها مشكلة نسبة ذروة إلى متوسط القدرة العالية (PAPR).

يعد الوصول المتعدد بتقسيم الموجة الحاملة الفردية (SC-FDMA) أحد الأساليب التي اقترحها مشروع شراكة الجيل الثالث (3GPP) لتقليل OFDMA PAPR ويستخدم الآن في الوصلة الصاعدة 4G. تم اقتراح تقنية الوصول المتعدد لتقسيم تسلسل الشفرة الفردي لتقسيم التردد الحامل الفردي (SC-FDMA DS-CDMA) في هذه الأطروحة لخفض PAPR لـنظام SC-FDMA.

في هذه الأطروحة ، بدأت سيناريوهات المحاكاة بمحاكاة نظام OFDMA لمعرفة أدائه من حيث PAPR و BER ثم محاكاة نظام SC-FDMA ومقارنته بنظام OFDMA. عندما تكون دالة التوزيع التراكمي التكميلية (CCDF) لـ PAPR تساوي 10^{-3} مع رسم خرائط الموجات الحاملة الفرعية المحلية وتعديل QPSK ، يكون PAPR لـ SC-FDMA هو 7 dB ، بينما يبلغ PAPR لـ OFDMA 9.8dB. يكون معدل الخطأ في البتات لنظام SC-FDMA هي 6.2×10^{-4} عند نسبة الإشارة إلى الضوضاء (SNR) تبلغ 17.5 dB، بينما يتطلب نظام OFDMA معدل SNR يبلغ 26.8 dB للوصول لنفس معدل الخطأ في البتات (BER).

نفذت بقية سيناريوهات المحاكاة النهج المقترح SC-FDMA-DS-CDMA وقارن أداءها مع طريقة SC-FDMA التقليدية. تم تنفيذ النظام المقترح باستخدام تقنيتي التعديل (QPSK و 16PSK) مع نوعين من خرائط الموجات الحاملة الفرعية (الموضعية والمتداخلة). أيضًا ، تم استخدام نموذجين لقناة الاتصال (AWGN و Rayleigh) ، مع أنواع متعددة من متواليات الكود (متواليات Walsh-Hadamard ، وشفرات OVSF ، ومتواليات الطول الأقصى "m-sequences" ، والرموز الذهبية). تم تنفيذ محاكاة النظام المقترحة على عدة مستخدمين ، بدءًا من 8 وحتى 128 مستخدمًا وباستخدام برنامج MATLAB.

عندما يكون CCDF لـ PAPR هو 2-10 في ظل تعيين الناقل الفرعي المحلي ، وتعديل QPSK ، ورموز Walsh ، فإن ال PAPR للنظام المقترح SC-FDMA-DSCDMA مع 8 مستخدمين هو 7.85dB ، بينما ال PAPR لنظام SC-FDMA تكون 8.9 dB . يكون معدل ال PAPR للنظام المقترح SC-FDMA-DSCDMA مع 32 مستخدمًا 10 dB ، مقارنة بـ PAPR لنظام SC-FDMA البالغ 10.4 dB . يحتوي نظام SC-FDMA-DSCDMA المقترح على PAPR يبلغ

11.26 dB مع 128 مستخدمًا ، مقارنة بـ 11.47 dB لـ SC-FDMA. اما من ناحية نسبة الاخطاء في البتات فان اداء النظام المقرح SC-FDMA-DSCDMAعلى نفس معدل الخطا لنظام SC-FDMAالتقليدي.

وزارة التعليم العالي والبحث العلمي
جامعة بابـل / كلية الهندسة
قسم الهندسة الكهربائية

تصميم و محاكاة نظام هجيني ذو شفرة مباشرة للوصول المتعدد بتقسيم الرمز و حامل منفرد للوصول المتعدد بتقسيم التردد

رســـالـــــة
مقدمة الى كلية الهندسة في جامعة بابل
وهي جزء من متطلبات نيل درجة الماجستير في الهندسة/ الهندسة الكهربائية/اتصالات

من قبل
محمد حمزة عويد عبد

اشـراف
الأستاذ الدكتور سمير جاسم محمد المرعب

١٤٤٤هـ ٢٠٢٢م